

1 **A Comparison of South Pacific Antarctic Sea Ice and Atmospheric Circulation**
2 **Reconstructions Since 1900**

3
4 Ryan L. Fogt¹, Quentin Dalaiden², and Gemma K. O'Connor³

5
6 ¹Department of Geography and Scalia Laboratory for Atmospheric Analysis, Ohio University,
7 Athens, OH, USA

8 ²Université catholique de Louvain (UCLouvain), Earth and Life Institute (ELI), Louvain-la-
9 Neuve, Belgium

10 ³Department of Earth and Space Sciences, University of Washington, Seattle, WA, USA

11
12 **Corresponding Author Address:** Dr. Ryan L. Fogt, Ohio University, 122 Clippinger
13 Laboratories, Athens OH 45701 USA email:fogtr@ohio.edu

14 Submitted to *Climate of the Past*
15
16

17 Abstract

18 The recent changes and record ~~minimal~~ lows in Antarctic sea ice extent implore the need
19 for longer estimates beyond the short satellite observation period commencing near 1979.

20 However, Antarctic sea ice extent reconstructions ~~since 1900~~ based on paleo records and those
21 generated based on instrumental observations from the Southern Hemisphere midlatitudes are
22 markedly different, especially prior to 1979. Here, these reconstructions are examined with the
23 goal of understanding the relative strengths and limitations of each reconstruction better so that
24 researchers using the various datasets can interpret them appropriately.

25 Overall, it is found that the different spatial and temporal resolutions of each dataset play
26 a secondary role to the inherent connections each reconstruction has with its ~~underlying~~ implied
27 atmospheric circulation. ~~Several~~ Five Southern Hemisphere pressure reconstructions spanning
28 the 20th century are thus examined further. There are different variability and trends poleward of
29 60°S between ~~paleo~~ proxy-based and station-based 20th century pressure reconstructions which
30 are connected to the disagreement between the Antarctic sea ice extent reconstructions examined
31 here. Importantly, ~~sensitivity-experiments~~ reconstructions based on only coral
32 ~~paleoclimatological~~ records provide the best agreement between the early pressure
33 reconstructions, suggesting a contributing role of tropical variability is present in the station-
34 based pressure (and therefore sea ice) reconstructions, ~~while high-latitude~~. ~~In contrast~~, ice core
35 ~~information strongly constrains paleo-based-only~~ reconstructions ~~(of both pressure provide a~~
36 ~~local, high-latitude constraint that creates differences between the proxy-based and sea~~
37 ~~ice) station-based reconstructions~~ near ~~the Antarctic continent~~ Antarctica. Our results reveal the
38 greatest consistencies and inconsistencies in available datasets and highlight the need to better

39 understand the relative roles of the tropics versus high latitudes in historical sea ice variability
40 around Antarctica.

41

42 **1. Introduction**

43 The climate of Antarctica is very complex and highly variable in space and time, influenced
44 by unique processes over the Southern Ocean, the surrounding sea ice, and the continent itself

45 ~~(Jones et al., 2016; Goyal et al., 2021; Raphael et al., 2016; Holland et al., 2022; Blanchard-~~

46 ~~Wrigglesworth et al., 2021). Although geographically remote from other continents in the~~

47 ~~Southern Hemisphere, it is also strongly modulated by large-scale patterns of climate variability,~~

48 ~~including teleconnections from the tropical oceans, in particular in West Antarctica (Li et al.,~~

49 ~~2021; Lachlan-Cope and Connolley, 2006; Ding et al., 2011). Some of the more pronounced and~~

50 ~~unique changes in Antarctic climate include a rapid acceleration and thinning of outlet glaciers in~~

51 ~~the Amundsen Sea embayment (near West Antarctica) (Rignot et al., 2019, 2013; Bamber et al.,~~

52 ~~2009; Smith et al., 2020), a strengthening of the atmospheric circulation (in particular in austral~~

53 ~~summer) since 1980 linked to stratospheric ozone depletion (Polvani et al., 2011; Banerjee et al.,~~

54 ~~2020), and record low total Antarctic sea ice extent set in 2017 (Turner et al., 2017), 2022~~

55 ~~(Turner et al., 2022; Wang et al., 2022), and 2023, following multiple decades of a slow~~

56 ~~equatorward growth in the sea ice edge from 1979-2016 (Parkinson, 2019; Hobbs et al.,~~

57 ~~2016). (Jones et al., 2016; Goyal et al., 2021; Raphael et al., 2016; Holland et al., 2022;~~

58 ~~Blanchard-Wrigglesworth et al., 2021). Although geographically remote from other continents~~

59 ~~in the Southern Hemisphere, it is also strongly modulated by large-scale patterns of climate~~

60 ~~variability, including teleconnections from the tropical oceans, in particular in West Antarctica~~

61 ~~(Li et al., 2021; Lachlan-Cope and Connolley, 2006; Ding et al., 2011). Some of the more~~

62 pronounced and unique changes in Antarctic climate include a rapid acceleration and thinning of
63 outlet glaciers in the Amundsen Sea embayment (near West Antarctica) (Rignot et al., 2019,
64 2013; Bamber et al., 2009; Smith et al., 2020), a strengthening of the atmospheric circulation (in
65 particular in austral summer) since 1980 linked to stratospheric ozone depletion (Polvani et al.,
66 2011; Banerjee et al., 2020), and record low total Antarctic sea ice extent set in 2017 (Turner et
67 al., 2017), 2022 (Turner et al., 2022; Wang et al., 2022), and 2023, following multiple decades of
68 a slow equatorward growth in the sea ice edge from 1979-2016 (Parkinson, 2019; Hobbs et al.,
69 2016).

70 ~~While the high degree of interannual variability makes it challenging to fully understand~~
71 ~~these processes and changes, knowledge of them is also compromised by the comparatively~~
72 ~~temporally short length of instrumental observations (Jones et al., 2016). The majority of~~
73 ~~Antarctic meteorological measurements of temperature, pressure, and wind extend back until the~~
74 ~~International Geophysical Year (1957–1958), giving roughly only 60 years of continuous~~
75 ~~measurements for much of the continent (although most are not located in the interior of the ice~~
76 ~~sheet) (Turner et al., 2004, 2020). The observational record for Antarctic sea ice is even shorter~~
77 ~~—beginning near 1978–1979 when modern satellites provided continuous measurements of the~~
78 ~~sea ice concentration surrounding the continent (Meier et al., 2021; Parkinson, 2019).~~

79 ~~Given the large year-to-year variability and the short observational records, other approaches~~
80 ~~must be employed in order to place the shorter records into a longer term context—a necessary~~
81 ~~step to better understand the potential uniqueness of ongoing changes across the continent and to~~
82 ~~provide more aid in deciphering possible mechanisms for these changes. One common approach~~
83 ~~is to produce reconstructions of past climate prior to direct observational measurements. For~~
84 ~~Antarctica, these reconstructions generally come in two main approaches. The first approach~~

85 ~~relies on paleoclimate records such as proxies from ice cores (typically the water isotopic content~~
86 ~~or snow accumulation) or ocean sediments to provide estimates of climate back centuries to~~
87 ~~millennia (Thomas et al., 2019; Steig et al., 2013; Thomas et al., 2017; Stenni et al., 2017).~~
88 ~~These paleoclimate data can be used directly to provide reconstructions of past climate if there is~~
89 ~~a strong physical relationship between the paleoclimate data and some aspect of observed~~
90 ~~climate; they can also be assimilated with climate model simulations to provide a more spatially~~
91 ~~complete reconstruction of climate across Antarctica (Dalaiden et al., 2021a; O'Connor et al.,~~
92 ~~2021, 2023). The second approach is based on instrumental observations in regions away from~~
93 ~~Antarctica through statistical models connecting the Antarctic climate with the climate across the~~
94 ~~Southern Hemisphere (Fogt et al., 2016a, b, 2019, 2022a; Fogt and Connolly, 2021). Assuming~~
95 ~~these relationships are stationary in time (Clark and Fogt, 2019), this approach creates~~
96 ~~reconstructions throughout the length of other Southern Hemisphere climate observations based~~
97 ~~on the relationship during the period of their overlap with Antarctic climate observations.~~

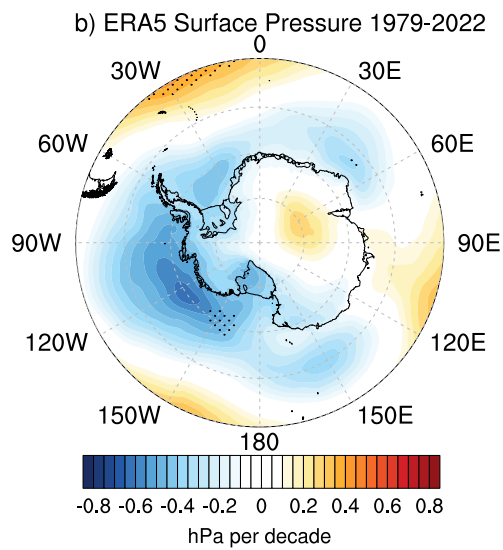
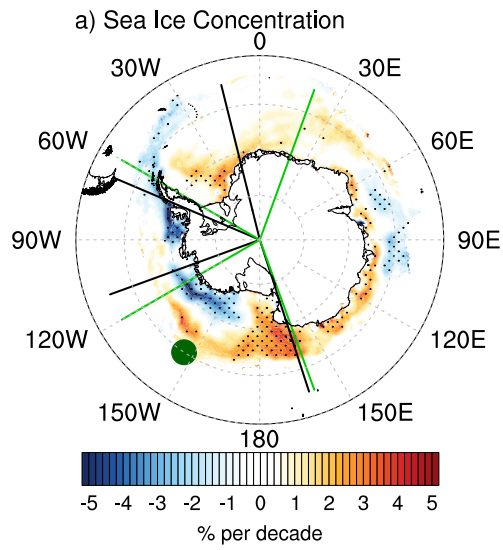
98 While the high degree of interannual variability makes it challenging to fully understand
99 these processes and changes, knowledge of them is also compromised by the comparatively
100 temporally short length of instrumental observations (Jones et al., 2016). The majority of
101 Antarctic meteorological measurements of temperature, pressure, and wind extend back until the
102 International Geophysical Year (1957-1958), giving roughly only 60 years of continuous
103 measurements for much of the continent (although most are not located in the interior of the ice
104 sheet) (Turner et al., 2004, 2020). The observational record for Antarctic sea ice is even shorter
105 – beginning in late 1978 when modern satellites provided continuous measurements of the sea
106 ice concentration surrounding the continent (Meier et al., 2021; Parkinson, 2019).

107 Given the large year-to-year variability and the short observational records in Antarctica,
108 other approaches must be employed to gain a longer term context – a necessary step to better
109 understand the potential uniqueness and possible mechanisms for these changes both now and
110 into the future. One common approach is to produce reconstructions of past climate prior to
111 direct observational measurements. For Antarctica, these reconstructions generally come in two
112 main approaches. The first approach relies on paleoclimate records such as proxies from ice
113 cores (typically the water isotopic content or snow accumulation) or ocean sediments to provide
114 estimates of climate back centuries to millennia (Thomas et al., 2019; Steig et al., 2013; Thomas
115 et al., 2017; Stenni et al., 2017). These paleoclimate data can be used directly to provide
116 reconstructions of past climate if there is a strong physical relationship between the paleoclimate
117 data and some aspect of observed climate; they can also be assimilated with climate model
118 simulations to provide a more spatially complete reconstruction of climate across Antarctica
119 (Dalaiden et al., 2021a; O’Connor et al., 2021, 2023). The second approach is based on
120 instrumental observations in regions away from Antarctica through statistical models connecting
121 the Antarctic climate with the climate across the Southern Hemisphere (Fogt et al., 2016a, b,
122 2019, 2022a; Fogt and Connolly, 2021). Assuming these relationships are stationary in time
123 (Clark and Fogt, 2019), this approach creates reconstructions throughout the length of other
124 Southern Hemisphere climate observations (most dating back to early 20th century or before)
125 based on the relationship during the period of their overlap with Antarctic climate observations.
126 The proxy-based and instrumental-based approaches have different strengths and weaknesses.
127 Paleo-based reconstructions can provide historical changes on longer timescales and in key
128 regions distant from stations; however, they are often limited to annual resolution and are
129 associated with uncertainties in the precise climate signals recorded. Station-based

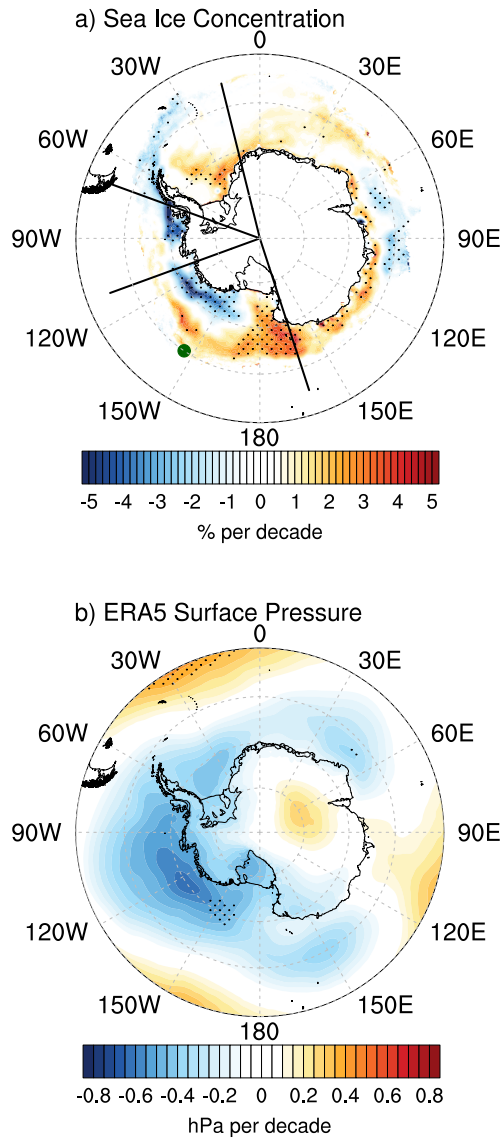
130 reconstructions can produce sub-annual resolutions with direct observations of climate but are
131 restricted temporally and spatially by station availability. Additionally, paleo-based
132 reconstructions have the advantage ~~to rely of relying~~ on measures of Antarctic climate variability
133 that are located closer to the Southern Ocean, whereas station-based reconstructions largely rely
134 on data from the Southern Hemisphere ~~midlatitude~~mid-latitude land masses. These differences
135 can lead to different estimates of Antarctic climate in the early 20th century (~~Fogt et al.,~~
136 ~~2022b~~);(Fogt et al., 2022b). In particular, one key area of differences suggested in earlier work
137 between these various reconstructions was in the south Pacific and Atlantic Oceans stretching
138 from the Ross Sea east to the Weddell Sea – regions of strong trends from observations (or
139 reanalyses) in both sea ice concentration / extent and sea level pressure (Fig. 1). Recently, Fogt
140 et al. (2022b) discussed this area as a key region where further analysis is needed on the
141 similarities and differences between the reconstructions to better understand their utility. This
142 paper will therefore extend the preliminary analysis of Fogt et al. (2022b) to ~~provide further~~
143 ~~comparison between proxy-based and instrumental-based analyze differences in (primarily West~~
144 ~~Antarctic annual mean) sea ice reconstructions of 20th century Southern Hemisphere sea ice~~
145 ~~extent to better understand the origins of their discrepancies~~, with a particular focus on the role
146 of the atmospheric circulation ~~throughout the 20th century as a primary mechanism for these~~
147 ~~differences~~.

148

Annual Mean Trends 1979-2020



Annual Mean Trends 1979-2020



150

151 **Figure 1.** a) Annual mean sea ice concentration trends (% per decade) over 1979–2020. The
152 solid black lines denote the sea ice sector boundaries from Parkinson (2019), while the solid
153 green lines represent the boundaries from Raphael and Hobbs (2014). The dark green dot marks
154 the location of the ice edge approximated by the Thomas and Abram (2016) reconstruction. b)
155 Annual mean ERA5 surface pressure trends (hPa per decade). In both plots, trends statistically
156 different from zero at $p < 0.05$ are stippled.
157

2. Data and Methods

~~Table 1 provides further info on the various reconstructions compared in this paper, while Fig. 2 shows the locations of data used in three separate reconstructions.~~ For station-based reconstructions, we use the Fogt et al. (2022a) seasonal sea ice extent reconstructions and the Fogt and Connolly (2021) merged pressure reconstructions. We also investigate three proxy-based reconstructions for sea ice extent (~~one of which is spatially complete~~), and two ~~spatially complete~~, proxy-based reconstructions for atmospheric pressure. Table 1 provides further information on the reconstructions compared in this paper, while Fig. 2 shows the locations of data used in three separate reconstructions.

2.1) Station and sea ice observations ~~and station-based reconstructions~~

Monthly mean atmospheric pressure and temperature observations across the Southern Hemisphere used in the Fogt et al. (2019) pressure and Fogt et al. (2022a) sea ice reconstruction (Fig. 2a) are primarily obtained from the University Corporation for Atmospheric Research (UCAR) Research Data Archive dataset ds570.0 (<https://rda.ucar.edu/datasets/ds570.0/#!description>). A few stations from this dataset have been patched and merged with nearby stations to provide the most complete and continuous observational record, following Fogt et al. (2022a). Some other station data have been corrected independently, as discussed in Fogt et al. (2022a).

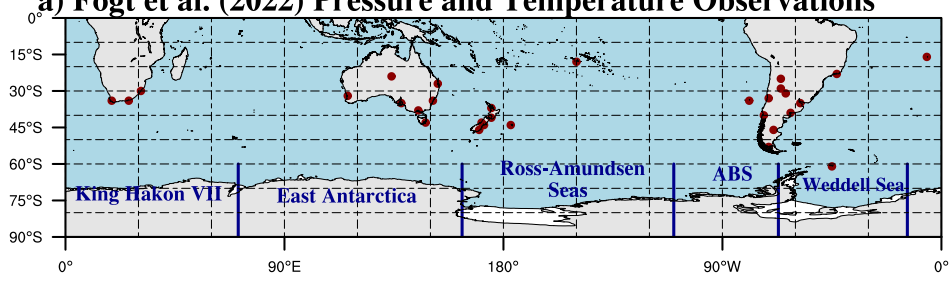
177 A few Antarctic pressure observations (Turner et al. 2014) are used to evaluate the pressure
178 variability throughout the 20th century. We combine the Byrd station (year round, 1957- 1970)
179 with the automatic weather station (AWS) data to provide the longest possible estimate in West
180 Antarctica. The combination of the Byrd temperature record has been completed and analyzed
181 in detail in earlier work (Bromwich et al. 2013), but the implications of the merged pressure
182 record have not yet been investigated. Similarly, we use the longest Antarctic Peninsula station
183 (Faraday/ Vernadsky, 1947-present) to represent conditions there. In the southern Weddell Sea
184 sector, we merge the pressure observations from the various locations of Halley station (1957-
185 present), as these are less influenced than temperature measurements at each site that show
186 discontinuities (King et al.). All of these stations are not included as predictor data in the Fogt
187 et al. (2016, 2019) pressure reconstructions. For the longest possible estimate, we also use
188 observations from Orcadas starting in 1903 (Zazulie et al. 2003) - the observations from this
189 station were directly included in the Fogt et al. (2019) spatial pressure reconstruction.

190 We also make use of the South Orkney fast ice duration time series from Murphy et al.
191 (1995, 2014) as a long-term observationally based estimate of historical sea ice conditions in the
192 Weddell Sea. This dataset was not used in any of the sea ice reconstructions evaluated here, so it
193 serves as an independent dataset to compare historical sea ice variations in the Weddell Sea.

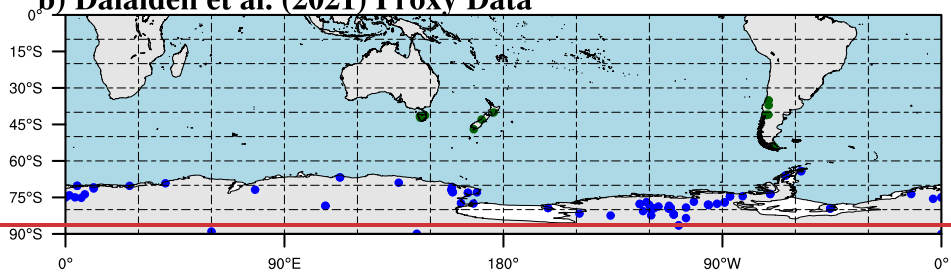
<u>Dataset and shortened name</u>	<u>Type (station-or paleo based)</u>	<u>Variable(s) used in this study</u>	<u>Data Used in Reconstruction</u>	<u>Time Period</u>	<u>Resolution (Temporal / Spatial)</u>
Fogt et al. (2022a) <u>FOGT22_STAT</u>	Station	Sea ice extent	Station pressure and temperature, indices of climate variability (Fig. 2a)	1905-2020	Seasonal, 5 sectors (Fig. 2a) + total sea ice extent
Fogt and Connolly (2021) <u>FC21_STAT</u>	Station	Near surface pressure	Fogt et al. (2019) reconstruction merged with NOAA 20CRv3 equatorward of 60°S	1905-2016	Seasonal, global, interpolated to 1°x1°
Abram et al. (2010) <u>AB10_PALEO</u>	Paleo	Sea ice extent	3 <u>methanesulphonic acid content from three</u> Antarctic Peninsula ice cores	1900-2004	Winter (August-October), 70°W – 100°W (Bellingshausen Sea, Fig. 1a)
Thomas and Abram (2016) <u>TA16_PALEO</u>	Paleo	Sea ice extent	Coastal West Antarctica ice core <u>methanesulphonic acid content from an ice core located off the Amundsen Sea coast</u>	1702-2010	Annual, ice edge at 146°W (Fig. 1a)
Dalaiden et al. (2021) <u>DAL21_ASSIM</u>	Paleo data assimilation with climate model prior (<u>fixed over time</u>)	Sea ice extent (derived from sea ice concentration); mean sea level pressure	Ice core $\delta^{18}\text{O}$ (<u>uncalibrated</u>) and <u>surfacesnow</u> accumulation; (<u>uncalibrated</u>); tree ring width data (<u>calibrated against temperature and precipitation</u> ; Fig. 2b); used isotope- enable <u>enabled</u> CESM1 last millennium ensemble as a prior (<u>natural variability</u>)	1800-2000	Sea ice extent: Annual, 5 sectors as in Raphael and Hobbs (2014) and Fogt et al. (2022a) Pressure: annual, global, 1°x1°
O'Connor et al. (2021) <u>OCON21_ASSIM</u>	Paleo data assimilation with climate model prior (<u>fixed over time</u>)	Mean sea level pressure	Global ice core, tree ring, and coral / sclerosponges (<u>Fig-all calibrated against temperature; tree-rings calibrated against temperature and precipitation</u> ; Fig. 2c); used CESM1 Pacific pacemaker ensemble (with external forcings) as a prior	1900-2005	Annual, global, 1°x1°
O'Connor et al. (2023) <u>OCON23_ASSIM</u>	Paleo data assimilation with climate model prior (<u>fixed over time</u>)	Mean sea level pressure from sensitivity experiments	One reconstruction using only ice core data (<u>calibrated against temperature</u>) and One reconstruction using only coral data (<u>calibrated against temperature</u>)	1900-2005	Annual, global, interpoated <u>interpolated</u> to 1°x1°

194 **Table 1.** Details on the various reconstruction datasets used in this study.

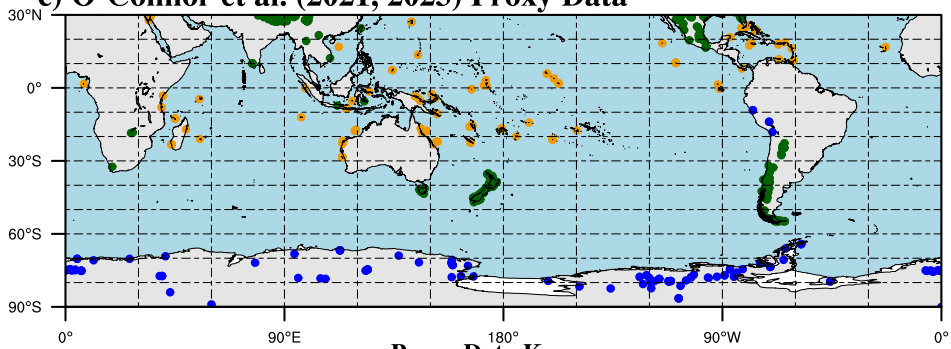
a) Fogt et al. (2022) Pressure and Temperature Observations



b) Dalaiden et al. (2021) Proxy Data



c) O'Connor et al. (2021, 2023) Proxy Data

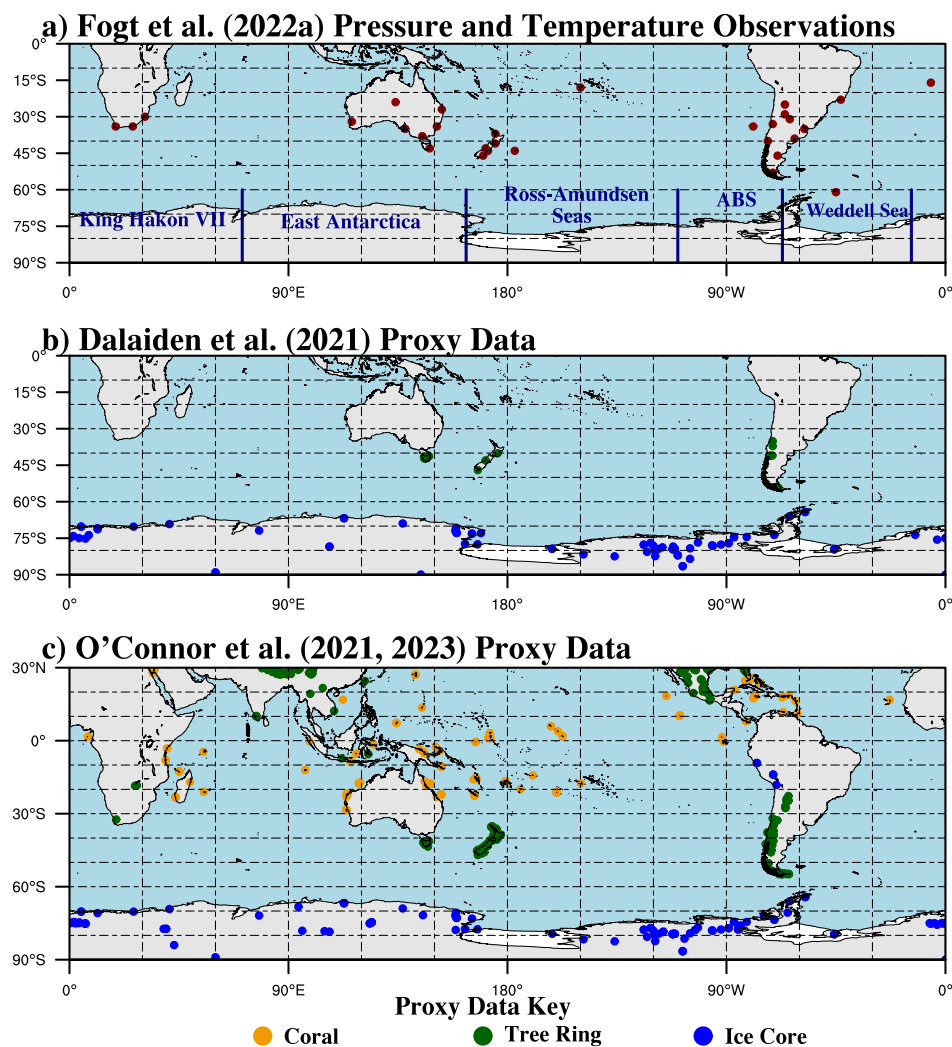


Proxy Data Key

● Coral

● Tree Ring

● Ice Core



196
 197 **Figure 2.** Map of a) temperature and pressure observations used in the Fogt et al. (2022a)
 198 seasonal sea ice reconstructions (the same pressure stations were used in the Fogt et al. (2019)
 199 and Fogt and Connolly (2021) pressure reconstruction); b) proxy data locations used in the
 200 Dalaiden et al. (2021) pressure and sea ice reconstructions; c) proxy data locations used in the
 201 O'Connor et al. (2021, 2023) pressure reconstructions. The Fogt et al. (2022a) seasonal sea ice
 202 reconstructions used only a subset of the available observations and also indices of atmospheric
 203 and oceanic variability in their reconstructions, depending on the sea ice sector being
 204 reconstructed (Table 1), depicted in a) (ABS= Amundsen-Bellingshausen Seas). For b), the ice
 205 core locations are a combination of the $\delta^{18}\text{O}$ and the surface accumulation measurements. For
 206 c), the coral proxies also include sclerosponges. Although the O'Connor et al. (2021, 2023)
 207 assimilated proxy data span the entire globe, only the data south of 30°N are shown as these have
 208 the strongest influence on the reconstruction near Antarctica.
 209

210 Observed sea ice concentration, from which sea ice extent is calculated, is obtained from the
211 Nimbus-7 Scanning Multichannel Microwave Radiometer (SMMR) and Defense Meteorological
212 Satellite Program (DMSP) Special Sensor Microwave Imager - Special Sensor Microwave
213 Imager/Sounder (SSM/I-SSMIS). ~~The Fogt et al. (2022a) sea ice extent reconstructions~~ We
214 specifically use the Climate Data Record (CDR) daily concentration fields from the National
215 Oceanic and Atmospheric Administration / National Snow and Ice Data Center (NOAA/NSIDC)
216 Climate Data Record of Passive Microwave Sea Ice Concentration, Version 4
217 (<https://nsidc.org/data/g02202>) (Meier et al., 2021). ~~The CDR algorithm output combines~~
218 ~~of~~ (Meier et al., 2021). ~~The CDR algorithm output combines~~ ice concentration estimates from the
219 National Aeronautics and Space Administration (NASA) Team algorithm and the NASA
220 Bootstrap algorithm, and are available at a 25 km x 25 km polar stereographic grid. Sea ice
221 extent is calculated as the ~~equatorward limit of the~~ cumulative area ~~bounded by of~~ grid cells with
222 at least 15% sea ice concentration ~~isoline~~; monthly, seasonal, and annual means are calculated
223 from the daily sea ice concentration data. Patching of a short temporal discontinuity of the sea
224 ice observations between December 1987 and January 1988 was done as in Fogt et al. (2022a).
225 Longitude bounds for the sea ice sectors used in this study follow ~~Raphael and Hobbs (2014)~~;
226 Raphael and Hobbs (2014), specifically defined as: Amundsen-Bellingshausen Seas (250°-
227 290°E), Weddell Sea (290°-346°E), and the Ross-Amundsen Sea (162°-250°E); see Figs. 1 and
228 2a for boundaries.

229 2.2) Station-based reconstructions

230 We use the best-fit reconstruction from the Fogt et al. (2022a) seasonal sea ice extent
231 reconstructions, hereafter FOGT22_STAT, conducted separately for the Raphael and Hobbs

232 (2014) sectors as well as for the total extent as the station-based sea ice extent reconstruction. To
233 get the annual mean, the four seasons were averaged together each year.

234 The seasonal spatially complete pressure reconstructions of Fogt et al. (2019) span the region
235 poleward of 60°S at 100km resolution, and are a kriging interpolation of individual Antarctic
236 station reconstructions from Fogt et al. (2016a,b). The Fogt et al. (2019) seasonal Antarctic
237 pressure reconstruction has been merged with the National Oceanic and Atmospheric
238 Administration (NOAA) 20th century reanalysis version 3 data ~~(Slivinski et al., 2019)~~(Slivinski
239 et al., 2019) equatorward of 60°S, as discussed in Fogt and Connolly (2021), hereafter
240 FC21_STAT, which we use for comparison in this study. We similarly average the F21_STAT
241 over the four seasons to calculate the annual mean for comparison.

242 *2.23) Paleo-based reconstructions*

243 While there are a few ocean sediment-derived sea ice extent reconstructions near the
244 Antarctic Peninsula relevant to this study, Thomas et al. (2019) note that the poorer temporal
245 resolution and lack of calibration of most marine sediments create challenges when combining
246 and comparing them to ice core-derived sea ice reconstructions. We therefore employ two main
247 ice core based reconstructions of sea ice extent, as in Fogt et al. ~~(2022b): Abram et al. (2010)~~
248 used a(2022b): Abram et al. (2010), which ends in 2004 (Table 1), used three ice cores from the
249 Antarctic Peninsula to reconstruct the winter sea ice extent from 70°W – 100°W, in the
250 Bellingshausen Sea (outlined in Fig. 1a). ~~The Abram et al. (2010) reconstruction ends in 2004.~~
251 ~~Further west, Thomas and Abram (2016) provide a reconstruction with annual resolution of the~~
252 ~~sea ice extent in the Ross Sea (marked in Fig. 1a). Both Abram et al. (2010) and Thomas and~~
253 ~~Abram (2016)1a), hereafter AB10_PALEO. Further west, Thomas and Abram (2016) provide a~~
254 reconstruction, hereafter TA16_PALEO, with annual resolution of the sea ice extent in the Ross

255 Sea (marked in Fig. 1a). Both AB10_PALEO and TA16_PALEO reconstructed the sea ice extent
256 based on the methanesulphonic acid (MSA) content – an indicator related to the algal blooms
257 occurring during the ice break-up periods - -from different Antarctic ice cores by calibrating
258 them against sea ice extent from satellite observations.

259 ~~As mentioned earlier, multiple ice core, tree ring, and coral proxy records can be assimilated~~
260 ~~with Earth System Model simulations to provide annual mean gridded estimates of not only sea~~
261 ~~ice extent and concentration, but also atmospheric pressure. We employ two such estimates of~~
262 ~~previous Antarctic climate in this study – those of Dalaiden et al. (2021) and O’Connor et al.~~
263 ~~(2021, 2023; no sea ice reconstruction), which both use proxy measurements but different data~~
264 ~~assimilation filters and different Earth System Model simulations as the data assimilation “prior”~~
265 ~~(the initial guess that is updated with proxy data) (Table 1). Although no sea ice nor atmospheric~~
266 ~~pressure observations are directly assimilated, the data assimilation relies on the covariance~~
267 ~~between assimilated observations and those variables given by the Earth System Model to~~
268 ~~reconstruct them (Widmann et al., 2010; Goosse et al., 2010; Hakim et al., 2016). The temporal~~
269 ~~variability thus only comes from proxy records, which are spatially interpolated during data~~
270 ~~assimilation. Therefore, the final reconstruction is dynamically consistent through all the~~
271 ~~reconstructed climate variables. For Dalaiden et al. (2021) we use the sea ice concentration,~~
272 ~~extent, and sea level pressure datasets generated using the isotope-enabled Community Earth~~
273 ~~System Model version 1 (CESM1) last millennium ensemble as the prior (Brady et al., 2019),~~
274 ~~and based on Southern Hemisphere ice cores and tree rings (Fig. 2b). We further use the~~
275 ~~O’Connor et al. (2021) pressure dataset generated using the CESM1 tropical Pacific pacemaker~~
276 ~~ensemble of simulations (Schneider and Deser, 2018) as the data assimilation prior, as this~~
277 ~~ensemble best represents historical external forcing and Pacific variability relative to other~~

278 ~~simulations (for more details see O'Connor et al., 2021). The O'Connor et al. (2021) dataset~~
279 ~~includes a global proxy database of ice cores, corals, and tree rings, synthesized by the~~
280 ~~PAGES2k working group (Fig. 2c) (PAGES2k Consortium et al., 2017), with additional snow~~
281 ~~accumulation records (Thomas et al., 2017). The comparison between the Dalaiden et al. (2021)~~
282 ~~reconstruction and the O'Connor et al. (2021) reconstruction reveals the roles of different~~
283 ~~filtering methods, proxy databases, and climate model priors. O'Connor et al. (2023) provide~~
284 ~~additional single-proxy reconstructions, using the same configuration as O'Connor et al. (2021),~~
285 ~~but based only on the assimilation of ice core or coral records. The comparison between these~~
286 ~~sensitivity experiments with O'Connor et al. (2021) allows a better understanding of the possible~~
287 ~~role of certain proxy data on the resulting reconstruction.~~

288

289 **3. Results**

290 *3.1 Comparison of Antarctic sea ice extent reconstructions*

291 *As alluded to in the introduction and Fogt et al. 2.4) Reconstructions based on paleo data* 292 *assimilation*

293 As mentioned earlier, multiple ice core, tree-ring, and coral proxy records can be assimilated
294 within Earth System Model simulations to provide annual mean gridded estimates of not only sea
295 ice extent and concentration, but also atmospheric pressure. We employ two such estimates of
296 previous Antarctic climate in this study- those of Dalaiden et al. (2021) and O'Connor et al.
297 (2021, 2023; no sea ice reconstruction), which both use proxy measurements but different data
298 assimilation filters and different Earth System Model simulations as the data assimilation “prior”
299 (the initial guess that is updated with proxy data) (Table 1). Although no sea ice nor atmospheric
300 pressure observations are directly assimilated, the data assimilation relies on the covariance

301 between the climate in the proxy locations and sea ice concentration or sea-level pressure, based
302 on covariance patterns in the data assimilation prior (Widmann et al., 2010; Goosse et al., 2010;
303 Hakim et al., 2016). The temporal variability thus only comes from proxy records, which are
304 spatially interpolated during data assimilation. Therefore, the final reconstruction is dynamically
305 consistent through all the reconstructed climate variables. For Dalaiden et al. (2021), hereafter
306 DAL21_ASSIM, we use the sea ice concentration, extent, and sea level pressure datasets
307 generated using the isotope-enabled Community Earth System Model version 1 (CESM1) last
308 millennium ensemble as the prior (Brady et al., 2019), and based on Southern Hemisphere ice
309 cores and tree rings (Fig. 2b). The sea ice extent from DAL21_ASSIM was calculated using the
310 Raphael and Hobbs (2014) boundaries to compare with FOGT_STAT. We further use the
311 O'Connor et al. (2021) pressure dataset, hereafter OCON21_ASSIM, generated using the
312 CESM1 tropical Pacific pacemaker ensemble of simulations (Schneider and Deser, 2018) as the
313 data assimilation prior, as this ensemble best represents historical external forcing and Pacific
314 variability relative to other simulations (for more details see O'Connor et al., 2021). The
315 OCON21_ASSIM dataset includes a global proxy database of ice cores, corals, and tree rings,
316 synthesized by the PAGES2k working group (Fig. 2c) (PAGES2k Consortium et al., 2017), with
317 additional snow accumulation records (Thomas et al., 2017; as in Dalaiden et al., 2021). It is
318 worth mentioning that the prior used in the DAL21_ASSIM and OCON21_ASSIM
319 reconstructions is fixed over time (i.e., each reconstructed year is based on the same prior) but
320 while the prior used in the OCON21_ASSIM reconstruction includes the anthropogenic forcing,
321 the reconstruction of DAL21_ASSIM solely relies on the natural climate variability as in Hakim
322 et al. (2016) and Steiger et al. (2018). Therefore, since the prior remains constant over time, the
323 temporal variability of the reconstruction only arises from the proxies. The comparison between

324 the DAL21_ASSIM reconstruction and the OCON21_ASSIM reconstruction reveals the roles of
325 different filtering methods, proxy databases, and atmospheric forcings used to form the climate
326 model priors. O'Connor et al. (2023), hereafter OCON23_ASSIM, provide additional single-
327 proxy reconstructions, using the same configuration as OCON21_ASSIM, but based only on the
328 assimilation of ice core or coral records. The comparison between these sensitivity experiments
329 with OCON21_ASSIM allows a better understanding of the possible role of certain proxy data
330 on the resulting reconstruction.

331

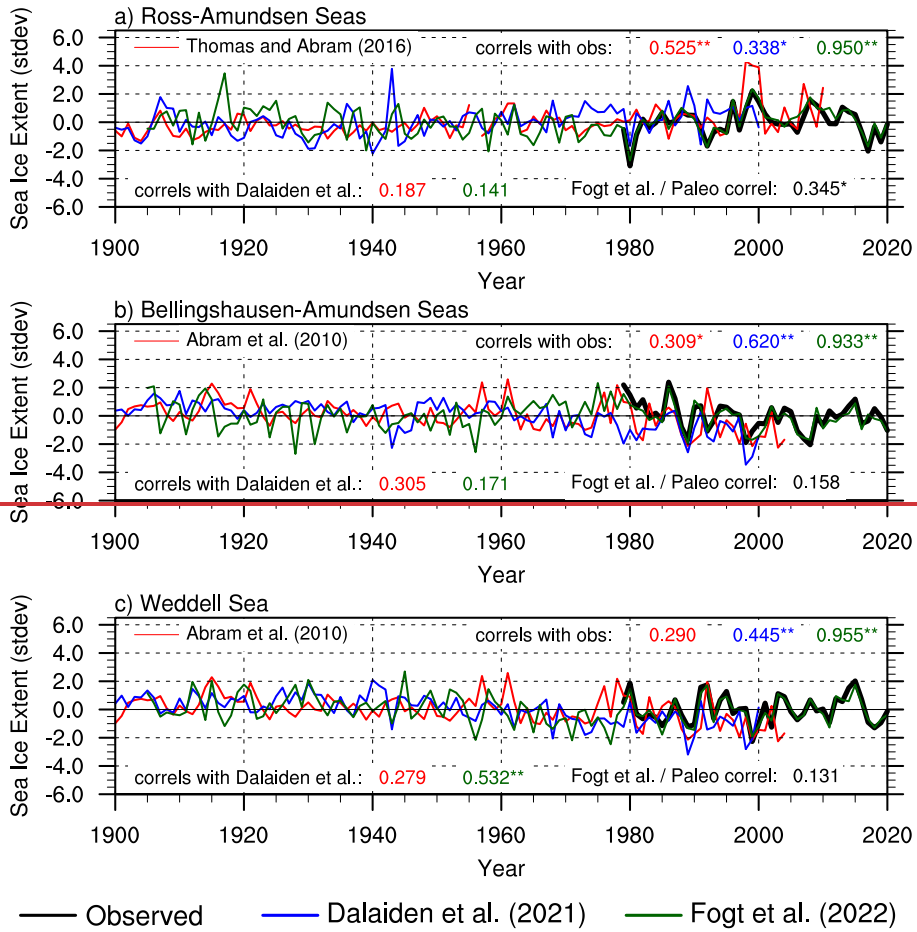
332 3. Results

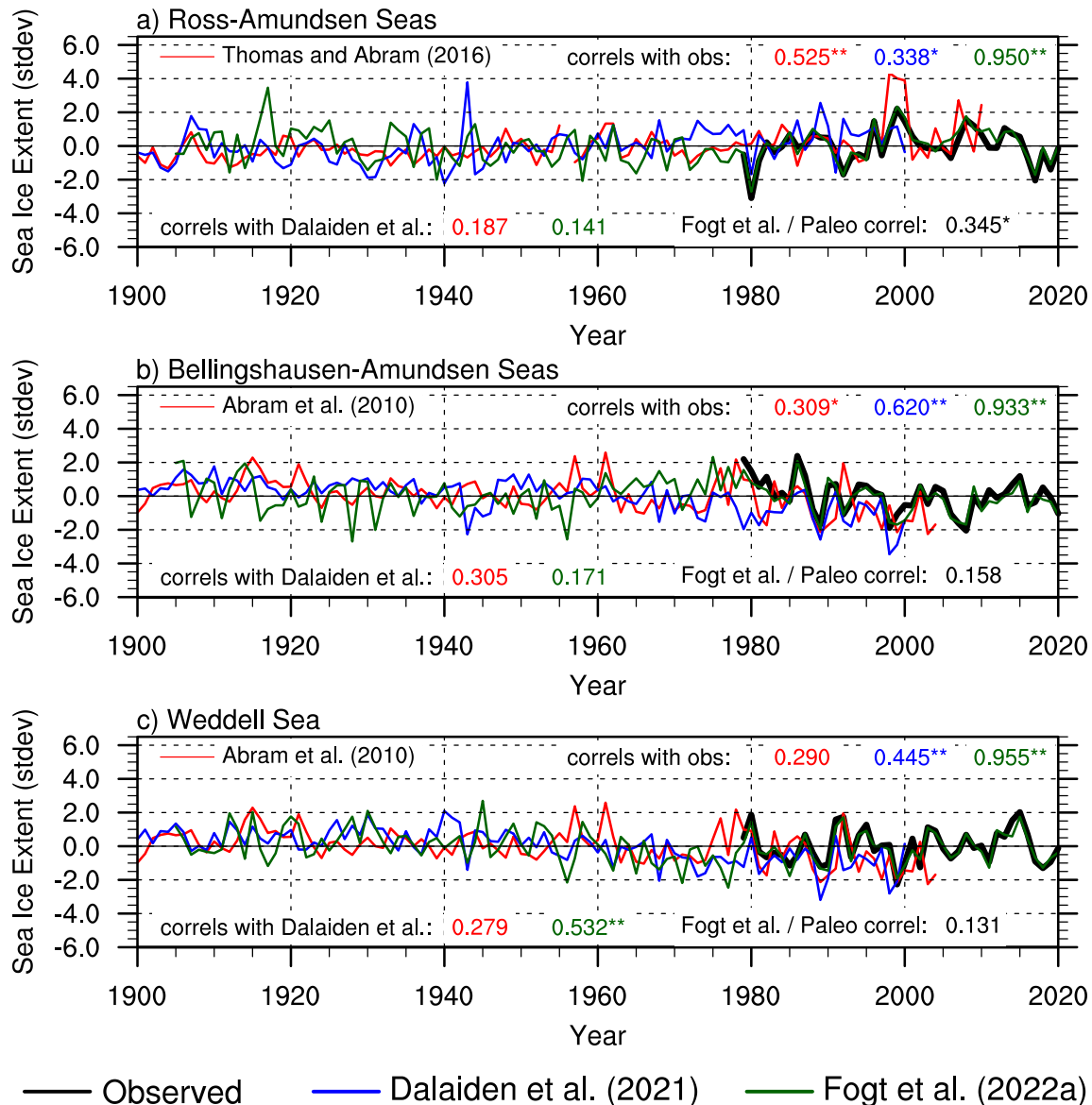
333 3.1) Comparison of Antarctic sea ice extent reconstructions

334 As alluded to in the introduction and Fogt et al. (2022a,b), there are substantial sea ice
335 extent differences between the station-based sea ice extent FOGT_STAT reconstructions of Fogt
336 et al. (2022a) and those based on paleo data, including from data assimilation-based
337 reconstructions. To investigate these differences further, the various time series of standardized
338 (to place on same scale) annual-mean sea ice extent anomalies from the Ross-Amundsen Sea
339 sector east to the Weddell Sea (see Fig. 1 for sector boundaries) are plotted in Fig. 3. Not
340 surprisingly, the correlations with observations (color-coded numbers at the Fogt et al. (2022a)
341 reconstructions with the observed data (green number in uppertop right of each panel in Fig. 3)
342 are the highest for the FOGT_STAT reconstructions ($p < 0.01$), as these reconstructions were
343 specifically statistically calibrated to provide the best match to the observations. However, the
344 correlations of the paleo-based reconstructions (including the Dalaiden et al.
345 (2021) DAL21_ASSIM reconstruction which is not directly calibrated to sea ice observations)
346 reconstructions are also uniformly positive, and the Thomas and Abram (2016) provides the

347 highest correlations of the paleo-based reconstructions in the Ross-Amundsen Seas (Fig. 3a,
348 $r=0.525, p<0.01$), while the Dalaiden et al. (2021) estimates from their data-assimilation-based
349 reconstruction are the highest correlations nearer to the Antarctic Peninsula in the
350 Bellingshausen-Amundsen (Fig. 3b, $r=0.620, p<0.01$) and Weddell Seas (Fig. 3c, $r=0.445,$
351 $p<0.01$).

352





354
 355 **Figure 3.** Annual mean sea ice extent timeseries from various reconstructions approximately
 356 related to the Raphael and Hobbs (2014) sea ice boundaries in Fig. 1 for the a) Ross-Amundsen
 357 Seas; b) Bellingshausen-Amundsen Seas; c) Weddell Sea. The Dalaiden et al. (2021) sectors
 358 have been adjusted to the Raphael and Hobbs (2014) boundaries.; paleo-based reconstructions
 359 are given in red and labeled separately for each panel. The correlations with satellite
 360 observations (in black) during the period of overlap are given in the top of each panel, with the
 361 colors denoting the individual timeseries: as given in the legend. At the bottom, correlations
 362 with the Dalaiden et al. (2021) and Fogt et al. (2022a) reconstructions are similarly provided. In
 363 each case, after adjusting the sample size by the lag1 correlation as needed, correlations
 364 significantly different from zero at $p < 0.05$ and $p < 0.01$ are marked with * and **, respectively.
 365

366

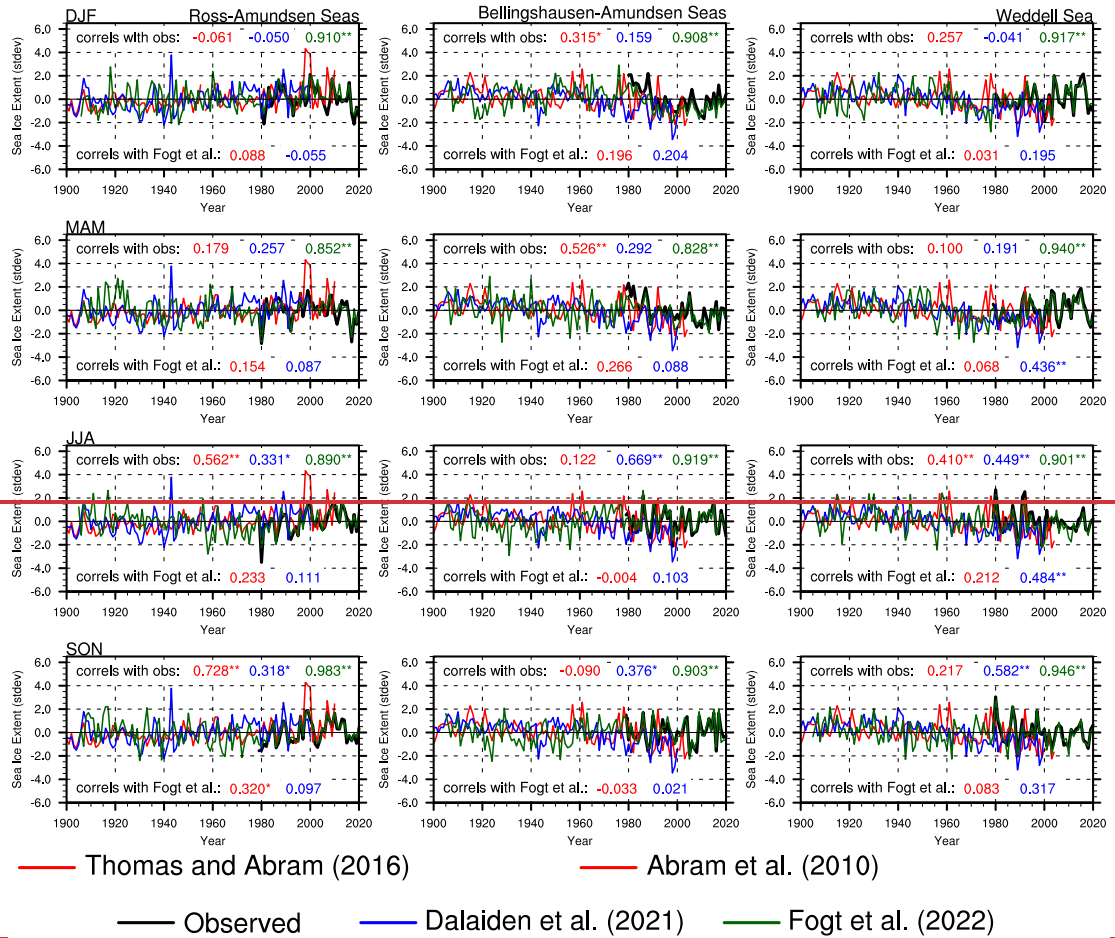
367 In contrast, ~~however,~~ the cross-correlations between the various sea ice extent
368 reconstructions (text at bottom of each panel in Fig. 3) are much weaker overall (numbers at
369 bottom of each plot), often falling below 0.30 (from 1905-2020, $p < 0.05$), ~~suggesting that~~. The
370 weak cross-correlations suggest the interannual variability in the ~~Dalaiden et al.~~
371 ~~(2021)~~ DAL21_ASSIM estimates ~~from a climate model that assimilates paleo data~~ and
372 ~~estimate those~~ from ice cores directly (both ~~Thomas~~ TA16_PALEO and ~~Abram (2016) and~~
373 ~~Abram et al. (2010)~~ AB10_PALEO) differ substantially; ~~part~~. Part of this difference could be
374 from a larger number of ice cores included in the ~~Dalaiden et al. (2021)~~ DAL21_ASSIM
375 reconstruction (~~Fig. 2b~~) than those of ~~Abram et al. (2010) and Thomas and Abram (2016)~~. ~~In,~~
376 smoothing out the ~~Bellingshausen-Amundsen sector~~ non-climatic noise (Fig. 3b), ~~even though the~~
377 ~~Dalaiden et al. (2021) estimate shows a correlation of $r = 0.620$ with observations (blue number,~~
378 ~~top of plot), the correlation of the Fogt et al. (2022a) data with the Dalaiden et al. (2021)~~
379 ~~estimate~~ 2b, Table 1). There is only $r = 0.171$ ($p > 0.05$) during 1905-2000. ~~Since the Fogt et al.~~
380 ~~(2022a) data are strongly correlated $r = 0.933$ ($p < 0.01$) with observations after 1979, the low~~
381 ~~correlations~~ slightly better agreement between these two estimates during 1905-2020 suggests they
382 ~~do not have similar interannual variability prior to 1979, as demonstrated in Fogt et al. (2022a,b).~~
383 ~~Of note, though, are a few cross-correlations that are near the same strength of the paleo-based~~
384 ~~estimates with observations, namely the Abram et al. (2010) correlation with the Dalaiden et al.~~
385 ~~(2021) estimates in the Bellingshausen-Amundsen Sea (Fig. 3b, $r = 0.305$, $p > 0.05$) and the Fogt et~~
386 ~~al. (2022) and Dalaiden et al. (2021) estimates in the Weddell Sea (Fig. the reconstructions in the~~
387 Weddell Sea, particularly for the FOGT_STAT and DAL21_ASSIM estimates (Fig. 3c, $r = 0.532$,
388 $p < 0.01$). ~~Even though there are some agreements, the overall linear trends in the data look~~
389 ~~notably different (to be addressed later), and there are sudden anomalies in each dataset that are~~

390 rarely replicated in others, including for the paleo-based reconstructions in the period of satellite
391 observations.

392 While it is straightforward to plot the timeseries together as in Fig. 3, understanding the
393 differences between them, especially prior to 1979, is much more complex, as the various
394 reconstructions were created inwith markedly distinct and incongruent methods (Table 1) and
395 data (Fig. 2). ~~Further, while they are all representing sea ice extent in some fashion, the~~
396 ~~reconstruction resolutions (Table 1) also indicates they are representing it in many different ways~~
397 ~~as well (some as the ice edge latitude at a specific point, some as an area, and all with different~~
398 ~~First, the various~~ temporal resolutions). ~~One important challenge is that the Fogt et al. (2022a)~~
399 ~~of each reconstruction may result in differences: the FOGT_STAT reconstructions were~~
400 ~~generated based on in Fig. 3 are averages of~~ seasonal ~~statistical relationships, producing~~
401 ~~reconstructions separately for the four meteorological seasons. These seasonal reconstructions~~
402 ~~were averaged together to give the annual mean values in Fig. 3 to compare with all the other~~
403 ~~paleo-based reconstructions that only have annual mean resolution (the exception being the~~
404 ~~MSA-based reconstruction of Abram et al. (2010) is for August-October, Table 1). Nonetheless,~~
405 and even though the paleo-based reconstructions often represent the annual mean, they may be
406 biased slightly to a particular time in the year affected primarily by the accumulation at the ice
407 core site(s) from which the paleo-based reconstructions were generated. To understand if the
408 relationships improve seasonally, Fig. 4 investigates the reconstructions agreement for each
409 sector (by column) and each season (rows).

410 ~~Compared~~In contrast to the annual mean data in Fig. 3, there are frequent negative
411 correlations between the various datasets and the observations (~~again except for the Fogt et al.~~
412 ~~(2022a) reconstructions that were explicitly calibrated to the seasonal observations~~), numbers at

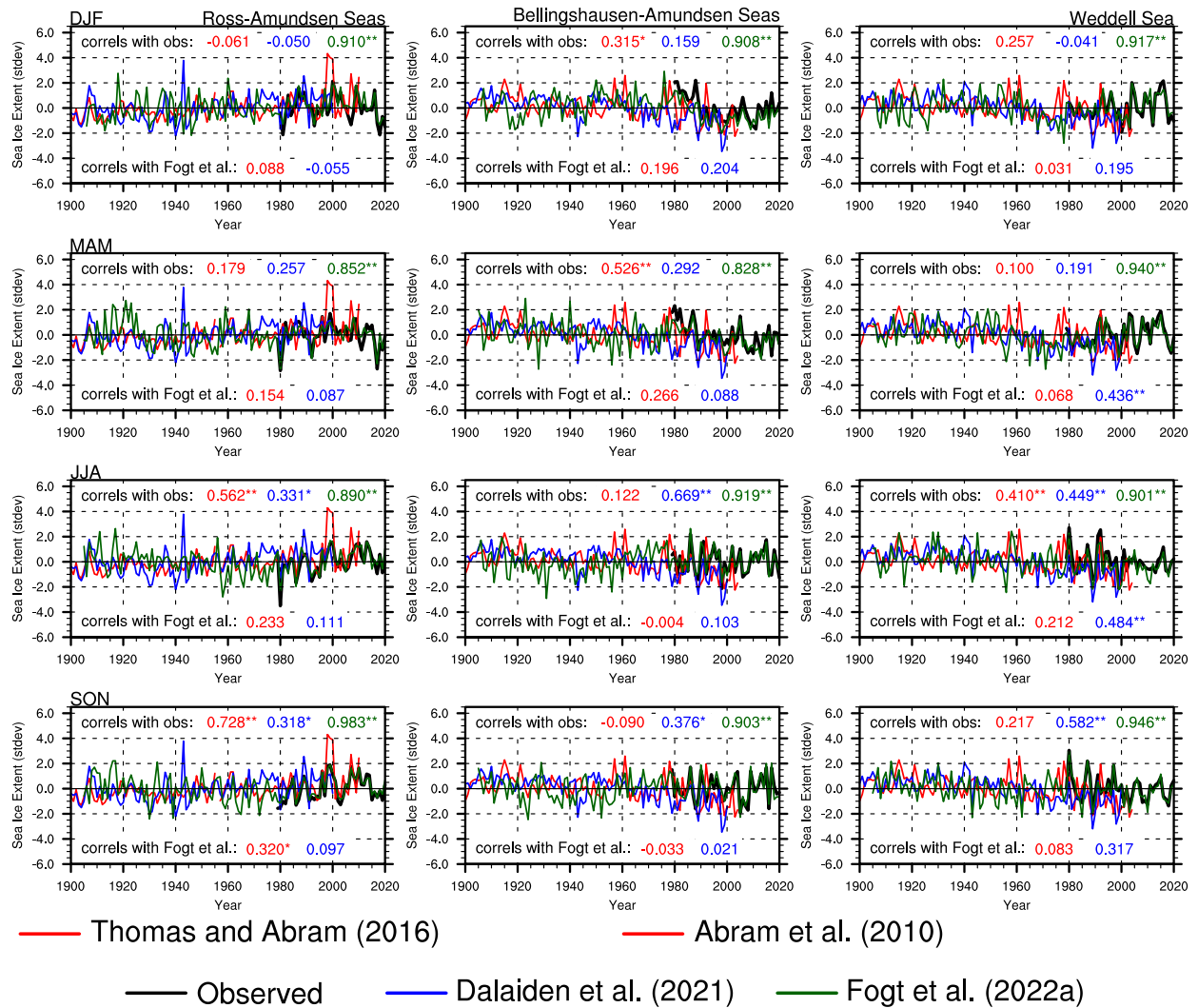
413 the top of each panel in Fig. 4) as well as between the paleo-based reconstructions and those
414 from ~~Fogt et al. (2022a)~~ given by the FOGT_STAT (numbers at the bottom of each panel in Fig.
415 ~~4).~~ For the Ross-Amundsen sector, ~~the Thomas and Abram (2016)~~ TA16_PALEO most closely
416 aligns with the austral winter (JJA) and austral spring (SON) seasons, near the seasonal
417 maximum sea ice extent. ~~The correlations with observations of the Thomas and Abram (2016)~~
418 ~~data exceed 0.56 ($p < 0.01$) in these seasons, higher than the correlation of the annual mean in Fig.~~
419 ~~3 ($r = 0.525$, $p < 0.02$); despite the higher correlations with the observations, the correlations of~~
420 ~~Thomas and Abram (2016) and the seasonal Fogt et al. (2022a) reconstructions however are~~
421 ~~slightly lower than for the annual ($r = 0.345$ for annual, max for SON is $r = 0.320$, both $p < 0.05$).~~
422 ~~As before, this suggests a reduction in the reconstruction cross correlations prior to satellite~~
423 ~~observations (i.e., before 1979). The seasonal relationships of the Abram et al. (2010)~~ The
424 seasonal relationships of the AB10_PALEO reconstruction are a bit more nuanced: it has
425 considerably higher correlations in MAM with observations in the Bellingshausen-Amundsen
426 sector ($r = 0.526$, $p < 0.01$), but the weakest correlations in this season in the Weddell sector
427 ($r = 0.10$, $p > 0.05$).



428

429 For the DAL21_ASSIM reconstruction, the relationships with observations are weakest in austral
 430 summer (Fig. 4, top row) for all sectors, and generally the highest during the second half of the
 431 year (Fig. 4, bottom two rows). Similarly, the correlations between the FOGT_STAT
 432 reconstruction and DAL21_ASSIM are typically highest in JJA.

433



434
 435 **Figure 4.** As in Fig. 3, but with the seasonal mean observations and reconstructions of Fogt et
 436 al. (2022a) with the annual mean paleo-based reconstructions. The Thomas and Abram
 437 (2016) paleo-based reconstruction is used for the Ross-Amundsen sector (left column), while the
 438 Abram et al. (2010) reconstruction is used for the other two sectors: (middle and right columns).
 439 The correlations are color coded following the legend. Correlations with observations are given
 440 at the top of each panel, and correlations with seasonally-varying Fogt et al. (2022a)
 441 reconstructions are given at the bottom of each panel.

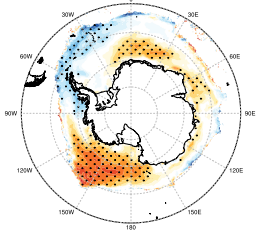
444 For the Dalaiden et al. (2021) estimates of sea ice from the data assimilation-based
 445 reconstruction, the relationships with observations are weakest in austral summer (top row) for
 446 all sectors, and generally the highest in austral winter and spring (bottom two rows).
 447 Interestingly, the correlations between the Fogt et al. (2022a) reconstruction and the estimates

448 ~~from Dalaiden et al. (2021) are in typically highest in JJA, and even exceed the correlations of~~
449 ~~the paleo-based reconstructions with observations in the Weddel sector in this season ($r=0.484$,~~
450 ~~$p<0.01$), suggesting that there is some shared interannual variability in these datasets prior to~~
451 ~~1979 in the winter season.~~

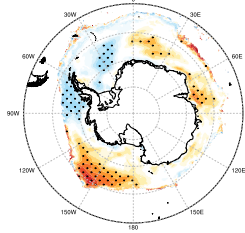
452
453 While the ~~seasonal~~ comparisons in Fig. 4 reveal that ~~better~~the agreement between the
454 various reconstructions is not uniform throughout the year, , the various spatial footprints of the
455 reconstructions can be achieved apart from the annual mean representation, there are other
456 factors that could lead toalso create differences in the reconstruction that would not be captured
457 by individual portions of the seasonal cyclebetween the reconstructions. In particular, while ice
458 core-based reconstructions can provide information directly over the continent on longer
459 timescales, their connections to Antarctic climate are geographically limited (Table 1), restricted
460 to the prominent pathway of tracers from the ocean/ice boundary near the ice edge to their
461 deposition at the ice core site (Thomas et al. 2019). In contrast, both the ~~Fogt et al.~~
462 ~~(2022a)~~FOGT_STAT and ~~Dalaiden et al. (2021)~~DAL21_ASSIM reconstructions represent the
463 cumulative sea ice area >15% in specific geographic boundaries (Figs. 1a and 2a). To
464 investigate the role the various spatial configurations may play in the differences between the
465 reconstructions, each annual mean reconstruction was correlated through time with the full
466 spatial field of annual mean sea ice concentration satellite observations (at each grid point
467 separately); these correlations are plotted in Fig. 5, with correlations statistically different from
468 zero at $p<0.05$ stippled. In Fig. 5, the correlation of the observed sea ice extent series for each
469 sector with the satellite sea ice concentration field is provided in the far left column for
470 comparison of the maximum expected correlation pattern and magnitude.

|471

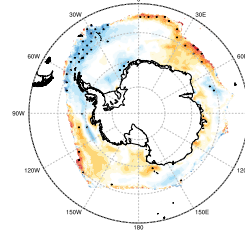
a) Ross-Amundsen Seas
Observed



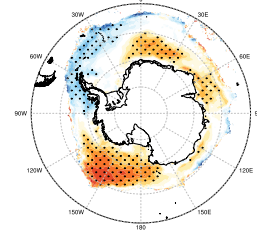
Thomas and Abram (2016)



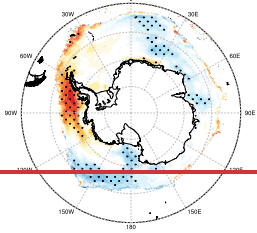
Dalaiden et al. (2021)



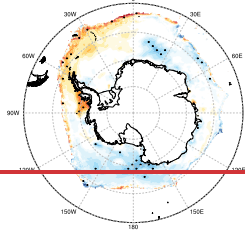
Fogt et al. (2022)



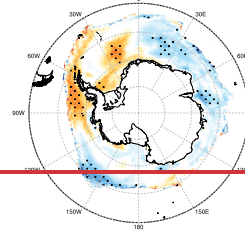
b) Bellingshausen-Amundsen Seas
Observed



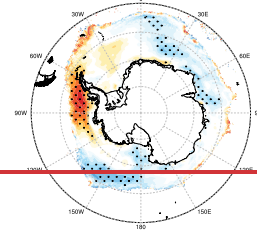
Abram et al. (2010)



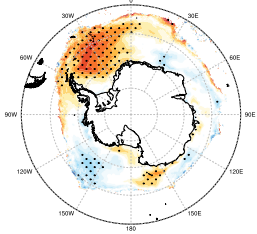
Dalaiden et al. (2021)



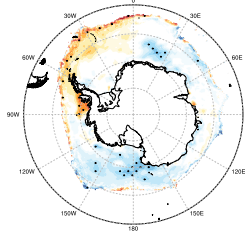
Fogt et al. (2022)



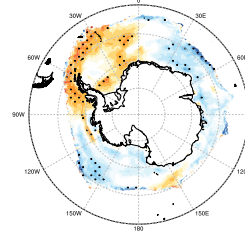
c) Weddell Sea
Observed



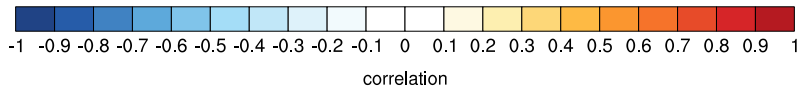
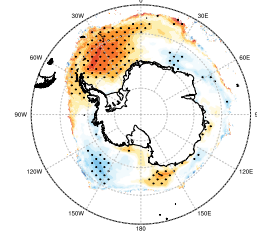
Abram et al. (2010)

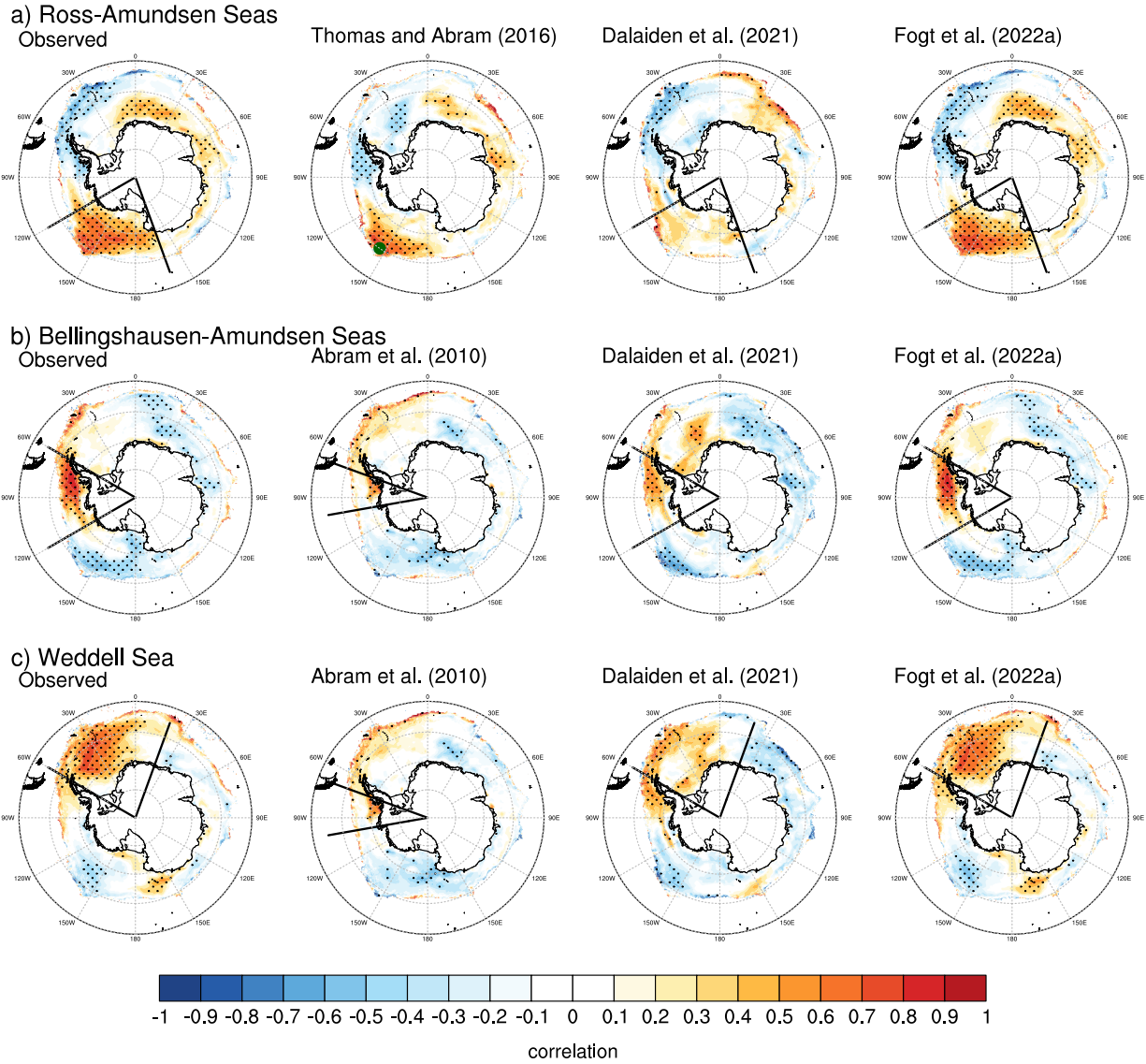


Dalaiden et al. (2021)



Fogt et al. (2022)





473
474
475
476
477
478
479
480
481

Figure 5. Correlations (1979-end of series) of annual mean sea ice extent timeseries with the observed annual mean sea ice concentration field, separated by the Raphael and Hobbs (2014) sectors, as in Fig. 3. The solid lines (or marker for Thomas and Abram (2016) represent the longitudinal boundaries of the observations or reconstructions for each sector (Table 1). In each row, correlations of the observed sea ice extent time series with the sea ice concentration are given for reference. a) Ross-Amundsen Seas; b) ~~Belingshausen~~Bellingshausen-Amundsen Seas; c) Weddell Sea.

482
483
484

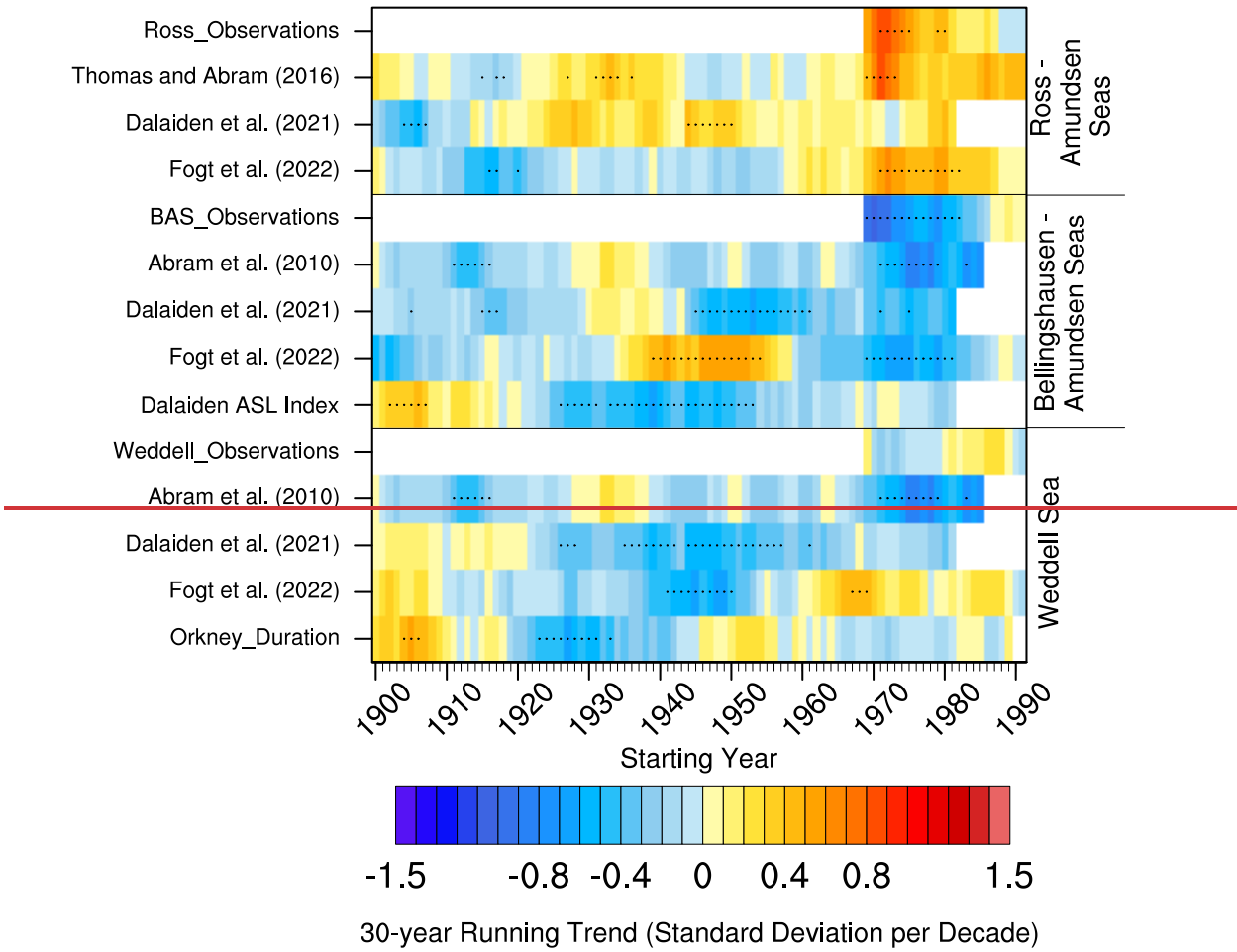
In the Ross-Amundsen sector (Fig. 5, top row), the ThomasTA16_PALEO and Abram (2016) and Fogt et al. (2022a)FOGT_STAT reconstructions represent the observed pattern well, although as expected the region of positive correlations with the Thomas and Abram

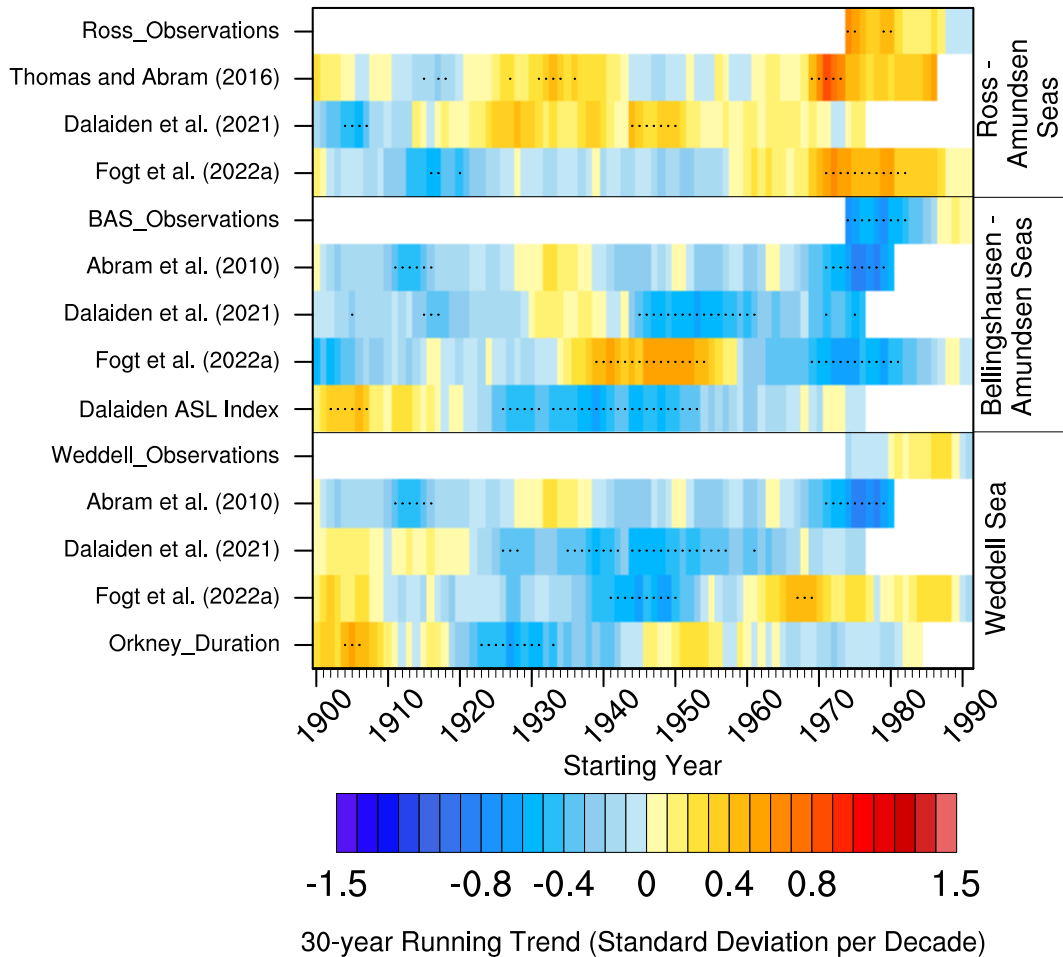
485 ~~(2016)~~TA16_PALEO is smaller and confined closer to the ice edge – their reconstruction is an
486 estimate of the ice edge at a point in the Ross Sea (Fig. 1, Table 1). While the ~~Dalaiden et al.~~
487 ~~(2021)~~DAL21_ASSIM spatial correlation field is notably weaker, it is important to remember
488 that unlike the other sea ice extent estimates examined here, this reconstruction was not
489 calibrated ~~in any way to sea ice, and was only extracted from the climate model simulations~~
490 ~~constrained by paleo data to sea ice observations.~~ Nonetheless, it still maintains a similar spatial
491 pattern of positive and negative correlations to the other datasets, suggesting that its geographic
492 representation is broadly similar to other datasets.

493 The ~~Abram et al. (2010)~~AB10_PALEO reconstruction shows a much weaker pattern of
494 correlations than the other estimates in the Bellingshausen-Amundsen and Weddell sectors
495 (middle and bottom rows of Fig. 5), while the ~~Dalaiden et al. (2021)~~DAL21_ASSIM estimates
496 align much better with observations in these sectors. The ~~Abram et al. (2010)~~AB10_PALEO
497 relationships with the sea ice concentrations only modestly improves seasonally (not shown).
498 Together, this suggests that the spatial (and to a lesser extent, seasonal) limitation of the ice
499 conditions represented by the ~~Abram et al. (2010)~~AB10_PALEO reconstruction is an important
500 contributing factor of its differences with the other sea ice extent estimates examined here. From
501 Fig. 5, the ~~Abram et al. (2010)~~AB10_PALEO reconstruction has significant correlations at the
502 far equatorward sea ice edge, stretching from the Bellingshausen Sea eastward across the
503 Antarctic Peninsula to the Weddell Sea, different ~~than~~from the 70°W-100°W region originally
504 suggested. This different spatial relationship in the annual mean (compared to the originally
505 published August – October) also explains why it has correlations with sea ice observations from
506 both the Bellingshausen-Amundsen and Weddell sectors (Figs. 3-4), albeit much weaker than
507 other reconstructions. This spatial relationship is to be expected as it is only based on three

508 Antarctic Peninsula ice cores (Table 1), compared to the array of ice cores used in
509 DAL21 ASSIM (Fig. 2b)

510 The timeseries in Figs. 3-4 suggest that while there are notable differences in the interannual
511 variability in the various reconstructions, there are also differences in longer-term changes and
512 especially the trends through time. Figure 6 investigates these discrepancies through the use of
513 30-year running trends, similar to that done in Fogt et al. (2022b), but including the Weddell
514 sector and other data sources.





516

517 **Figure 6.** 30-year running trends (standard deviations per decade) of the annual mean sea ice
 518 extent timeseries in Fig. 3. Individual 30-year trends that are statistically different from zero at
 519 $p < 0.05$ are stippled. For the Weddell Sea, the fast ice duration at the Orkney islands from
 520 Murphy et al. (1995) is also provided. For the Bellingshausen-Amundsen Sea region, the ASL
 521 index from Dalaiden et al. (2021), defined as the annual mean 500 hPa geopotential ~~height~~
 522 from 60°-75°S, 170°E – 70°W, is also shown. Trends are only calculated if 25 years or more
 523 are available in each 30-year window.

524

525 One clear pattern in the satellite-observed trends discussed in the introduction and shown in
 526 Fig. 1a is the opposing nature of positive sea ice extent trends (equatorward movement of the ice
 527 edge) in the Ross Sea and negative sea ice extent trends in the Bellingshausen-Amundsen sector
 528 (Fig. 6). ~~As suggested in Fogt et al. (2022a) in their investigation of the total Antarctic sea ice~~
 529 ~~extent trends and evident in Fig. 6, these~~ These trends reverse and weaken after the 2016 sudden

530 decline, (Fig. 6; Fogt et al. 2022a), but still demonstrate opposite behavior, strongly tied to the
531 atmospheric circulation around the Amundsen Sea low (Hosking et al., 2013; Raphael et al.,
532 2016; Holland and Kwok, 2012). (Hosking et al., 2013; Raphael et al., 2016; Holland and Kwok,
533 2012). While the various reconstructions capture the observed trends (including their statistical
534 significance), there are marked differences in the signs of the trends prior to the satellite
535 observations around 1979. In particular, paleo-based sea ice extent estimates generally
536 ~~display indicate~~ that the observed trends are part of a long-term continuous trend of the same sign
537 throughout much of the 20th century ~~(i.e., that there are increases in the Ross Sea sector and~~
538 ~~decreases in the Bellingshausen Sea region throughout the 20th century);~~; this story is also
539 consistent in the Weddell sector, as the paleo-based reconstructions only show statistically
540 significant trends prior to 1979 that are the same sign as the observed trends after 1979. In
541 contrast, the Fogt et al. (2022a) FOGT_STAT reconstructions show a pronounced shift in the
542 trend sign and magnitude through time. The Fogt et al. (2022a) FOGT_STAT sea ice
543 reconstruction trends are characterized with statistically significant positive trends in the middle
544 20th century in the Bellingshausen-Amundsen sector (opposite the decreases after 1979 there),
545 and statistically significant negative trends in the Ross Sea in the early 20th century, with a
546 prolonged period of weaker negative trends throughout the 20th century, opposite to the strong
547 positive trends in the satellite observations starting in 1979 (Fig. 6). In the Weddell sector,
548 where there is a better agreement between the Fogt et al. (2022a) FOGT_STAT and Dalaiden et
549 al. (2021) DAL21_ASSIM estimates (Figs. 3-5), the trends align better through time. Moreover,
550 these trends and their temporal changes in both significance and sign are broadly aligned with
551 the South Orkney fast ice duration dataset of Murphy et al. (1995); Murphy et al. (1995), with

552 positive trends in the first portion of the 20th century that change to negative trends through much
553 of the middle 20th century, to weak trends during the satellite observation period.

554 While the seasonal and spatial differences between the various reconstructions evaluated in
555 Figs. 2-35 undoubtedly play a role (especially for the ~~Abram et al. (2010)AB10_PALEO~~
556 reconstruction), Fig. 56 suggests that changes in the underlying implied atmospheric circulation
557 are also playing a role. In observations (Fig. 1a), the differing sea ice extent trends in the
558 Bellingshausen and Ross Seas are largely tied to the atmospheric circulation around the
559 Amundsen Sea low and implied sea ice drift changes (~~Holland and Kwok, 2012; Holland,~~
560 ~~2014).~~(Holland and Kwok, 2012; Holland, 2014). Although there are no long-term direct
561 observations, the ASL index extracted from the pressure field in ~~the proxy-based~~DAL21_ASSIM
562 reconstructions ~~of Dalaiden et al. (2021) show~~shows changes through time that are nearly
563 opposite the ~~Fogt et al. (2022a)FOGT_STAT~~ reconstructions for the Bellingshausen-Amundsen
564 sector ~~in the early and middle 20th centuries~~, potentially confirming that underlying atmospheric
565 circulation changes are a dominant contribution to the different sea ice changes.

566 While reconstruction uncertainty will always play a role in differences between various
567 historical estimates, the comparisons of the various sea ice reconstructions thus far suggest that:
568 a) the ~~Abram et al. (2010)AB10_PALEO~~ is primarily different from other reconstructions
569 because of its different spatial footprint; b) the methodology used to create the reconstructions or
570 their temporal resolution does not play a consistent role, as correlations between the proxy-based
571 reconstructions as well as with the station-based reconstructions vary considerably; c) the
572 atmospheric circulation associated with the sea ice reconstructions appears to be a dominant
573 mechanism for differences between them. To investigate this further, the role of implied changes

574 in the atmospheric circulation underlying the proxy-based and station-based reconstructions is
575 therefore the focus for the remainder of this paper.

576 3.2) *Connection to the atmospheric circulation changes and comparison of Antarctic sea level*
577 *pressure reconstructions*

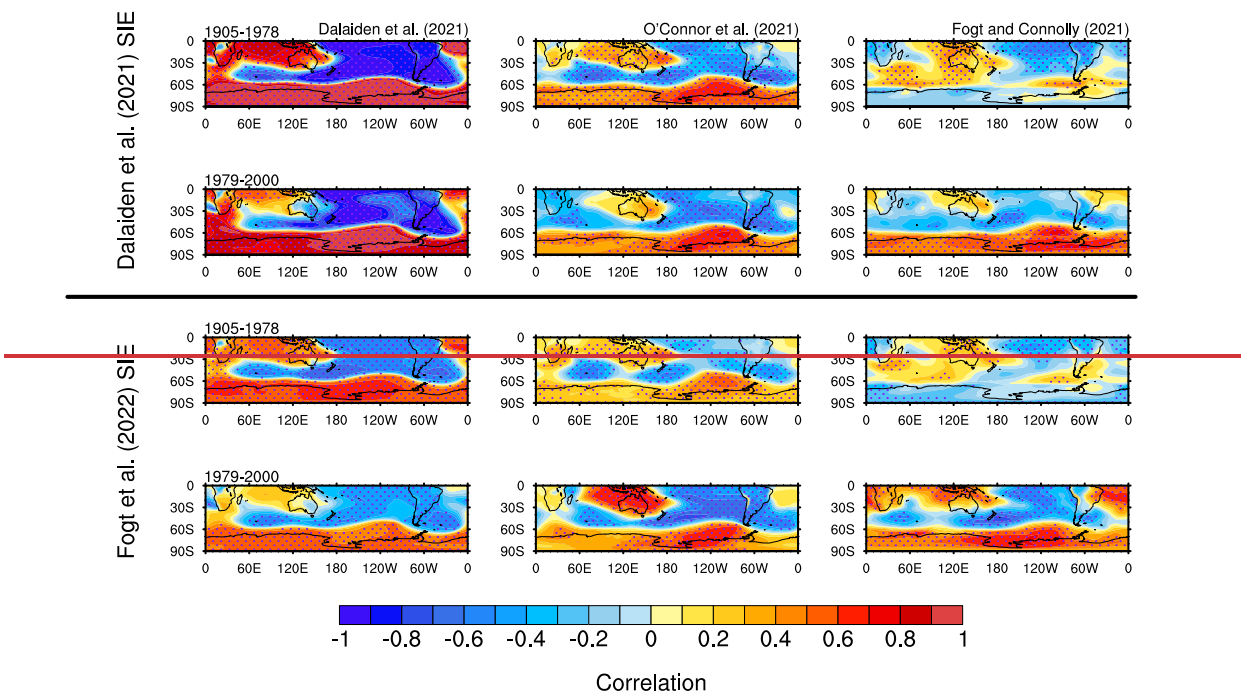
578 ~~Since 20th-century atmospheric reanalyses have been shown to have long-term artificial~~
579 ~~pressure trends throughout the early and middle 20th-century (Schneider and Fogt, 2018; Fogt et~~
580 ~~al., 2020), our analysis of the relationship between sea ice extent and the atmospheric circulation~~
581 ~~is focused on other estimates of pressure. In particular, for consistency we employ estimates of~~
582 ~~pressure from reconstructions generated using proxy data assimilation with various climate~~
583 ~~model priors and proxy datasets, including the Dalaiden et al. (2021) and O'Connor et al.~~
584 ~~(2021,2023) datasets (Table 1). For a station-based estimate, we also investigate the Fogt and~~
585 ~~Connolly (2021) dataset, which is a blend interpolated seasonal Antarctic station pressure~~
586 ~~reconstructions south of 60°S (Fogt et al., 2019, 2017), and the NOAA 20th-century reanalysis~~
587 ~~version 3 equatorward of 60°S (Table 1). Since the Antarctic station pressure reconstructions~~
588 ~~were generated using a similar statistical technique as the Fogt et al. (2022a) sea ice extent~~
589 ~~reconstructions, this allows for an evaluation of other estimates that are expected to provide~~
590 ~~similar temporal variability as the Fogt et al. (2022a) sea ice extent reconstructions.~~

591 Since 20th century atmospheric reanalyses have been shown to have long-term artificial
592 pressure trends throughout the early and middle 20th century (Schneider and Fogt, 2018; Fogt et
593 al., 2020), our analysis of the relationship between sea ice extent and the atmospheric circulation
594 is focused on other estimates. In particular, we examine pressure reconstructions generated
595 using proxy data assimilation with various climate model priors and proxy datasets, including the

596 DAL21_ASSIM and O'Connor et al. (2021, 2023) datasets (Table 1), as well as a station-based
597 estimate, FC21_STAT,

598 Figure 7 displays the correlations for the Weddell sector sea ice extent from ~~Dalaiden et al.~~
599 ~~(2021) with the (top rows) DAL21_ASSIM and (bottom rows) FOGT_STAT with three~~ gridded
600 pressure datasets ~~in the top rows, and the Weddell sector sea ice extent reconstructions from Fogt~~
601 ~~et al. (2022a) with the same gridded datasets in the bottom rows.~~ The gridded pressure datasets
602 are grouped by columns, and further broken into the pre-satellite sea ice observation period of
603 1905-1978 (top rows of each section) and satellite-era sea ice observation period (1979-2000).
604 Overall the patterns are quite similar in each of the panels, reflecting the broad similarities of the
605 sea ice reconstructions in the Weddell sector (Figs. 3-5). Here, the sea ice extent reconstructions
606 show a strong positive correlation with pressure over the Antarctic continent that changes to
607 negative correlations with pressure in the Pacific Ocean from the midlatitudes and equatorward,
608 including South America. For both the ~~Dalaiden et al. (2021)~~ DAL21_ASSIM and ~~O'Connor et~~
609 ~~al. (2021)~~ OCON21_ASSIM pressure datasets, regardless of the sea ice extent estimate (top or
610 bottom half of Fig. 7), these relationships exist in a similar fashion throughout time, suggesting

Weddell Sea SIE Extent and Pressure Correlations



Weddell Sea SIE Extent and Pressure Correlations

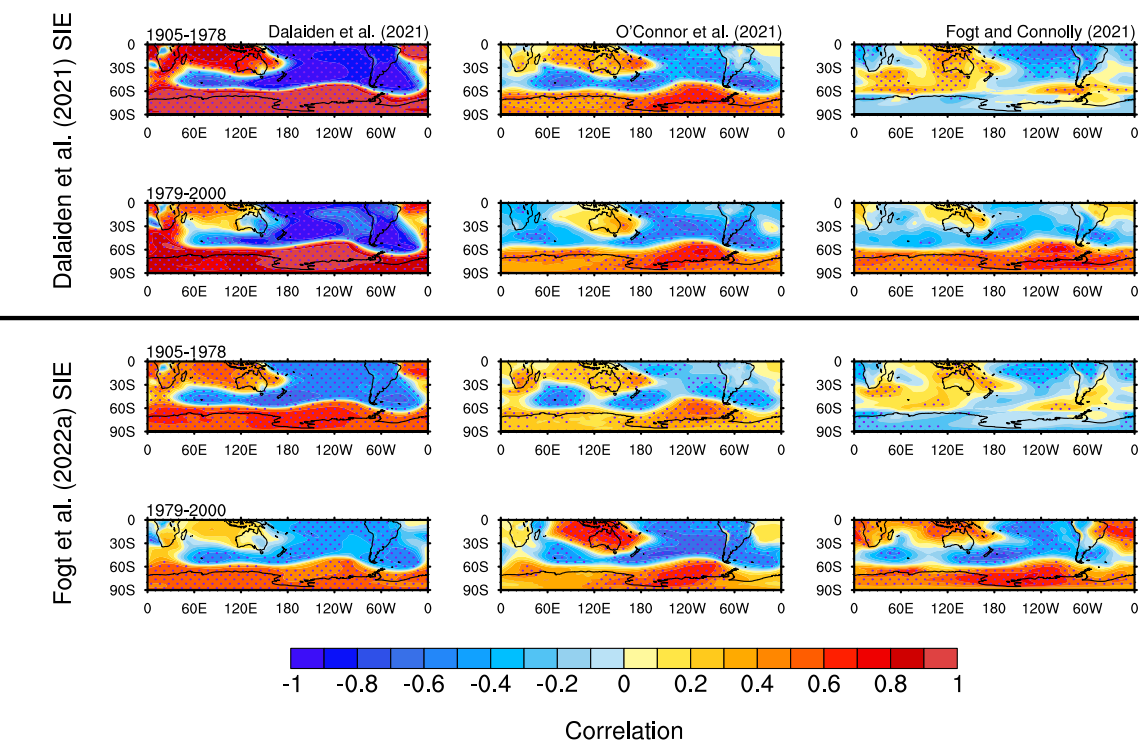


Figure 7. Annual mean correlations of (top half) Dalaiden et al. (2021) and (bottom half) Fogt et al. (2022a) sea ice extent correlations for the Weddell Sea with three 20th century spatially complete pressure reconstructions (columns). In each half, the top row are for correlations in the

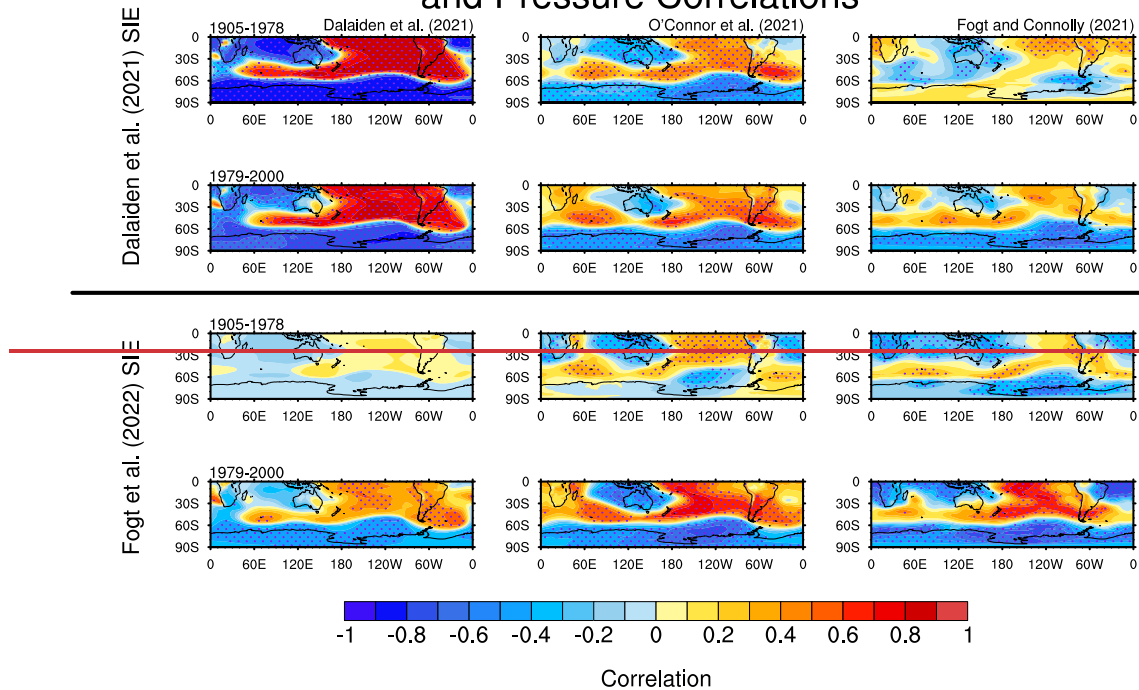
616 pre-satellite period, 1905-1978, and the bottom are for 1979-2000. The pressure reconstructions
617 are (left column) Dalaiden et al. (2021), (middle column) O'Connor et al. (2021), and (right
618 column) Fogt and Connolly (2021). Correlations statistically different from zero at $p < 0.05$ are
619 stippled.

620
621 the Weddell sea ice maintains a similar relationship with pressure across the entire Southern
622 Hemisphere from data assimilation-based products ~~with a fixed prior.~~ However, ~~when~~
623 ~~comparing with~~ for the ~~Fogt and Connolly (2021) FC21_STAT~~ pressure dataset, the relationship
624 ~~between~~ with Weddell sea ice extent, regardless of the sea ice extent estimate (~~Dalaiden et al.~~
625 ~~(2021) DAL21_ASSIM~~ or ~~Fogt et al. (2022a) FOGT_STAT~~) shows a change in ~~the relationship~~
626 ~~over Antarctica, flipping to a weakly negative (generally not statistically significant)~~
627 ~~correlation~~ sign poleward of 60°S in the 1905-1978 (right column in Fig. 7). While the trends in
628 the Weddell sea ice extent change less dramatically through time than in the Ross, Amundsen,
629 and Bellingshausen sectors (Fig. 6), there are still changes in the sea ice extent trends in the
630 Weddell sector in the ~~Fogt et al. (2022a) FOGT_STAT~~ reconstruction, with perhaps too strongly
631 positive sea ice extent trends at the end of the 20th century (compared to observations) juxtaposed
632 by negative sea ice extent trends in the middle twentieth century (Fig. 6). If the statistical
633 relationship between the atmospheric circulation and sea ice extent changed in time (Fig. 7, right
634 column), this could be linked (at least statistically, and perhaps incorrectly) to the changes in the
635 sea ice extent trends displayed in the ~~Fogt et al. (2022a) sea ice extent FOGT_STAT~~
636 reconstructions, but not in the paleo-reconstructions (Fig. 6).

637 Interestingly, when examining the correlation of sea ice extent reconstructions in the Ross-
638 Amundsen sector ~~with (Fig. 8), this sea ice-pressure relationship across~~ the various ~~gridded~~
639 ~~historical pressure~~ datasets (Fig. 8), ~~this pattern is not fully maintained, and there are more~~
640 ~~differences in the spatial correlation patterns not only between the two sea ice extent estimates,~~

641 ~~but also dependent on the various~~ apparent for the DAL21_ASSIM pressure ~~datasets (columns in~~
642 ~~Fig. 8)-dataset~~. For the ~~Dalaiden et al. (2021)~~DAL21_ASSIM sea ice extent estimate (Fig. 8, left
643 column), the pressure relationships are maintained throughout time, and are even stronger in the
644 1905-1978 period for the ~~Dalaiden et al. (2021)~~DAL21_ASSIM pressure estimate. As in the
645 Weddell sector, the correlation pattern of the ~~Dalaiden et al. (2021)~~DAL21_ASSIM sea ice
646 extent estimate with the ~~the Fogt and Connolly (2021)~~FC21_STAT pressure dataset in the Ross-
647 Amundsen sector again changes through time poleward of 60°S over the Antarctic continent,
648 from overall weakly positive and insignificant correlations from 1905-1978 to statistically
649 significant ($p < 0.05$) negative correlations after 1979 (Fig. 8, top two rows of rightmost column).
650 A notable exception however is off the coast of West Antarctica, in the vicinity of the Amundsen
651 Sea low, where correlations remain significantly ($p < 0.05$) negative throughout time, highlighting
652 the key role of this feature for regional sea ice variability (~~Hosking et al., 2013; Raphael et al.,~~
653 ~~2016~~).
654

Ross - Amundsen Sea SIE Extent and Pressure Correlations



655 _____
 656 ([Hosking et al., 2013](#); [Raphael et al., 2016](#)). However, for the `FOGT_STAT` ~~Figure 8. As in Fig.~~
 657 ~~7, but for the sea ice extent reconstructions for the Ross Amundsen Seas sector.~~
 658

659 ~~For the [Fogt et al. \(2022a\)](#) sea ice extent reconstructions (bottom two rows in Fig. 8), a~~
 660 different story emerges. The correlations, while of a generally similar sign, are weaker for all
 661 pressure datasets (columns in Fig. 8) in the 1905-1978 period compared to the 1979-2000 period.
 662 In particular, the statistically significant ($p < 0.05$) negative correlations within the region of the
 663 Amundsen Sea low are maintained throughout time, especially in the [Fogt and Connolly](#)
 664 ~~(2021)~~`FC21_STAT` pressure dataset (Fig. 8, right column, bottom two rows); these are reduced
 665 however when using the [Dalaiden et al. \(2021\)](#)`DAL21_ASSIM` pressure dataset with the [Fogt et](#)
 666 ~~al. (2022a)~~`FOGT_STAT` sea ice extent reconstruction (Fig. 8, left column, bottom two rows).
 667
 668

Ross - Amundsen Sea SIE Extent and Pressure Correlations

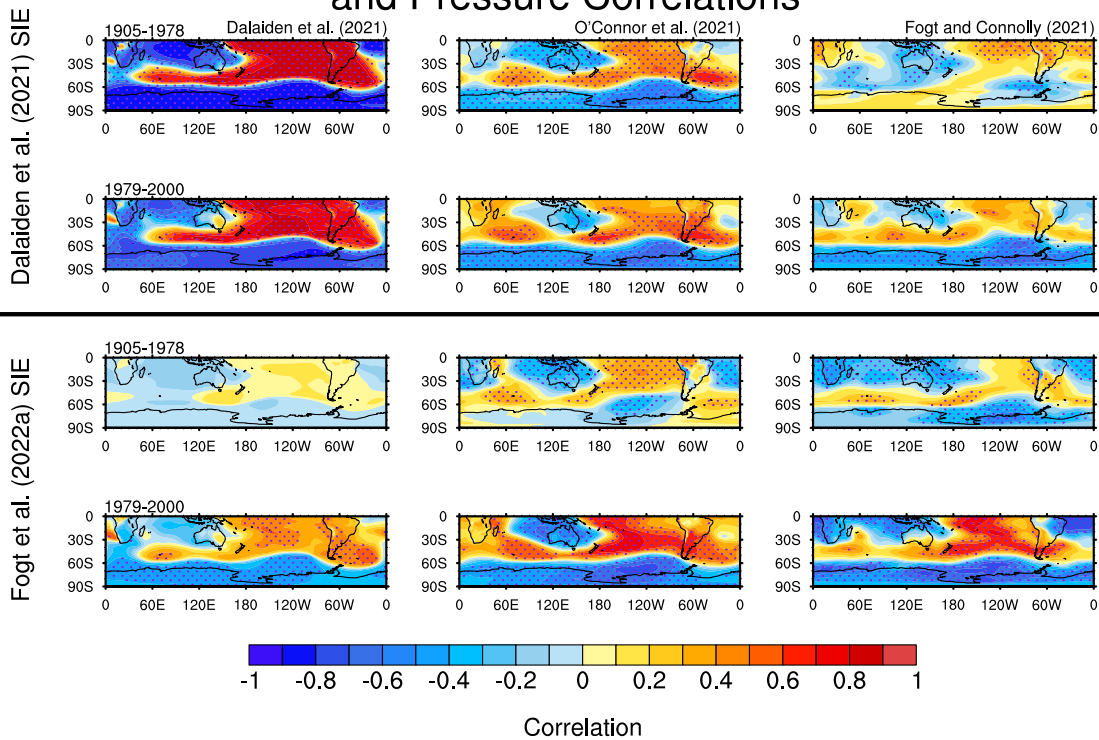


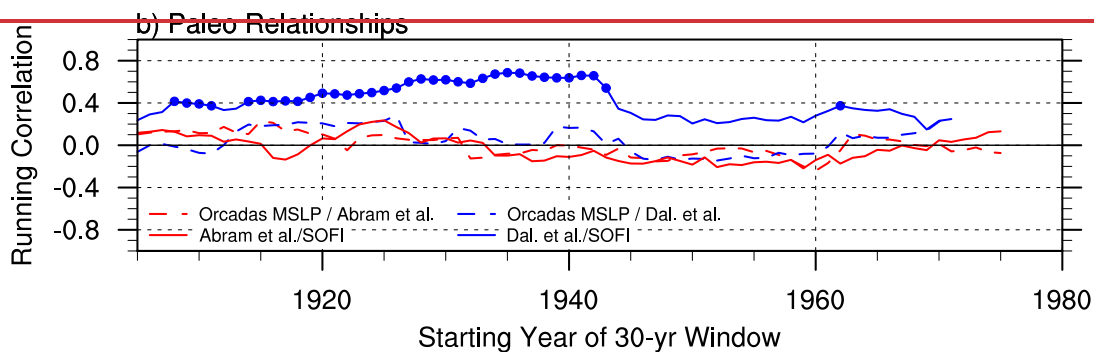
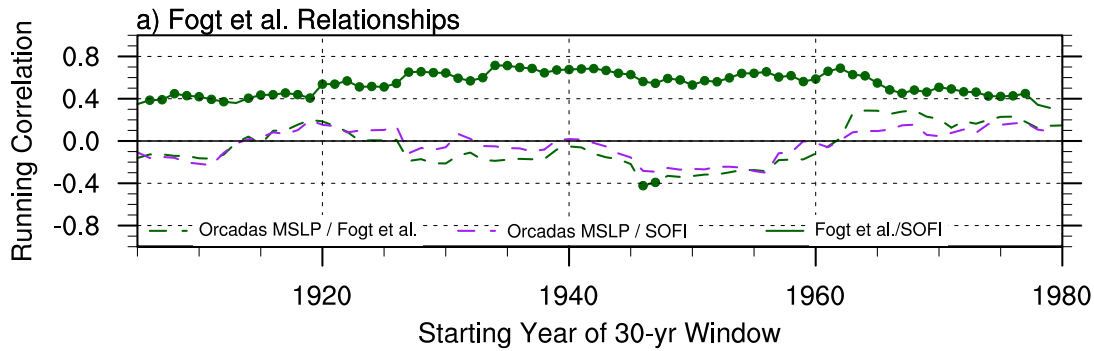
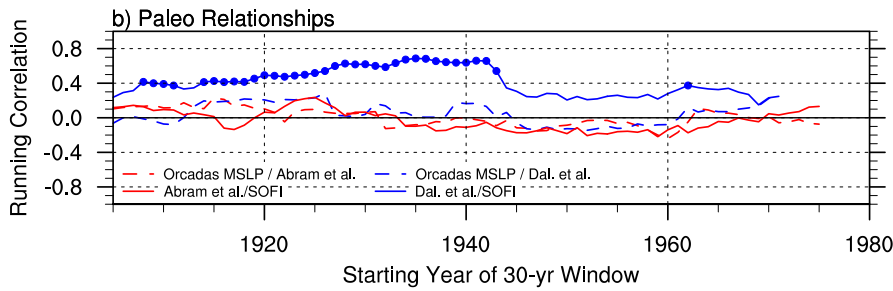
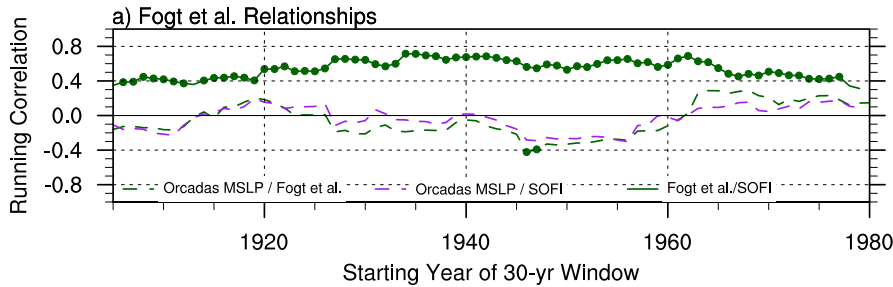
Figure 8. As in Fig. 7, but for the sea ice extent reconstructions for the Ross-Amundsen Seas sector.

Are changes in time of the sea ice – pressure relationship in time in the Weddell sector from Fig. 7 a real feature, or is this an artifact of the reconstructions (sea ice extent, pressure, or both) generated by their limitations? While there are no direct spatially complete observations of sea ice or pressure throughout the full 20th century, the Weddell sector is one of the few places with longer historical observations of both pressure ~~and sea ice conditions, afforded by the observations collected at Orcadas station (60.7°S, 44.7°W) since 1903 (Zazulie et al., 2010), and the fast ice duration series around this island from Murphy et al., afforded by the observations collected at Orcadas station (60.7°S, 44.7°W) since 1903 (Zazulie et al., 2010), and sea ice conditions, represented by the fast-ice duration series around Orcadas from Murphy et al. (1995).~~

The running correlations of these key observations with sea ice estimates are provided in Fig. 9 as the only observation-based investigation into the possible reality of a time-varying sea ice /

684 pressure relationship within the Weddell ~~sea~~Sea. In Fig. 9a, the annual mean ~~Fogt et al.~~
685 ~~(2022a)~~FOGT_STAT Weddell sea ice extent reconstruction maintains a statistically significant
686 ($p < 0.05$) positive relationship throughout time with the South Orkney fast ice (SOFI) record
687 (solid lines, Fig. 9a). ~~Given this, it is not surprising then that both the relationship between the~~
688 ~~Fogt et al. (2022a) Weddell sea ice extent reconstruction and the~~Although usually not
689 statistically significant, both FOGT_STAT SOFI duration similarly change sign through time
690 with the pressure at Orcadas station (dashed lines in Fig. 9a), ~~potentially confirming~~which is
691 consistent with the ~~spatial~~Weddell SIE-gridded pressure correlation change through time
692 presented in the right column of Fig. 7. While the Weddell sea ice extent estimate from ~~Dalaiden~~
693 ~~et al. (2021)~~DAL21_ASSIM also is positively correlated through time with the SOFI duration
694 (solid blue line, Fig. 9b, albeit only significant [$p < 0.05$] for 30-year windows ~~starting prior to~~
695 ~~1945~~in the early 20th century), the Orcadas observed pressure and Weddell sea ice extent
696 estimate from ~~Dalaiden et al. (2021)~~ are ~~weakly correlated ($p > 0.05$), near zero through time~~
697 ~~(although still with some deviation in sign, but not~~DAL21_ASSIM have no statistically
698 ~~meaningful)~~significant correlations. There is therefore ~~much~~ stronger support ~~offor~~ changes in
699 the relationship of high latitude pressure and Weddell sea ice from the statistically-generated sea
700 ice and pressure reconstructions than there is from the paleo-based reconstructions, consistent
701 with Fig. 7.

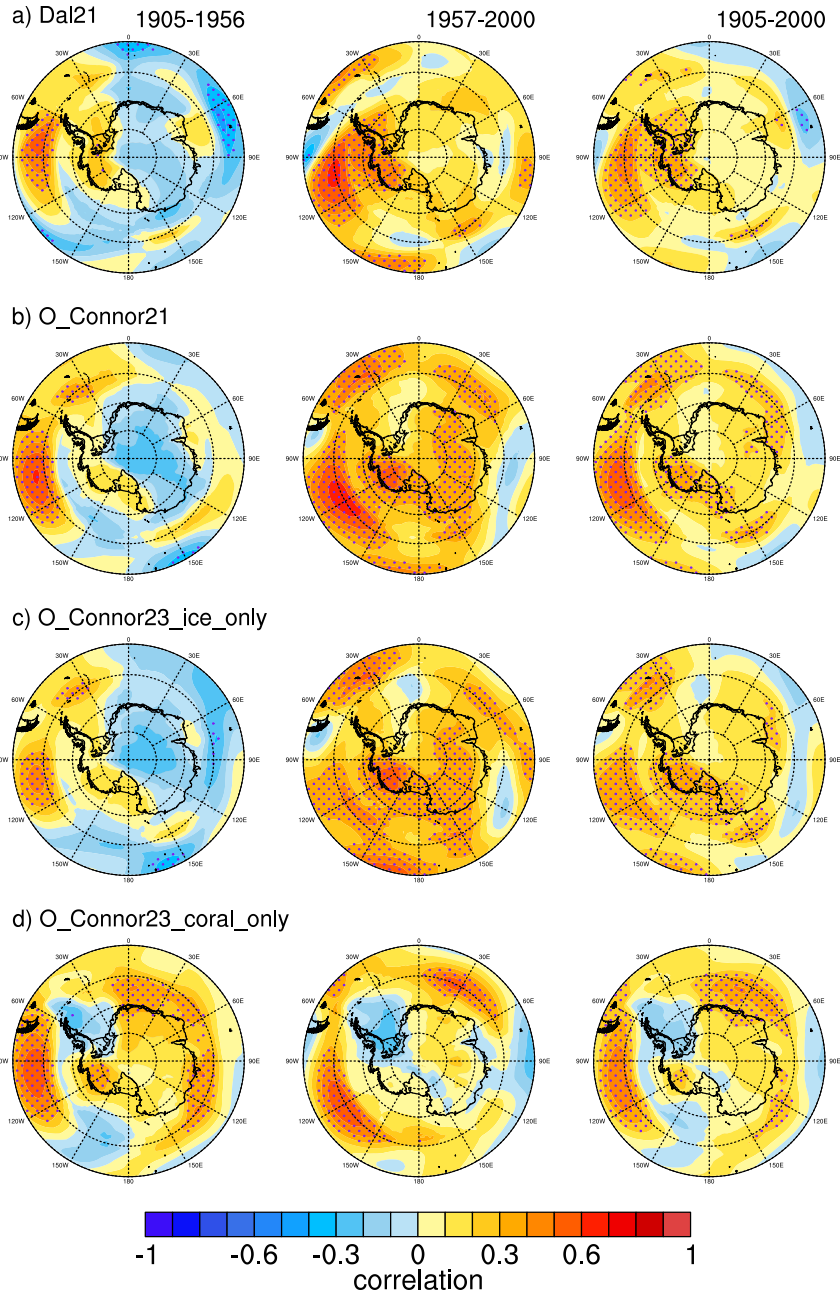
702

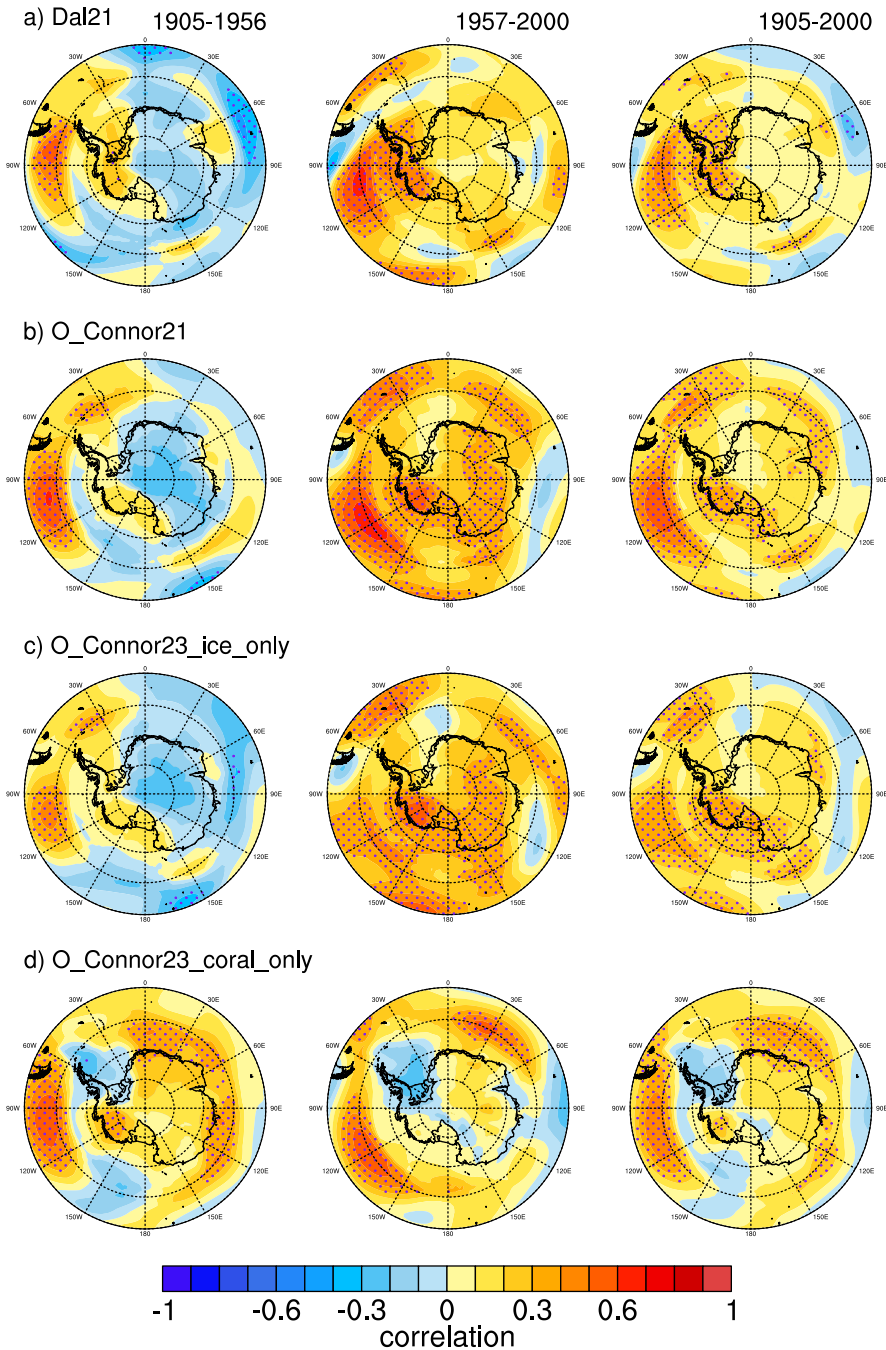


703
 704 **Figure 9.** 30-year running correlations between pairs of the South Orkney Fast Ice (SOFI)
 705 duration from Murphy et al. (1995, 2014), various sea ice extent estimates, or Orcadas station
 706 mean sea level pressure. Correlations significantly different from zero at $p < 0.05$ are marked
 707 with a circle.

708
 709
 710 3.3) Differences in atmospheric pressure reconstructions

711 The connections of the various sea ice reconstructions with the atmospheric circulation in
712 Figs. 7-9 suggest, just like with the sea ice, that there are also differences in the underlying
713 atmospheric circulation from the ~~Fogt and Connolly (2021)~~FC21_STAT dataset and the
714 ~~Dalaiden et al. (2021) and O'Connor et al. (2021)~~DAL21_ASSIM and OCON21_ASSIM proxy-
715 data assimilation datasets. While some of these differences were discussed in O'Connor et al.
716 (2021), it is not clear how they may impact sea ice changes through time. To understand these
717 differences better and the role they may play in the differences in the sea ice reconstructions,
718 correlations between the various annual mean gridded pressure datasets ~~are provided in Fig. 10.~~
719 ~~To help pinpoint the sensitivity of the correlations to the paleo data assimilated into the climate~~
720 ~~model, the O'Connor et al. (2021) pressure reconstruction was expanded by separately~~
721 ~~examining reconstructions assimilating ice core and coral data only from O'Connor et al. (2023).~~
722 ~~We examine these separately to better isolate them~~ Table 1 are provided in Fig. 10.
723





725 **Figure 10.** Correlations of annual mean pressure at each grid point between the various paleo-
 726 based reconstructions with the Fogt and Connolly (2021) reconstruction. a) Dalaiden et al.
 727 (2021); b) O'Connor et al. (2021); c) O'Connor et al. (2023) ice core-based proxies only; d)
 728 O'Connor et al. (2023) coral-based proxies only. The columns denote three time periods: 1905-
 729 1956 (left column, prior to Antarctic data), 1957-2000 (middle column), and the full period of
 730 overlap 1905-2000 (right column). Correlations statistically different from zero at $p < 0.05$ are
 731 stippled. All datasets were linearly detrended over the specific time period prior to calculating
 732 the correlations; further details on each dataset is provided in Table 1 and the proxy locations are
 733 given in Fig. 2.

734 ~~role~~ Prior to the start of tropical paleo data constraints (from corals) and those primarily from
735 Antarctica (from ice cores, Fig. 2e) on the comparison of these most Antarctic pressure
736 reconstructions with the Fogt and Connolly (2021) data. In observations, during the 1905-1956
737 time period (left column, Fig. 10), there are similar correlation patterns between for the
738 DAL21_ASSIM, OCON21_ASSIM, and the Dalaiden et al. (2021), O'Connor et al. (2021), and
739 the O'Connor et al. (2023) OCON23_ASSIM (ice core only) datasets, suggesting that the ice
740 core data provide a strong constraint to the pressure variability in the paleo-based assimilation
741 reconstructions near Antarctica, and that the inclusion of external forcing in the data assimilation
742 prior (for the O'Connor et al. (2021, 2023) reconstructions) has minimal influence. Meanwhile,
743 there are positive and even statistically significant ($p < 0.05$) correlations between the O'Connor
744 et al. (2023) OCON23_ASSIM (coral only) and Fogt and Connolly (2021) FC21_STAT datasets
745 (Fig. 10d, left column) in the early period. This suggests that tropical teleconnections, captured
746 by the coral paleo data, play an important role in the interannual variability in the Fogt and
747 Connolly (2021) dataset. Given that the predictor data for the Fogt and Connolly (2021) dataset
748 is confined to the Southern Hemisphere landmasses large distances away from Antarctica, it is
749 not surprising that there is better agreement with the coral-only dataset of O'Connor et al. (2023)
750 and Fogt and Connolly (2021) pressure dataset over Antarctica. However, given the different
751 pattern with the paleo-based datasets (left column, Fig. 10a-c), it is also clear that the local ice
752 core variability over Antarctica is opposite that of the coral-based tropical variability (especially
753 over East Antarctica, where tropical teleconnections to Antarctica are generally weaker; Li et al.,
754 2021), with the former dominating the overall reconstruction for the paleo-based datasets.
755 Notably, during 1957-2000 the agreement improves from 1905-1956 for the full reconstructions
756 (Fig. 10a-b, middle column, especially for the O'Connor et al. reconstructions) as well as the ice

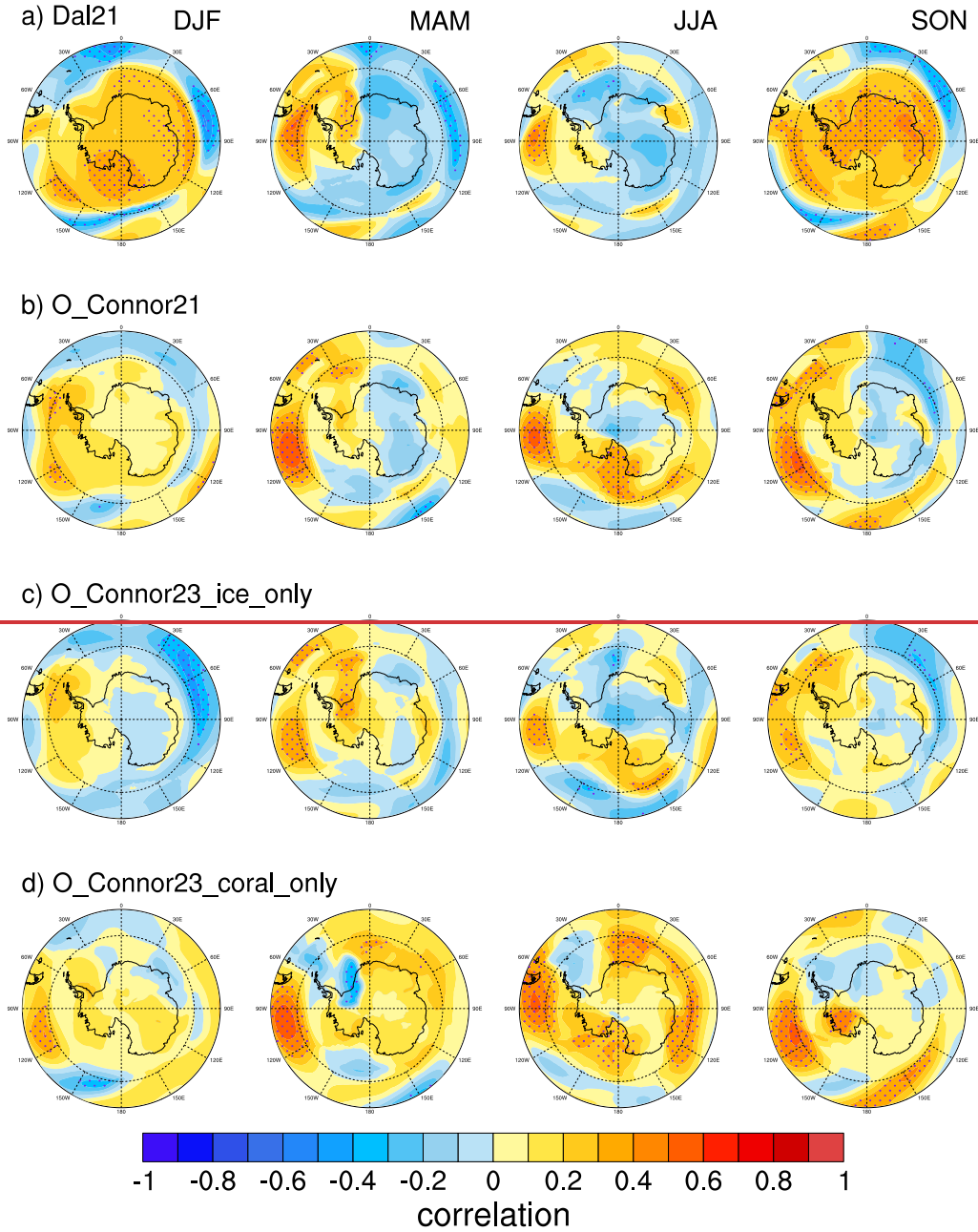
757 ~~core-only reconstruction from O'Connor et al. (2023, Fig. 10e, middle column), while the~~
758 ~~agreement weakens for the coral-only reconstruction (Fig. 10d, middle column). This suggests~~
759 ~~the Fogt and Connolly (2021)FC21_STAT dataset. However, it is also clear the local ice core~~
760 ~~variability over Antarctica, which dominates the reconstructions in Figs. 10a-c, is opposite to~~
761 ~~that of the coral-based tropical variability (Fig 10d.), especially over East Antarctica, where~~
762 ~~tropical teleconnections to Antarctica are generally weaker (Li et al., 2021).~~

763 During 1957-2000, the agreement improves from 1905-1956 for all but the
764 OCON23_ASSIM coral-only reconstructions (Fig. 10, middle column). This suggests that the
765 FC21_STAT dataset aligns more with tropical variability in the early 20th century, which
766 dominates its response, but more with ice core related variability in the latter half of the 20th
767 century, which dominates the paleo-based data assimilation reconstructions near Antarctica.
768 Further, given the greater skill in the O'Connor et al. (2021, 2023) reconstructions relative to
769 Dalaiden et al. (2021)DAL21_ASSIM in the later period, this also ~~suggests~~suggests that including
770 external forcing in the climate model prior is important.

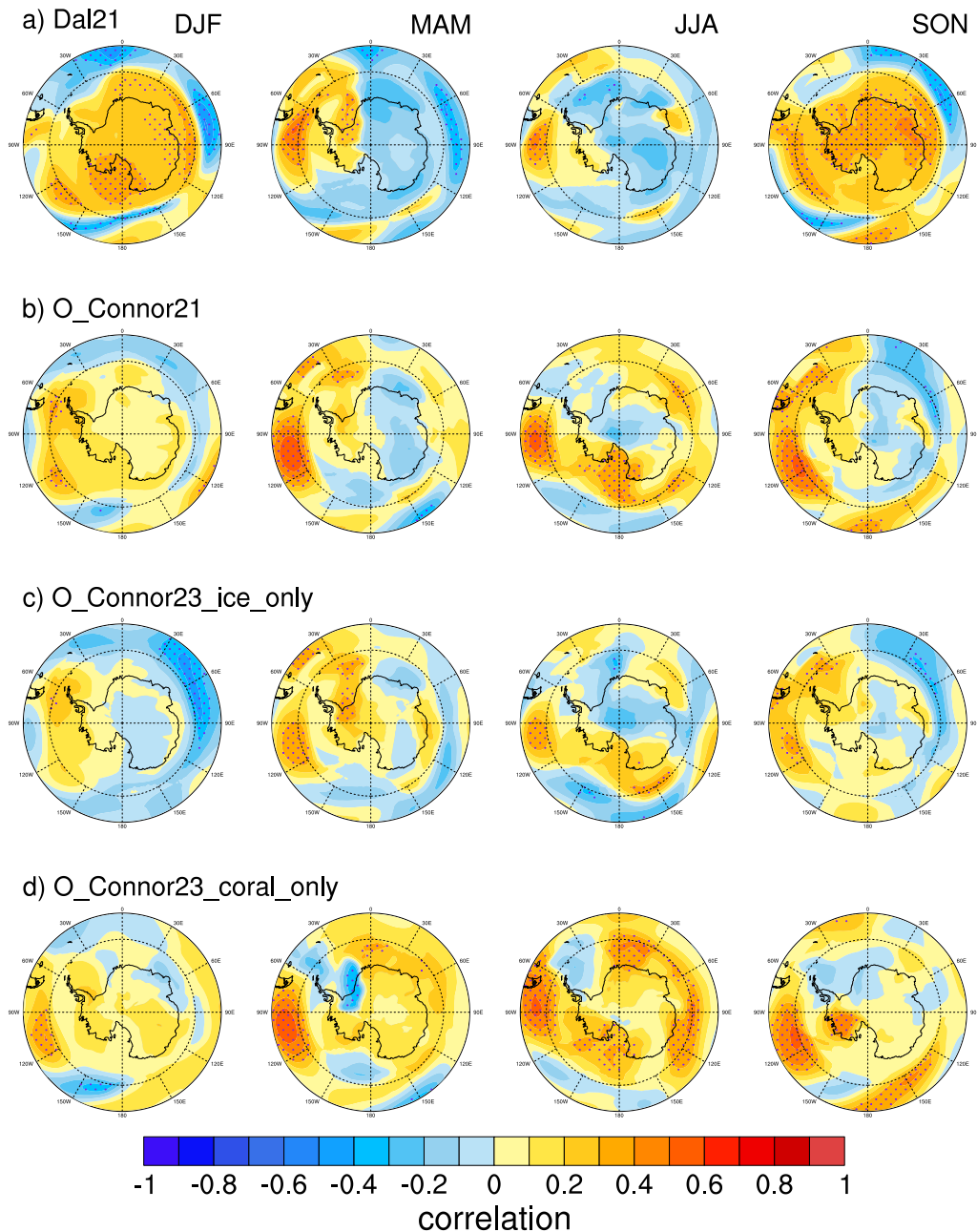
771 Since there was some effect of seasonality on the relationship between the paleo-based and
772 statistically based sea ice reconstructions in Fig. 4, we examine the correlations for each season
773 ~~(like with the Fogt et al. (2022a) sea ice reconstructions, the Fogt and Connolly (2021) pressure~~
774 ~~datasets were constructed seasonally, and annually averaged for Fig. 10, Table 1)~~ in the 1905-
775 1956 period in Fig. 11. ~~However, for~~For the pressure datasets, the change in seasonal skill in
776 Fig. 11 is dampened compared to that for Antarctic sea ice extent in Fig. 4. There are more
777 correlations statistically significant ($p < 0.05$) for the Dalaiden et al. (2021)DAL21_ASSIM
778 dataset in DJF and SON, likely tied to when the skill of the Fogt and Connolly
779 (2021)FC21_STAT dataset is the highest. For the O'Connor et al. (2021,2023) datasets (Figs.

780 11b-d), the agreement is slightly better over the Ross Sea and West Antarctica in winter. This
781 improvement is due to contributions from both ice cores and corals, with the corals providing
782 enhanced agreement off the coast and across East Antarctica (Figs. [10e11c,d](#)). The ice core-only
783 reconstruction provides better agreement over West Antarctica in SON (Fig. [10d11d](#), right
784 column). Another interesting feature, worthy of further study, is the opposite
785 [agreementcorrelation](#) in the Weddell Sea in MAM between the ice core-only reconstruction (Fig.
786 [10e11c](#), significantly [$p<0.05$] positively correlated) and the coral-only reconstruction (Fig.
787 [10d11d](#), significantly [$p<0.05$] negatively correlated); the significant positive correlations over
788 the Weddell Sea onto the Antarctic continent in MAM are also seen in the [Dalaiden et al.](#)
789 [\(2021\)DAL21_ASSIM](#) reconstruction, related to the ice core constraints (since this dataset does
790 not assimilate coral proxies).

Seasonal Correlations with Fogt and Connolly (2021), 1905-1956



Seasonal Correlations with Fogt and Connolly (2021), 1905-1956

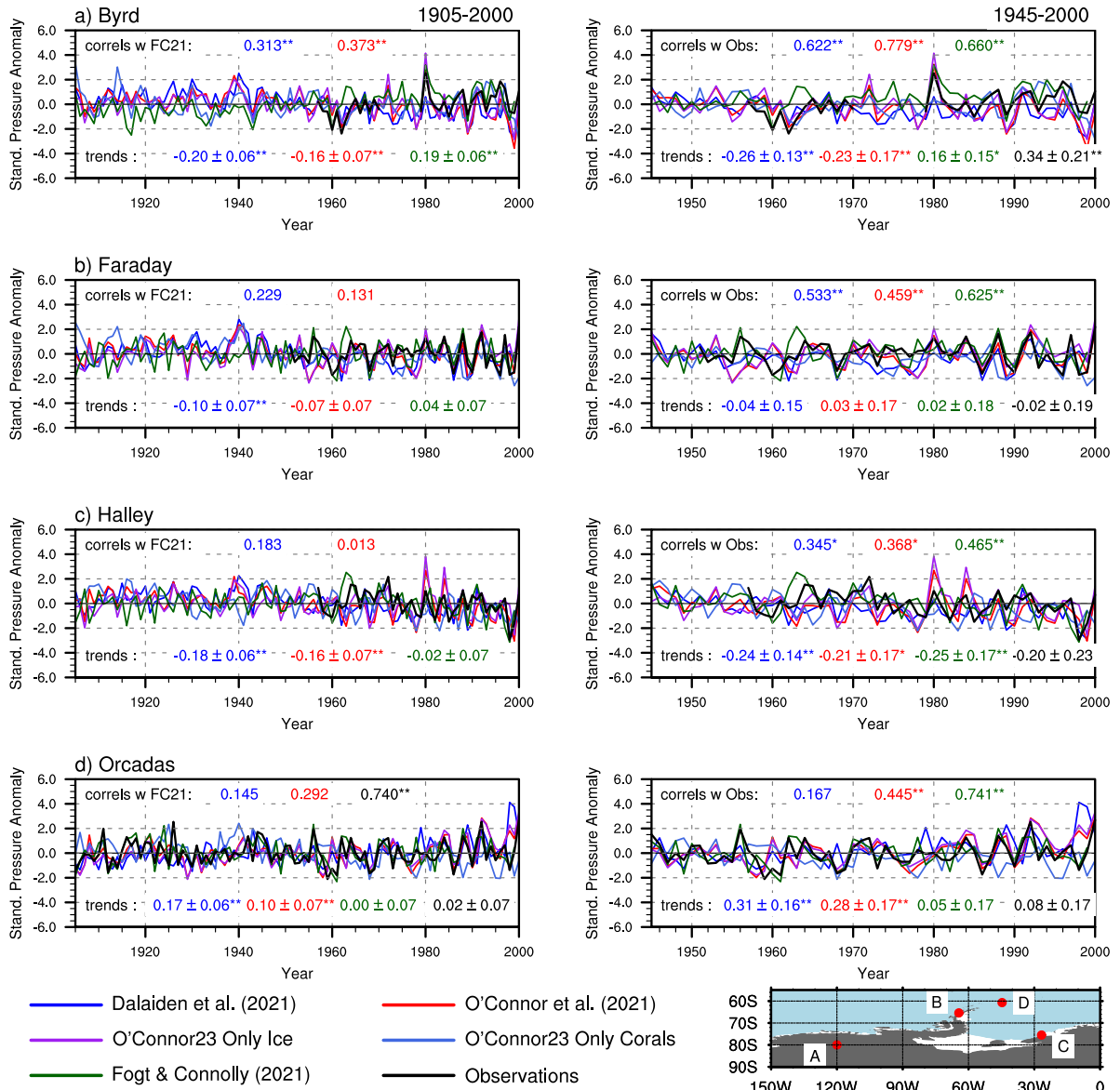


792
793
794
795
796

Figure 11. As in Fig. 10, but for correlations of the annual mean pressure reconstructions with the seasonal mean reconstruction of Fogt and Connolly (2021) during 1905-1956. The columns, from left to right, represent DJF, MAM, JJA, and SON, respectively.

797 To ~~more-completely~~further evaluate these datasets, annual mean comparisons with select
798 observations are conducted in Fig. 12 using the ~~gridpoints~~grid points nearest to the station
799 locations (for reference, a map of the stations is provided in the legend of Fig. 12). In the full
800 period 1905-2000 (left column), correlations of the paleo-based datasets with the ~~Fogt and~~
801 ~~Connolly (2021)~~FC21_STAT dataset are generally near zero, and only significant (here, $p < 0.01$)
802 over the West Antarctic continent at Byrd station: ~~(Fig. 12a)~~. The correlations with the
803 observations ~~improve after 1945~~ (right column in Fig. ~~12~~, near the start of data at Faraday),
804 most now significant at $p < 0.01$, are generally higher than with FC21_STAT, especially for the
805 ~~O'Connor et al. (2021)~~OCON21_ASSIM dataset. The inclusion of more proxy data in the
806 ~~O'Connor et al. (2021)~~OCON21_ASSIM dataset (Fig. 2c) and the inclusion of an
807 anthropogenically forced prior (Table 1) likely lead to overall better agreement with the
808 observations than for the ~~Dalaiden et al. (2021)~~DAL21_ASSIM dataset; however both of these
809 paleo-~~based~~assimilation datasets use a moderately coarse spatial resolution prior that may limit
810 their comparison at a single point. It is also important to note that while the ~~Fogt and Connolly~~
811 ~~(2021)~~FC21_STAT correlations are overall higher than the ~~paleo-based~~other reconstructions, this
812 dataset is calibrated directly to these observations, and for Orcadas, direct observations (and not
813 a reconstruction) are used, ~~hence why the correlations are strong in both time periods at this~~
814 ~~location, black correlation values at top of the figures in the bottom row of Fig. 12).~~
815 ~~More striking than the change in correlation in Fig. 12 are the changes in the linear trends~~
816 ~~through time across the various datasets (given by the values at the bottom of each panel).~~

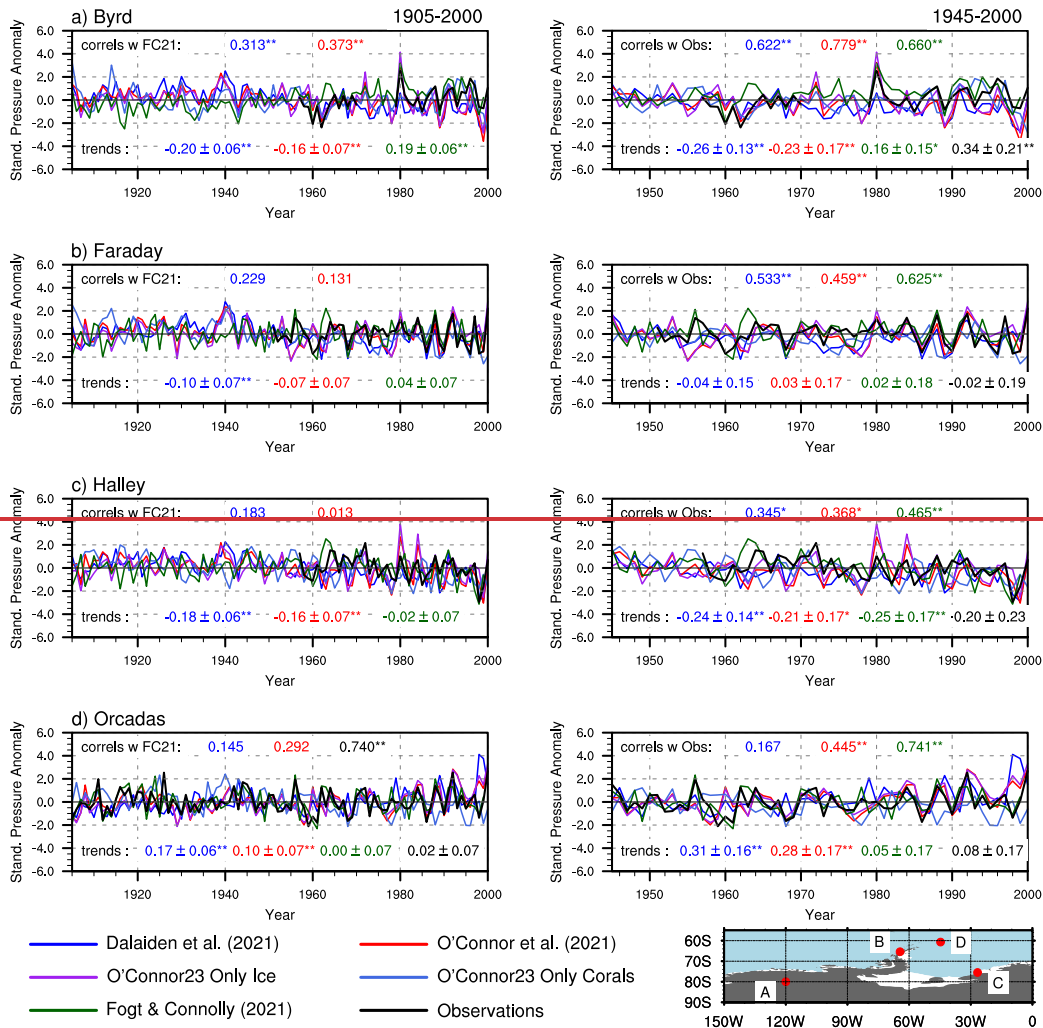
Annual Mean Pressure Comparisons and Trends with Observation Data



817

818 In the full time period (1905–2000, left column of Fig. 12), both the Dalaiden et al. (2021) and
 819 O'Connor et al. (2021) datasets show statistically significant ($p < 0.01$) pressure decreases at Byrd
 820 and Halley stations (Figs. 12a,e), but statistically significant ($p < 0.01$) pressure increases at
 821 Orcadas (Fig. 12d). The Fogt and Connolly (2021) dataset, in strong contrast, shows significant
 822 ($p < 0.05$) pressure increases at Byrd in both time periods (consistent with observations after 1957,

Annual Mean Pressure Comparisons and Trends with Observation Data



823
 824 **Figure 12.** Timeseries of standardized pressure anomalies at various locations given in the map
 825 at the bottom right- (i.e., A = panel a). The observations, mostly starting around 1957 (1903 for
 826 Orcadas, panel d), are shown in black. For the left column, correlations given at the top of each
 827 panel are with the Fogt and Connolly (2021) dataset during 1905-2020, and trends at the bottom
 828 are calculated for the 1905-2020 period. For the right column, the correlations are with the
 829 observations, and both correlations and trends are calculated during 1945-2020. In all panels,
 830 correlations and trends are color-coded based on the timeseries color in the legend, with values
 831 significantly different from zero at $p < 0.05$ and $p < 0.01$ -are marked with * and **, respectively.
 832

833 The changes in the linear trends through time across the various datasets (given by the color-
834 coded values at the bottom of each panel) are also noteworthy in Fig. 12. In the full time period
835 (1905-2000, left column of Fig.

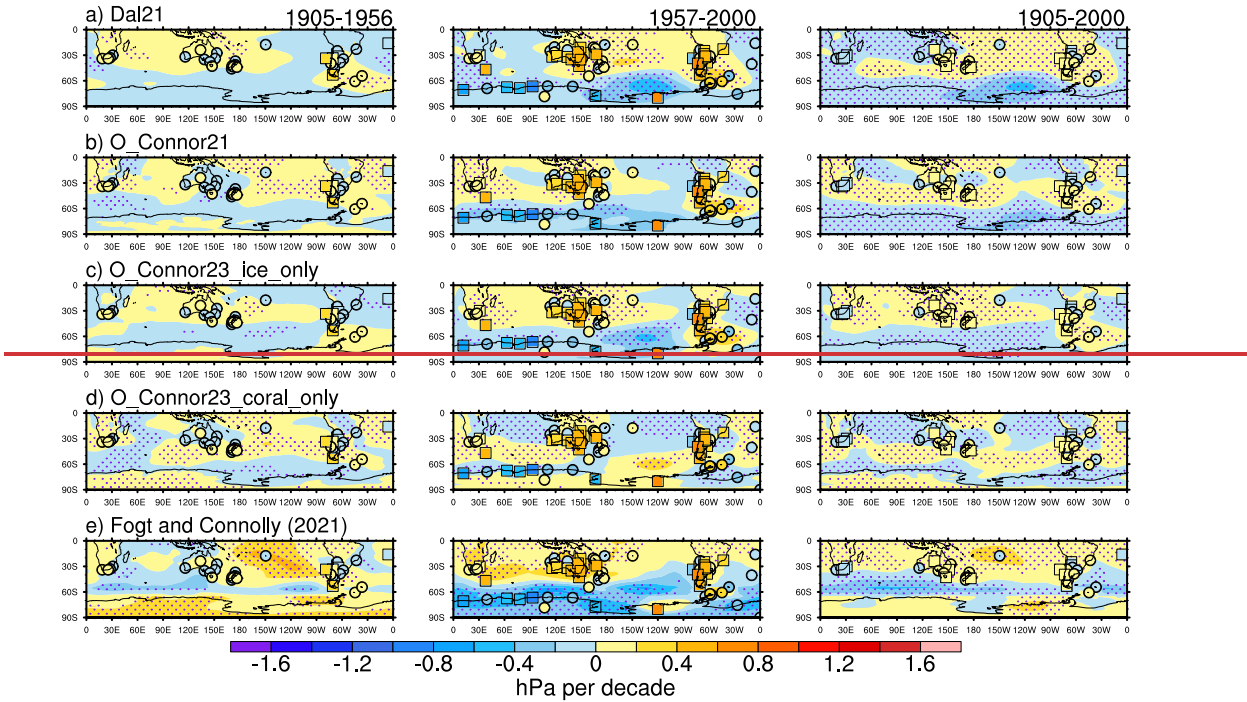
836
837 Fig.12), both the DAL21_ASSIM and OCON21_ASSIM datasets show statistically
838 significant ($p<0.01$) pressure decreases at Byrd and Halley stations (Figs. 12a,c), but statistically
839 significant ($p<0.01$) pressure increases at Orcadas (Fig. 12d). The FC21_STAT dataset, in
840 strong contrast, shows significant ($p<0.05$) pressure increases at Byrd in both time periods
841 (consistent with observations after 1957, Fig. 12a), and only significant ($p<0.01$) pressure
842 decreases at Halley station after 1945 (Fig. 12c, right column). The much stronger and
843 sometimes different signed trends in the paleo-basedassimilation pressure reconstructions
844 compared to the Fogt and Connolly (2021)FC21_STAT dataset during 1905-2020, and even with
845 most observations after 1945, are undoubtedly a strong contributor to the differences seen in the
846 Antarctic sea ice extent reconstructions-between the paleo-based and statistically based
847 reconstructions; there are statistically significant differences in the underlying atmospheric
848 circulation used to generate these reconstructions that connect to their differences in trends seen
849 in Figs. 3 and 6.

850 Both the Dalaiden et al. (2021) and O'Connor et al. (2021) studies focus on marked pressure
851 decreases in the region of the Amundsen Sea low, which as discussed earlier, has a strong role in
852 regional sea ice conditions examined in this study (Hosking et al., 2013; Raphael et al., 2016;
853 Holland and Kwok, 2012);(Hosking et al., 2013; Raphael et al., 2016; Holland and Kwok, 2012).
854 It is much more challenging to investigate the reality of these long term changes in this region, as
855 there are no direct observations (the closest stations are represented by those in Fig. 12), and).

856 Further the ~~Fogt and Connolly (2021)~~FC21_STAT dataset shows the lowest skill (compared to
857 the ERA-Interim reanalysis) spatially in this region; ~~(Fogt et al. 2019)~~, consistent with the fact
858 that even contemporary reanalyses show the greatest disparity (in terms of pressure correlations
859 and trends) in this region as well ~~(Fogt et al., 2018)~~~~(Fogt et al., 2018)~~. Given the disparities in
860 trends seen from observation locations in Fig. 12, it is not surprising that the datasets also have
861 dramatically different trends in this region, which have similar implications for differences in sea
862 ice extent trends. To visualize this in perspective, a full spatial comparison across the Southern
863 Hemisphere of the pressure trends in the various datasets in three time periods, along with
864 available observations, is provided in Fig. ~~13 as a final comparison of these products~~13.

865 First, for the period of Antarctic observations (1957-2000, middle column of Fig. 13),
866 observations indicate statistically significant (boxes, $p < 0.05$) pressure decreases only over
867 coastal East Antarctica, with insignificant positive annual mean trends over the East Antarctic
868 plateau at Vostok (~~78.5°S, 106.9°E, the~~ only observation plotted in central East Antarctica in Fig.
869 13~~).~~, consistent with ERA5 surface pressure trends during 1979-2022 in Fig. 1b~~).~~. At Byrd
870 station in central West

Spatial Trends with Observations

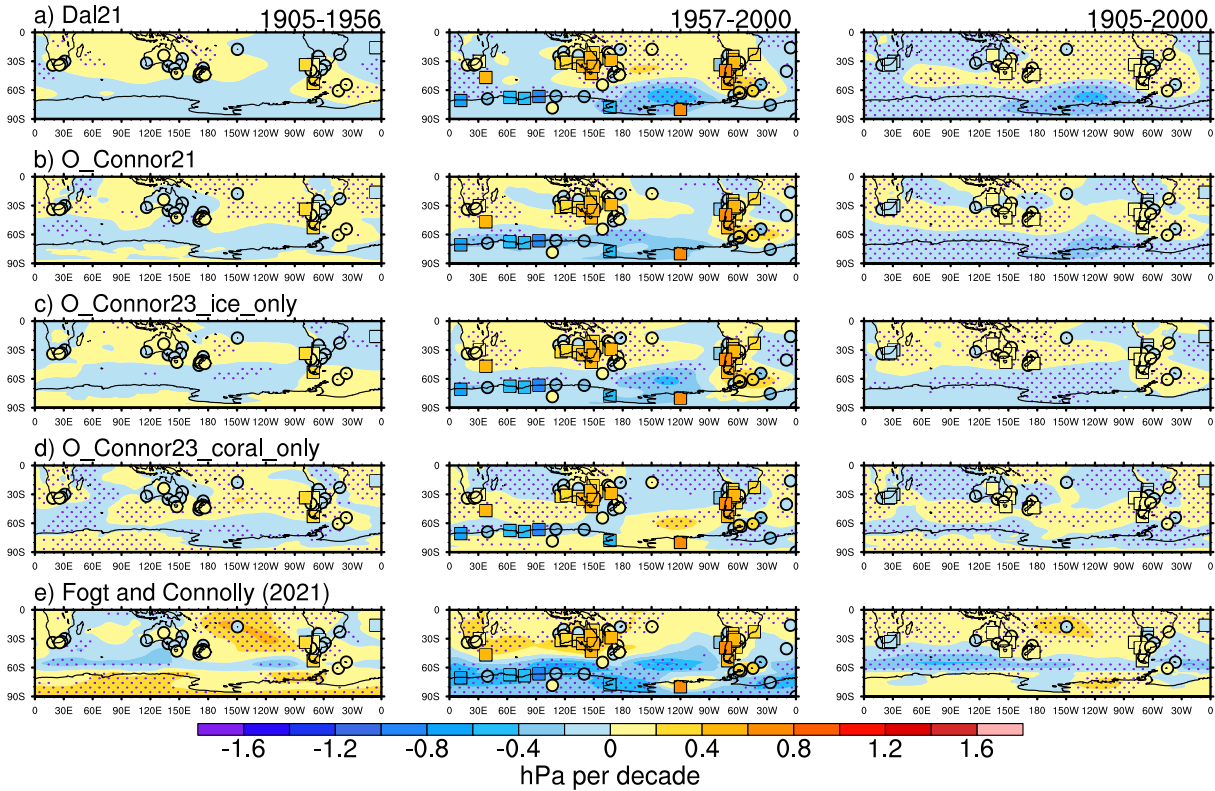


871
 872 **Figure 13.** Linear near-surface annual mean pressure trends (hPa per decade) for 1905–1956
 873 (left column), 1957–2000 (middle column), and 1905–2000 (right column) for various datasets in
 874 each row a) Dalaiden et al. (2021); b) O’Connor et al. (2021) proxy reconstruction c) O’Connor
 875 et al. (2023) reconstruction with only ice core proxies; d) O’Connor et al. (2023) reconstruction
 876 with only coral proxies; e) Fogt and Connolly (2021) station-based reconstruction. Trends from
 877 observation data, where available, are plotted using the same color scale on top of the gridded
 878 pressure trends. Stippling indicates gridded pressure trends significantly different from zero at
 879 $p < 0.05$, boxes indicate trends in observations significantly different from zero at $p < 0.05$.

880
 881
 882 Antarctica, statistically significant positive trends (annual mean) are observed (also seen in
 883 Fig. 12a). The various datasets capture these patterns to differing degrees: paleo-based. Paleo-
 884 data assimilation datasets generally only have statistically significant negative trends along the
 885 Antarctic coastline, consistent with the positive annual mean SAM trend (~~Fogt and Marshall,~~
 886 2020), (Fogt and Marshall, 2020), but only capture positive trends in the Antarctic interior in
 887 coral-only reconstruction (middle column Figs. 13a-d). Indeed, the coral-only reconstruction has
 888 positive pressure trends everywhere over Antarctica except along the Antarctic Peninsula and

889 Weddell Sea (Fig. 13d, middle column), and therefore is the only dataset to miss the observed
890 significant negative pressure trends along the East Antarctic coastline. Meanwhile, the ~~Fogt and~~
891 ~~Connolly (2021)FC21_STAT~~ dataset ~~incorrectly has~~ is the only one to have significant ($p < 0.05$)
892 negative, instead of the observed positive, pressure trends over the East Antarctic plateau, but it
893 does capture a regional pressure increase in West Antarctica (Figs. 13e middle column, Fig. 12).
894 The ~~Dalaiden et al. (2021)DAL21_ASSIM~~ dataset has a marked significant deepening of the
895 Amundsen Sea low during 1957-2000 (Fig. 13a, middle column), which is largely driven by ice
896 core paleo data (Fig. 2b), and thus reduced in the ~~O'Connor et al. (2021)OCON21_ASSIM~~
897 dataset by the inclusion of coral data (Figs. 13b-d; Fig. 2c). This suggests that if the significant
898 pressure increases over West Antarctica are correct, there is likely might be a tropical signal,
899 either internal or forced, to these positive trends (to be discussed in more detail later). In the
900 midlatitudes during 1957-2000, the coral-only reconstruction (Fig. 13d) captures the pattern seen
901 in observations the best (the ~~Fogt and Connolly (2021)FC21_STAT~~ dataset is not independent of
902 observations in these locations since it is merely the 20th century reanalysis north of 60°S, Table
903 1). It should be noted that there are large inconsistencies withbetween observations at Tahiti in
904 the central tropical Pacific and the 20CRv3, as discussed in ~~Fogt and Connolly~~
905 ~~(2021)FC21_STAT.~~
906 For the early 20th-century during

Spatial Trends with Observations



907
908
909
910
911
912
913
914
915
916

Figure 13. Linear near-surface annual mean pressure trends (hPa per decade) for 1905-1956, (left column), 1957-2000 (middle column), and 1905-2000 (right column) for various datasets in each row a) Dalaiden et al. (2021); b) O'Connor et al. (2021) proxy reconstruction c) O'Connor et al. (2023) reconstruction with only ice core proxies; d) O'Connor et al. (2023) reconstruction with only coral proxies; e) Fogt and Connolly (2021) station-based reconstruction. Trends from observation data, where available, are plotted using the same color scale on top of the clear gridded pressure trends. Stippling indicates gridded pressure trends significantly different from zero at $p < 0.05$, boxes indicate trends in observations significantly different from zero at $p < 0.05$

917 Figure 13 clearly demonstrates the difference in trends in 1905-1956 between the Fogt and
918 Connolly (2021)FC21_STAT dataset and those of Dalaiden et al. (2021) and O'Connor et al
919 (2021) is distinct.DAL21_ASSIM and OCON21_ASSIM. Pressure trends over the Antarctic
920 continent reverse in the Fogt and Connolly (2021) dataset,FC21_STAT dataset (significantly
921 positive in early 20th century, Fig. 13e left column, significantly negative in late 20th century,
922 Fig. 13e right column) while they remain insignificant in most paleo-basedassimilation datasets.
923 It is interesting however that the coral-only reconstruction from O'Connor et al. (2023)
924 OCON23_ASSIM (Fig. 13d) also produces statistically significant positive trends over
925 Antarctica in all time periods, consistent with the Fogt and Connolly (2021)FC21_STAT dataset
926 during 1905-1956, and aligning with the period when these two datasets agree the most (Figs.
927 11-12). Notably, this coral-only dataset agrees the best with observations in the midlatitudesmid-
928 latitudes during 1905-1956 (Fig. 13d, left column), and is quite similar to the pattern in the early
929 20th century from the full OCON21_ASSIM dataset in the midlatitudes (Fig. 13b, left column),
930 suggesting a primary role of the coral records in constraining the solution in the midlatitudes.

931 The larger sample size afforded by the full time period from 1905-2000 yields more
932 statistically significant trends across the Southern Hemisphere in the paleo-baseddata
933 assimilation datasets (Figs. 13a-d, right column) that are overall similar in structure to the trends
934 in the paleo-based datasets during 1957-2000 (Figs. 13a-d, middle column). The coral-only
935 dataset slightly produces better agreement with the midlatitude observations, capturing the
936 significant negative trends over South Africa that are also hinted at by insignificant negative
937 pressure trends at Perth in southwestern Australia. In comparing the paleo-based with the station-
938 based Fogt and Connolly (2021)FC21_STAT datasets, the biggest differences are the trends
939 poleward of 60°S, which are insignificant except for pressure increases ($p < 0.05$) over West

940 Antarctica in the [Fogt and Connolly \(2021\)FC21_STAT](#) dataset due to the cancellation of
941 different trends in the early and late 20th century in this dataset (Fig. 13e). Compared to the other
942 sources of differences in the Antarctic sea ice reconstructions examined earlier, this connection
943 to the implied changes (or lack thereof) in the atmospheric circulation in the 20th century are a
944 dominant contributing factor to the differences in the linear trends among the Antarctic sea ice
945 estimates seen in Fig. 2; this similar conclusion was reached in Fogt et al. (2022b) using a much
946 more limited analysis.

947

948 **4. Discussion**

949 While this study largely focuses on causes for the differences between various sea ice and
950 pressure reconstructions, it is important to note that there are broad similarities as well,
951 especially in the Weddell sector where cross-correlations are strongest, even stronger in some
952 seasons than in the annual mean. Further, each of these datasets has their own limitations due to
953 their methodology and assumptions made in their reconstruction procedure, and that every
954 reconstruction is only an estimate and is not without error. Nonetheless, the differences in the
955 sea ice extent reconstruction trends (and to a lesser degree, the interannual variability) largely
956 appear to hinge on whether or not there was a change in the atmospheric circulation in the high
957 southern latitudes (poleward of 60°S) in the 20th century. [Paleo-based assimilation](#)
958 reconstructions, constrained by ice core records over Antarctica, have similar pressure trends
959 through time, which influence the proxy-based sea ice extent reconstructions. In contrast,
960 station-based reconstructions of both pressure and Antarctic sea ice extent show trends that
961 change through time, which reduces their similarities with proxy-based reconstructions (for both
962 sea ice extent and pressure) in the early 20th century. Given that coral-only reconstructions from

963 ~~O'Connor et al. (2023)~~OCON23_ASSIM agree better with the ~~Fogt and Connolly~~
964 ~~(2021)~~FC21_STAT dataset in the early 20th century, there ~~it~~ is possible that if there was indeed a
965 reversal of atmospheric circulation trends, ~~that these had~~there was a tropical association to them.
966 Nonetheless, the analysis here shows an important influence of the implied atmospheric
967 circulation on Antarctic sea ice variations in both proxy-based and station-based sea ice extent
968 reconstructions, consistent with findings from observations and models (~~Sun and Eisenman,~~
969 ~~2021; Blanchard-Wrigglesworth et al., 2021).~~(Sun and Eisenman, 2021; Blanchard-
970 Wrigglesworth et al., 2021).

971 In looking more closely at the analysis presented here, the limited observational data always
972 present a challenge. In particular, in the vicinity of the Amundsen Sea low, Byrd station in West
973 Antarctica (see map in Fig. ~~H12~~) is the only observational record spanning over 30 years in the
974 150°-90°W sector poleward of 60°S (not including the South Pole). ~~While weather observations~~
975 ~~started at this station in 1957, it shut down for a period in the 1970s, and was replaced by an~~
976 ~~automatic weather station nearby. While there has been considerable work done to patch the~~
977 ~~temperature record at this station (Bromwich et al., 2012), there could be measurement-specific~~
978 ~~errors that lead to the~~Importantly, this merged observation record shows statistically significant
979 ($p < 0.05$) annual mean pressure increases from 1957-2000, while the positive pressure trends at
980 Vostok station in East Antarctica are not significant. While there has been considerable work
981 done to patch the temperature record at this station (Bromwich et al., 2012), there could be
982 measurement-specific errors that lead to the statistically significant positive trend at this station
983 in the observational dataset that may at least partially explain the regional differences in pressure
984 (across West Antarctica and extending northward into the Amundsen and Bellingshausen Seas)
985 between the paleo-~~based~~data assimilation pressure datasets and those of ~~Fogt and Connolly~~

986 ~~(2021)~~FC21_STAT. However, the AWS in the later portion of the record is at a slightly higher
987 elevation than the station observations in the earlier part of the data, which would generate
988 negative pressure trends based on unadjusted instrument elevation changes, opposite the positive
989 annual mean trends seen here. There is also a strong seasonal pattern to the positive pressure
990 trends over West Antarctica, as shown in Fogt et al. (2018). Further work is needed to investigate
991 the Byrd pressure data source, as well to employ historical data from ship logbooks and early
992 expeditions (~~Edinburgh and Day, 2016; De La Mare, 2009; Fogt et al., 2020; Lorrey et al.,~~
993 ~~2022~~)(Edinburgh and Day, 2016; de La Mare, 2009; Fogt et al., 2020; Lorrey et al., 2022) to
994 better understand possible atmospheric circulation shifts in the high southern latitudes prior to
995 1957. Additionally, each kind of observations (e.g., paleo or instrumental observations) has its
996 own advantages and weaknesses. Combining these two sources of information could provide a
997 more accurate reconstruction of historical surface climate changes.

998 5. Conclusions

999 The analysis presented in this paper has evaluated various sea ice extent reconstructions
1000 spanning the Ross Sea eastward to the Weddell sea, and pressure reconstructions across the
1001 entire Southern Hemisphere to explain the differences between the sea ice extent reconstructions.
1002 Overall, better agreement in the sea ice extent reconstructions was found in the Weddell sea,
1003 despite possible changes in the relationship sea ice shares with the atmospheric pressure in this
1004 region throughout the 20th century. In the Ross and Bellingshausen seas, the agreement is
1005 weaker, and appears to be more strongly tied to the atmospheric circulation. For ice core based
1006 reconstructions studied here, the ~~Thomas and Abram (2016)~~TA16_PALEO reconstruction is
1007 fairly consistent with other reconstructions in the Ross sea, while the differing spatial and
1008 temporal representation of the ~~Abram et al. (2010)~~AB10_PALEO reconstruction make it

1009 challenging to effectively compare to other datasets. Overall, paleo-based data assimilation and
1010 station-based pressure reconstructions give notably different trends from the Ross Sea east to the
1011 Weddell Sea throughout the 20th century, especially in the vicinity of the Amundsen Sea low, a
1012 semi-permanent pressure cell known to strongly modulate Antarctic sea ice in the Ross,
1013 Amundsen, and Bellingshausen Seas (~~Hosking et al., 2013; Raphael et al., 2016~~).~~(Hosking et al.,~~
1014 2013; Raphael et al., 2016). There is often better agreement in OCON21_ASSIM
1015 reconstructions based solely on coral proxy data with the FC21_STAT reconstruction, especially
1016 in the early 20th century. This likely suggests that signals from the tropics, which may or may
1017 not include external forcing, tropical variability governs the relationships within the
1018 FC21_STAT, while reconstructions based on ice-cores provide a more local constraint to
1019 reconstructions near the Antarctic continent. In the latter half of the 20th century, the warming
1020 trend in the tropical Pacific can explain the pressure increases found in the coral-only
1021 reconstructions in the South Pacific; however, it is unclear how to reconcile that with the
1022 Amundsen Sea Low deepening found in the ice core-only reconstructions and all-proxy
1023 reconstructions. The relative contributions of the tropics, local internal variability, and external
1024 forcing to historical trends remains highly uncertain and deserves further investigation, in
1025 agreement with previous studies (e.g., Holland et al., 2022).

1026 While this study has determined that many of the differences in ~~the paleo-based and~~
1027 ~~statistically generated~~ Antarctic sea ice extent reconstructions are tied primarily to their
1028 connection to the underlying atmospheric circulation, it is not able to determine the validity of
1029 changes in the atmospheric circulation in the early to mid 20th century. Further data extraction
1030 from ship logbooks (~~Lorrey et al., 2022~~),~~(Lorrey et al., 2022)~~, new climate model simulations
1031 assimilating both paleo data and observations, and isolated forcing simulations in coupled

1032 climate model simulations may help to understand this potential atmospheric circulation change.
1033 Nonetheless, this study has helped to better understand the differences and relative strengths and
1034 limitations of not only the Antarctic sea ice reconstructions examined here, but also several
1035 pressure reconstructions. It is thus hoped that future users of these valuable datasets will
1036 exercise the necessary caution when analyzing them given the knowledge of the processes they
1037 represent well, and other mechanisms that they may not reproduce as reliably.

1038

1039 ~~Code and~~ Data Availability

1040 ~~The Fogt et al. (2022a) sea ice reconstructions can be obtained from the National Snow and Ice~~
1041 ~~Data Center dataset G10039 (<https://nsidc.org/data/g10039/versions/1>) (Fogt et al., 2023). The~~
1042 ~~Fogt et al. The FOGT_STAT sea ice reconstructions can be obtained from the National Snow~~
1043 ~~and Ice Data Center dataset G10039 (<https://nsidc.org/data/g10039/versions/1>) (Fogt et al.,~~
1044 ~~2023). The Fogt et al. (2019) and Fogt and Connolly (2021) pressure reconstructions can be~~
1045 ~~downloaded from figshare (<https://doi.org/10.6084/m9.figshare.c.6765447.v1>). Data for the~~
1046 ~~Dalaiden et al. (2021)<https://doi.org/10.6084/m9.figshare.c.6765447.v1>). Data for the~~
1047 ~~DAL21_ASSIM sea ice extent and pressure reconstructions are available on Zenodo~~
1048 ~~(<https://zenodo.org/record/4770179>). The O'Connor et al.~~
1049 ~~(2021)<https://zenodo.org/record/4770179>). The OCON21_ASSIM pressure reconstructions are~~
1050 ~~available on Zenodo ([https://zenodo.org/record/5507607#.Y6OOI-](https://zenodo.org/record/5507607#.Y6OOI-yIb0o)~~
1051 ~~yIb0o~~<https://zenodo.org/record/5507607#.Y6OOI-yIb0o>) and the ~~sensitivity~~
1052 ~~reconstructions from O'Connor et al. (2023)OCON23_ASSIM can also be downloaded from~~
1053 ~~Zenodo (<https://zenodo.org/record/8007655><https://zenodo.org/record/8007655>).~~

1054

1055 Author Contributions

1056 RLF and QD designed the study. All authors contributed to writing and editing the manuscript,
1057 and RLF produced the figures.

1058

1059 **Competing Interests**

1060 The authors declare no competing interests.

1061

1062 **Acknowledgments**

1063 RLF acknowledges support from the U.S. National Science Foundation Office of Polar Programs

1064 award #1744998. QD is a Research Fellow within the F.R.S.-FNRS (Belgium).

1065

1066

1067 **References**

- 1068 Abram, N. J., Thomas, E. R., McConnell, J. R., Mulvaney, R., Bracegirdle, T. J., Sime, L. C., and
1069 Aristarain, A. J.: Ice core evidence for a 20th century decline of sea ice in the Bellingshausen
1070 Sea, Antarctica, *Journal of Geophysical Research*, 115, <https://doi.org/10.1029/2010JD014644>,
1071 2010.
- 1072 Bamber, J. L., Riva, R. E. M., Vermeersen, B. L. A., and LeBrocq, A. M.: Reassessment of the
1073 Potential Sea-Level Rise from a Collapse of the West Antarctic Ice Sheet, *Science*, 324, 901–903,
1074 <https://doi.org/10.1126/science.1169335>, 2009.
- 1075 Banerjee, A., Fyfe, J. C., Polvani, L. M., Waugh, D., and Chang, K.-L.: A pause in Southern
1076 Hemisphere circulation trends due to the Montreal Protocol, *Nature*, 579, 544–548,
1077 <https://doi.org/10.1038/s41586-020-2120-4>, 2020.
- 1078 Blanchard-Wrigglesworth, E., Roach, L. A., Donohoe, A., and Ding, Q.: Impact of Winds and
1079 Southern Ocean SSTs on Antarctic Sea Ice Trends and Variability, *Journal of Climate*, 34, 949–
1080 965, <https://doi.org/10.1175/JCLI-D-20-0386.1>, 2021.
- 1081 Brady, E., Stevenson, S., Bailey, D., Liu, Z., Noone, D., Nusbaumer, J., Otto-Bliesner, B. L., Tabor,
1082 C., Tomas, R., Wong, T., Zhang, J., and Zhu, J.: The Connected Isotopic Water Cycle in the
1083 Community Earth System Model Version 1, *J Adv Model Earth Syst*, 11, 2547–2566,
1084 <https://doi.org/10.1029/2019MS001663>, 2019.
- 1085 Bromwich, D. H., Nicolas, J. P., Monaghan, A. J., Lazzara, M. A., Keller, L. M., Weidner, G. A., and
1086 Wilson, A. B.: Central West Antarctica among the most rapidly warming regions on Earth,
1087 *Nature Geoscience*, 6, 139–145, <https://doi.org/10.1038/ngeo1671>, 2012.
- 1088 Clark, L. and Fogt, R.: Southern Hemisphere Pressure Relationships during the 20th Century—
1089 Implications for Climate Reconstructions and Model Evaluation, *Geosciences*, 9, 413,
1090 <https://doi.org/10.3390/geosciences9100413>, 2019.
- 1091 Dalaiden, Q., Goosse, H., Rezsöhazy, J., and Thomas, E. R.: Reconstructing atmospheric
1092 circulation and sea ice extent in the West Antarctic over the past 200 years using data
1093 assimilation, *Clim Dyn*, 57, 3479–3503, <https://doi.org/10.1007/s00382-021-05879-6>, 2021a.
- 1094 Dalaiden, Q., Goosse, H., Rezsöhazy, J., and Thomas, E. R.: Reconstructing atmospheric circulation
1095 and sea ice extent in the West Antarctic over the past 200 years using data assimilation,
1096 <https://doi.org/10.5281/ZENODO.4770178>, 2021b.
- 1097 De La Mare, W. K.: Changes in Antarctic sea ice extent from direct historical observations and
1098 whaling records, *Climatic Change*, 92, 461–493, <https://doi.org/10.1007/s10584-008-9473-2>,
1099 2009.
- 1100 Ding, Q., Steig, E. J., Battisti, D. S., and Küttel, M.: Winter warming in West Antarctica caused by
1101 central tropical Pacific warming, *Nature Geoscience*, 4, 398–403,
1102 <https://doi.org/10.1038/ngeo1129>, 2011.

1103 Edinburgh, T. and Day, J. J.: Estimating the extent of Antarctic summer sea ice during the Heroic
1104 Age of Antarctic Exploration, *The Cryosphere*, 10, 2721–2730, [https://doi.org/10.5194/te-10-](https://doi.org/10.5194/te-10-2721-2016)
1105 [2721-2016](https://doi.org/10.5194/te-10-2721-2016), 2016.

1106 Fogt, R. L. and Connolly, C. J.: Extratropical Southern Hemisphere Synchronous Pressure
1107 Variability in the Early Twentieth Century, *Journal of Climate*, 34, 5795–5811,
1108 <https://doi.org/10.1175/JCLI-D-20-0498.1>, 2021.

1109 Fogt, R. L. and Marshall, G. J.: The Southern Annular Mode: Variability, trends, and climate
1110 impacts across the Southern Hemisphere, *WIREs Climate Change*, 11,
1111 <https://doi.org/10.1002/wcc.652>, 2020.

1112 Fogt, R. L., Goergens, C. A., Jones, M. E., Witte, G. A., Lee, M. Y., and Jones, J. M.: Antarctic
1113 station-based seasonal pressure reconstructions since 1905: 1. Reconstruction evaluation:
1114 Antarctic Pressure Evaluation, *Journal of Geophysical Research: Atmospheres*, 121, 2814–2835,
1115 <https://doi.org/10.1002/2015JD024564>, 2016a.

1116 Fogt, R. L., Jones, J. M., Goergens, C. A., Jones, M. E., Witte, G. A., and Lee, M. Y.: Antarctic
1117 station-based seasonal pressure reconstructions since 1905: 2. Variability and trends during the
1118 twentieth century., *Journal of Geophysical Research: Atmospheres*, 121, 2836–2856,
1119 <https://doi.org/10.1002/2015JD024565>, 2016b.

1120 Fogt, R. L., Goergens, C. A., Jones, J. M., Schneider, D. P., Nicolas, J. P., Bromwich, D. H., and
1121 Dusselier, H. E.: A twentieth-century perspective on summer Antarctic pressure change and
1122 variability and contributions from tropical SSTs and ozone depletion, *Geophysical Research*
1123 *Letters*, 44, 9918–9927, <https://doi.org/10.1002/2017GL075079>, 2017.

1124 Fogt, R. L., Clark, L. N., and Nicolas, J. P.: A New Monthly Pressure Dataset Poleward of 60°S
1125 since 1957, *Journal of Climate*, 31, 3865–3874, <https://doi.org/10.1175/JCLI-D-17-0879.1>, 2018.

1126 Fogt, R. L., Schneider, D. P., Goergens, C. A., Jones, J. M., Clark, L. N., and Garberoglio, M. J.:
1127 Seasonal Antarctic pressure variability during the twentieth century from spatially complete
1128 reconstructions and CAM5 simulations, *Climate Dynamics*, [https://doi.org/10.1007/s00382-](https://doi.org/10.1007/s00382-019-04674-8)
1129 [019-04674-8](https://doi.org/10.1007/s00382-019-04674-8), 2019.

1130 Fogt, R. L., Belak, C. P., Jones, J. M., Slivinski, L. C., and Compo, G. P.: An Assessment of Early
1131 20th-Century Antarctic Pressure Reconstructions using Historical Observations, *International*
1132 *Journal of Climatology*, <https://doi.org/10.1002/joc.6718>, 2020.

1133 Fogt, R. L., Sleinkofer, A. M., Raphael, M. N., and Handcock, M. S.: A regime shift in seasonal
1134 total Antarctic sea ice extent in the twentieth century, *Nat. Clim. Chang.*, 12, 54–62,
1135 <https://doi.org/10.1038/s41558-021-01254-9>, 2022a.

1136 Fogt, R. L., Dalaiden, Q., and Zarembka, M. S.: Understanding differences in Antarctic sea ice-
1137 extent reconstructions in the Ross, Amundsen, and Bellingshausen seas since 1900, *PAGES Mag.*,
1138 30, 74–75, <https://doi.org/10.22498/pages.30.2.74>, 2022b.

1139 Fogt, R. L., Raphael, M. N., and Handcock, M. S.: Seasonal Antarctic Sea Ice Extent
1140 Reconstructions, 1905–2020, Version 1, <https://doi.org/10.7265/55X7-WE68>, 2023.

1141 Goosse, H., Crespin, E., De Montety, A., Mann, M. E., Renssen, H., and Timmermann, A.:
1142 Reconstructing surface temperature changes over the past 600 years using climate model
1143 simulations with data assimilation, *J. Geophys. Res.*, *115*, D09108,
1144 <https://doi.org/10.1029/2009JD012737>, 2010.

1145 Goyal, R., Jucker, M., Sen Gupta, A., and England, M. H.: Generation of the Amundsen Sea Low
1146 by Antarctic Orography, *Geophys Res Lett*, *48*, <https://doi.org/10.1029/2020GL091487>, 2021.

1147 Hakim, G. J., Emile-Geay, J., Steig, E. J., Noone, D., Anderson, D. M., Tardif, R., Steiger, N., and
1148 Perkins, W. A.: The last millennium climate reanalysis project: Framework and first results, *J.*
1149 *Geophys. Res. Atmos.*, *121*, 6745–6764, <https://doi.org/10.1002/2016JD024751>, 2016.

1150 Hobbs, W. R., Massom, R., Stammerjohn, S., Reid, P., Williams, G., and Meier, W.: A review of
1151 recent changes in Southern Ocean sea ice, their drivers and forcings, *Global and Planetary*
1152 *Change*, *143*, 228–250, <https://doi.org/10.1016/j.gloplacha.2016.06.008>, 2016.

1153 Holland, P. R.: The seasonality of Antarctic sea ice trends, *Geophys. Res. Lett.*, *41*, 4230–4237,
1154 <https://doi.org/10.1002/2014GL060172>, 2014.

1155 Holland, P. R. and Kwok, R.: Wind-driven trends in Antarctic sea-ice drift, *Nature Geoscience*, *5*,
1156 872–875, <https://doi.org/10.1038/ngeo1627>, 2012.

1157 Holland, P. R., O’Connor, G. K., Bracegirdle, T. J., Dutrieux, P., Naughten, K. A., Steig, E. J.,
1158 Schneider, D. P., Jenkins, A., and Smith, J. A.: Anthropogenic and internal drivers of wind
1159 changes over the Amundsen Sea, West Antarctica, during the 20th and 21st centuries, *The*
1160 *Cryosphere*, *16*, 5085–5105, <https://doi.org/10.5194/tc-16-5085-2022>, 2022.

1161 Hosking, J. S., Orr, A., Marshall, G. J., Turner, J., and Phillips, T.: The Influence of the Amundsen–
1162 Bellinghausen Seas Low on the Climate of West Antarctica and Its Representation in Coupled
1163 Climate Model Simulations, *Journal of Climate*, *26*, 6633–6648, <https://doi.org/10.1175/JCLI-D-12-00813.1>, 2013.

1165 Jones, J. M., Gille, S. T., Goosse, H., Abram, N. J., Canziani, P. O., Charman, D. J., Clem, K. R.,
1166 Crosta, X., de Lavergne, C., Eisenman, I., England, M. H., Fogt, R. L., Frankcombe, L. M.,
1167 Marshall, G. J., Masson-Delmotte, V., Morrison, A. K., Orsi, A. J., Raphael, M. N., Renwick, J. A.,
1168 Schneider, D. P., Simpkins, G. R., Steig, E. J., Stenni, B., Swingedouw, D., and Vance, T. R.:
1169 Assessing recent trends in high latitude Southern Hemisphere surface climate, *Nature Climate*
1170 *Change*, *6*, 917–926, <https://doi.org/10.1038/nclimate3103>, 2016.

1171 Lachlan Cope, T. and Connolley, W.: Teleconnections between the tropical Pacific and the
1172 Amundsen–Bellinghausens Sea: Role of the El Niño/Southern Oscillation, *Journal of Geophysical*
1173 *Research: Atmospheres*, *111*, <https://doi.org/10.1029/2005JD006386>, 2006.

1174 Li, X., Cai, W., Meehl, G. A., Chen, D., Yuan, X., Raphael, M., Holland, D. M., Ding, Q., Fogt, R. L.,
1175 Markle, B. R., Wang, G., Bromwich, D. H., Turner, J., Xie, S. P., Steig, E. J., Gille, S. T., Xiao, C.,
1176 Wu, B., Lazzara, M. A., Chen, X., Stammerjohn, S., Holland, P. R., Holland, M. M., Cheng, X.,
1177 Price, S. F., Wang, Z., Bitz, C. M., Shi, J., Gerber, E. P., Liang, X., Goosse, H., Yoo, C., Ding, M.,
1178 Geng, L., Xin, M., Li, C., Dou, T., Liu, C., Sun, W., Wang, X., and Song, C.: Tropical teleconnection
1179 impacts on Antarctic climate changes, *Nat Rev Earth Environ*, <https://doi.org/10.1038/s43017-021-00204-5>, 2021.

1181 Lorrey, A. M., Pearce, P. R., Allan, R., Wilkinson, C., Woolley, J. M., Judd, E., Mackay, S., Rawhat,
1182 S., Slivinski, L., Wilkinson, S., Hawkins, E., Quesnel, P., and Compo, G. P.: Meteorological data
1183 rescue: Citizen science lessons learned from Southern Weather Discovery, *Patterns*, *3*, 100495,
1184 <https://doi.org/10.1016/j.patter.2022.100495>, 2022.

1185 Meier, W., Fetterer, F., Windnagel, A., and Stewart, S.: NOAA/NSIDC Climate Data Record of
1186 Passive Microwave Sea Ice Concentration, Version 4, <https://doi.org/10.7265/EFMZ-2T65>,
1187 2021.

1188 Murphy, E. J., Clarke, A., Symon, C., and Priddle, J.: Temporal variation in Antarctic sea-ice:
1189 analysis of a long term fast-ice record from the South Orkney Islands, *Deep Sea Research Part I:
1190 Oceanographic Research Papers*, *42*, 1045–1062, [https://doi.org/10.1016/0967-0637\(95\)00057-
1191 D](https://doi.org/10.1016/0967-0637(95)00057-D), 1995.

1192 O’Connor, G. K., Steig, E. J., and Hakim, G. J.: Strengthening Southern Hemisphere Westerlies
1193 and Amundsen Sea Low Deepening Over the 20th Century Revealed by Proxy Data Assimilation,
1194 *Geophysical Research Letters*, *48*, <https://doi.org/10.1029/2021GL095999>, 2021.

1195 O’Connor, G. K., Holland, P. R., Steig, E. J., Dutrieux, P., and Hakim, G. J.: Drivers and rarity of
1196 the strong 1940s westerly wind event over the Amundsen Sea, West Antarctica, *Ice
1197 sheets/Climate Interactions*, <https://doi.org/10.5194/tc-2023-16>, 2023.

1198 PAGES2k Consortium, Emile-Geay, J., McKay, N. P., Kaufman, D. S., Von Gunten, L., Wang, J.,
1199 Anchukaitis, K. J., Abram, N. J., Addison, J. A., Curran, M. A. J., Evans, M. N., Henley, B. J., Hao,
1200 Z., Martrat, B., McGregor, H. V., Neukom, R., Pederson, G. T., Stenni, B., Thirumalai, K., Werner,
1201 J. P., Xu, C., Divine, D. V., Dixon, B. C., Gergis, J., Mundo, I. A., Nakatsuka, T., Phipps, S. J.,
1202 Routson, C. C., Steig, E. J., Tierney, J. E., Tyler, J. J., Allen, K. J., Bertler, N. A. N., Björklund, J.,
1203 Chase, B. M., Chen, M. T., Cook, E., De Jong, R., DeLong, K. L., Dixon, D. A., Ekaykin, A. A., Ersek,
1204 V., Filipsson, H. L., Francus, P., Freund, M. B., Frezzotti, M., Gaire, N. P., Gajewski, K., Ge, Q.,
1205 Goosse, H., Gornostaeva, A., Grosjean, M., Horiuchi, K., Hormes, A., Husum, K., Isaksson, E.,
1206 Kandasamy, S., Kawamura, K., Kilbourne, K. H., Koç, N., Leduc, G., Linderholm, H. W., Lorrey, A.
1207 M., Mikhalenko, V., Mortyn, P. G., Motoyama, H., Moy, A. D., Mulvaney, R., Munz, P. M., Nash,
1208 D. J., Oerter, H., Opel, T., Orsi, A. J., Ovchinnikov, D. V., Porter, T. J., Roop, H. A., Saenger, C.,
1209 Sano, M., Sauchyn, D., Saunders, K. M., Seidenkrantz, M. S., Severi, M., Shao, X., Sicre, M. A.,
1210 Sigl, M., Sinclair, K., St. George, S., St. Jacques, J. M., Thamban, M., Kuwar Thapa, U., Thomas, E.
1211 R., Turney, C., Uemura, R., Viau, A. E., Vladimirova, D. O., Wahl, E. R., White, J. W. C., Yu, Z., and

1212 Zinke, J.: A global multiproxy database for temperature reconstructions of the Common Era, *Sci*
1213 *Data*, 4, 170088, <https://doi.org/10.1038/sdata.2017.88>, 2017.

1214 Parkinson, C. L.: A 40-y record reveals gradual Antarctic sea ice increases followed by decreases
1215 at rates far exceeding the rates seen in the Arctic, *Proc Natl Acad Sci USA*, 116, 14414–14423,
1216 <https://doi.org/10.1073/pnas.1906556116>, 2019.

1217 Polvani, L. M., Waugh, D. W., Correa, G. J. P., and Son, S.-W.: Stratospheric Ozone Depletion:
1218 The Main Driver of Twentieth-Century Atmospheric Circulation Changes in the Southern
1219 Hemisphere, *Journal of Climate*, 24, 795–812, <https://doi.org/10.1175/2010JCLI3772.1>, 2011.

1220 Raphael, M. N. and Hobbs, W.: The influence of the large-scale atmospheric circulation on
1221 Antarctic sea ice during ice advance and retreat seasons, *Geophys. Res. Lett.*, 41, 5037–5045,
1222 <https://doi.org/10.1002/2014GL060365>, 2014.

1223 Raphael, M. N., Marshall, G. J., Turner, J., Fogt, R. L., Schneider, D., Dixon, D. A., Hosking, J. S.,
1224 Jones, J. M., and Hobbs, W. R.: The Amundsen Sea Low: Variability, Change, and Impact on
1225 Antarctic Climate, *Bulletin of the American Meteorological Society*, 97, 111–121,
1226 <https://doi.org/10.1175/BAMS-D-14-00018.1>, 2016.

1227 Rignot, E., Jacobs, S., Mouginot, J., and Scheuchl, B.: Ice Shelf Melting Around Antarctica,
1228 *Science*, 341, 266–270, <https://doi.org/10.1126/science.1235798>, 2013.

1229 Rignot, E., Mouginot, J., Scheuchl, B., van den Broeke, M., van Wessem, M. J., and Morlighem,
1230 M.: Four decades of Antarctic Ice Sheet mass balance from 1979–2017, *Proceedings of the*
1231 *National Academy of Sciences*, 116, 1095–1103, <https://doi.org/10.1073/pnas.1812883116>,
1232 2019.

1233 Schneider, D. P. and Deser, C.: Tropically driven and externally forced patterns of Antarctic sea
1234 ice change: reconciling observed and modeled trends, *Clim Dyn*, 50, 4599–4618,
1235 <https://doi.org/10.1007/s00382-017-3893-5>, 2018.

1236 Schneider, D. P. and Fogt, R. L.: Artifacts in Century-Length Atmospheric and Coupled
1237 Reanalyses Over Antarctica Due to Historical Data Availability, *Geophysical Research Letters*, 45,
1238 964–973, <https://doi.org/10.1002/2017GL076226>, 2018.

1239 Slivinski, L. C., Compo, G. P., Whitaker, J. S., Sardeshmukh, P. D., Giese, B. S., McColl, C., Allan,
1240 R., Yin, X., Vose, R., Titchner, H., Kennedy, J., Spencer, L. J., Ashcroft, L., Brönnimann, S., Brunet,
1241 M., Camuffo, D., Cornes, R., Cram, T. A., Crouthamel, R., Domínguez-Castro, F., Freeman, J. E.,
1242 Gergis, J., Hawkins, E., Jones, P. D., Jourdain, S., Kaplan, A., Kubota, H., Le Blancq, F., Lee, T.,
1243 Lorrey, A., Luterbacher, J., Maugeri, M., Mock, C. J., Moore, G. W. K., Przybylak, R., Pudmenzky,
1244 C., Reason, C., Slonosky, V. C., Smith, C., Tinz, B., Trewin, B., Valente, M. A., Wang, X. L.,
1245 Wilkinson, C., Wood, K., and Wyszyn'ski, P.: Towards a more reliable historical reanalysis:
1246 Improvements for version 3 of the Twentieth-Century Reanalysis system, *Quarterly Journal of*
1247 *the Royal Meteorological Society*, <https://doi.org/10.1002/qj.3598>, 2019.

1248 Smith, B., Fricker, H. A., Gardner, A. S., Medley, B., Nilsson, J., Paolo, F. S., Holschuh, N.,
1249 Adusumilli, S., Brunt, K., Csatho, B., Harbeck, K., Markus, T., Neumann, T., Siegfried, M. R., and
1250 Zwally, H. J.: Pervasive ice sheet mass loss reflects competing ocean and atmosphere processes,
1251 *Science*, 368, 1239–1242, <https://doi.org/10.1126/science.aaz5845>, 2020.

1252 Steig, E. J., Ding, Q., White, J. W. C., Küttel, M., Rupper, S. B., Neumann, T. A., Neff, P. D.,
1253 Gallant, A. J. E., Mayewski, P. A., Taylor, K. C., Hoffmann, G., Dixon, D. A., Schoenemann, S. W.,
1254 Markle, B. R., Fudge, T. J., Schneider, D. P., Schauer, A. J., Teel, R. P., Vaughn, B. H., Burgener, L.,
1255 Williams, J., and Korotkikh, E.: Recent climate and ice sheet changes in West Antarctica
1256 compared with the past 2,000 years, *Nature Geosci*, 6, 372–375,
1257 <https://doi.org/10.1038/ngeo1778>, 2013.

1258 Stenni, B., Curran, M. A. J., Abram, N. J., Orsi, A., Goursaud, S., Masson-Delmotte, V., Neukom,
1259 R., Goosse, H., Divine, D., van Ommen, T., Steig, E. J., Dixon, D. A., Thomas, E. R., Bertler, N. A.
1260 N., Isaksson, E., Ekaykin, A., Werner, M., and Frezzotti, M.: Antarctic climate variability on
1261 regional and continental scales over the last 2000 years, *Climate of the Past*, 13, 1609–1634,
1262 <https://doi.org/10.5194/cp-13-1609-2017>, 2017.

1263 Sun, S. and Eisenman, I.: Observed Antarctic sea ice expansion reproduced in a climate model
1264 after correcting biases in sea ice drift velocity, *Nat Commun*, 12, 1060,
1265 <https://doi.org/10.1038/s41467-021-21412-z>, 2021.

1266 Thomas, E. R. and Abram, N. J.: Ice core reconstruction of sea ice change in the Amundsen-Ross
1267 Seas since 1702 A.D., *Geophys. Res. Lett.*, 43, 5309–5317,
1268 <https://doi.org/10.1002/2016GL068130>, 2016.

1269 Thomas, E. R., Van Wessem, J. M., Roberts, J., Isaksson, E., Schlosser, E., Fudge, T. J., Vallelonga,
1270 P., Medley, B., Lenaerts, J., Bertler, N., Van Den Broeke, M. R., Dixon, D. A., Frezzotti, M., Stenni,
1271 B., Curran, M., and Ekaykin, A. A.: Regional Antarctic snow accumulation over the past 1000
1272 years, *Clim. Past*, 13, 1491–1513, <https://doi.org/10.5194/cp-13-1491-2017>, 2017.

1273 Thomas, E. R., Allen, C. S., Etourneau, J., King, A. C. F., Severi, M., Winton, V. H. L., Mueller, J.,
1274 Crosta, X., and Peck, V. L.: Antarctic Sea Ice Proxies from Marine and Ice Core Archives Suitable
1275 for Reconstructing Sea Ice over the Past 2000 Years, *Geosciences*, 9, 506,
1276 <https://doi.org/10.3390/geosciences9120506>, 2019.

1277 Turner, J., Colwell, S. R., Marshall, G. J., Lachlan Cope, T. A., Carleton, A. M., Jones, P. D., Lagun,
1278 V., Reid, P. A., and Iagovkina, S.: The SCAR READER project: Toward a high quality database of
1279 mean Antarctic meteorological observations, *J. Clim.*, 17, 2890–2898,
1280 [https://doi.org/10.1175/1520-0442\(2004\)017<2890:TSRPTA>2.0.CO;2](https://doi.org/10.1175/1520-0442(2004)017<2890:TSRPTA>2.0.CO;2), 2004.

1281 Turner, J., Phillips, T., Marshall, G. J., Hosking, J. S., Pope, J. O., Bracegirdle, T. J., and Deb, P.:
1282 Unprecedented springtime retreat of Antarctic sea ice in 2016: The 2016 Antarctic Sea Ice
1283 Retreat, *Geophysical Research Letters*, 44, 6868–6875, <https://doi.org/10.1002/2017GL073656>,
1284 2017.

1285 [Turner, J., Marshall, G. J., Clem, K., Colwell, S., Phillips, T., and Lu, H.: Antarctic temperature](#)
1286 [variability and change from station data, *Int J Climatol*, 40, 2986–3007,](#)
1287 <https://doi.org/10.1002/joc.6378>, 2020.

1288 [Turner, J., Holmes, C., Caton Harrison, T., Phillips, T., Jena, B., Reeves Francois, T., Fogt, R.,](#)
1289 [Thomas, E. R., and Bajish, C. C.: Record Low Antarctic Sea Ice Cover in February 2022,](#)
1290 [Geophysical Research Letters](#), 49, <https://doi.org/10.1029/2022GL098904>, 2022.

1291 [Wang, J., Luo, H., Yang, Q., Liu, J., Yu, L., Shi, Q., and Han, B.: An Unprecedented Record Low](#)
1292 [Antarctic Sea-ice Extent during Austral Summer 2022, *Adv. Atmos. Sci.*, 39, 1591–1597,](#)
1293 <https://doi.org/10.1007/s00376-022-2087-1>, 2022.

1294 [Widmann, M., Goosse, H., Van Der Schrier, G., Schnur, R., and Barkmeijer, J.: Using data](#)
1295 [assimilation to study extratropical Northern Hemisphere climate over the last millennium, *Clim.*](#)
1296 [Past](#), 6, 627–644, <https://doi.org/10.5194/cp-6-627-2010>, 2010.

1297 [Zazulie, N., Rusticucci, M., and Solomon, S.: Changes in Climate at High Southern Latitudes: A](#)
1298 [Unique Daily Record at Orcadas Spanning 1903–2008, *Journal of Climate*, 23, 189–196,](#)
1299 <https://doi.org/10.1175/2009JCLI3074.1>, 2010.

1300 [Abram, N. J., Thomas, E. R., McConnell, J. R., Mulvaney, R., Bracegirdle, T. J., Sime, L. C., and](#)
1301 [Aristarain, A. J.: Ice core evidence for a 20th century decline of sea ice in the Bellingshausen](#)
1302 [Sea, Antarctica, *Journal of Geophysical Research*, 115, <https://doi.org/10.1029/2010JD014644>,](#)
1303 [2010.](#)

1304 [Bamber, J. L., Riva, R. E. M., Vermeersen, B. L. A., and LeBrocq, A. M.: Reassessment of the](#)
1305 [Potential Sea-Level Rise from a Collapse of the West Antarctic Ice Sheet, *Science*, 324, 901–903,](#)
1306 <https://doi.org/10.1126/science.1169335>, 2009.

1307 [Banerjee, A., Fyfe, J. C., Polvani, L. M., Waugh, D., and Chang, K.-L.: A pause in Southern](#)
1308 [Hemisphere circulation trends due to the Montreal Protocol, *Nature*, 579, 544–548,](#)
1309 <https://doi.org/10.1038/s41586-020-2120-4>, 2020.

1310 [Blanchard-Wrigglesworth, E., Roach, L. A., Donohoe, A., and Ding, Q.: Impact of Winds and](#)
1311 [Southern Ocean SSTs on Antarctic Sea Ice Trends and Variability, *Journal of Climate*, 34, 949–](#)
1312 [965, <https://doi.org/10.1175/JCLI-D-20-0386.1>, 2021.](#)

1313 [Brady, E., Stevenson, S., Bailey, D., Liu, Z., Noone, D., Nusbaumer, J., Otto-Bliesner, B. L., Tabor,](#)
1314 [C., Tomas, R., Wong, T., Zhang, J., and Zhu, J.: The Connected Isotopic Water Cycle in the](#)
1315 [Community Earth System Model Version 1, *J Adv Model Earth Syst*, 11, 2547–2566,](#)
1316 <https://doi.org/10.1029/2019MS001663>, 2019.

1317 [Bromwich, D. H., Nicolas, J. P., Monaghan, A. J., Lazzara, M. A., Keller, L. M., Weidner, G. A., and](#)
1318 [Wilson, A. B.: Central West Antarctica among the most rapidly warming regions on Earth,](#)
1319 [Nature Geoscience](#), 6, 139–145, <https://doi.org/10.1038/ngeo1671>, 2012.

1320 [Clark, L. and Fogt, R.: Southern Hemisphere Pressure Relationships during the 20th Century—](#)
1321 [Implications for Climate Reconstructions and Model Evaluation, *Geosciences*, 9, 413,](#)
1322 <https://doi.org/10.3390/geosciences9100413>, 2019.

1323 [Dalaiden, Q., Goosse, H., Rezsöhazy, J., and Thomas, E. R.: Reconstructing atmospheric](#)
1324 [circulation and sea-ice extent in the West Antarctic over the past 200 years using data](#)
1325 [assimilation, *Clim Dyn*, 57, 3479–3503, https://doi.org/10.1007/s00382-021-05879-6](#), 2021a.

1326 [Dalaiden, Q., Goosse, H., Rezsöhazy, J., and Thomas, E.: Reconstructing atmospheric circulation](#)
1327 [and sea-ice extent in the West Antarctic over the past 200 years using data assimilation,](#)
1328 <https://doi.org/10.5281/ZENODO.4770178>, 2021b.

1329 [De La Mare, W. K.: Changes in Antarctic sea-ice extent from direct historical observations and](#)
1330 [whaling records, *Climatic Change*, 92, 461–493, https://doi.org/10.1007/s10584-008-9473-2](#),
1331 [2009.](#)

1332 [Ding, Q., Steig, E. J., Battisti, D. S., and Küttel, M.: Winter warming in West Antarctica caused by](#)
1333 [central tropical Pacific warming, *Nature Geoscience*, 4, 398–403,](#)
1334 <https://doi.org/10.1038/ngeo1129>, 2011.

1335 [Edinburgh, T. and Day, J. J.: Estimating the extent of Antarctic summer sea ice during the Heroic](#)
1336 [Age of Antarctic Exploration, *The Cryosphere*, 10, 2721–2730, https://doi.org/10.5194/tc-10-](#)
1337 [2721-2016](#), 2016.

1338 [Fogt, R. L. and Connolly, C. J.: Extratropical Southern Hemisphere Synchronous Pressure](#)
1339 [Variability in the Early Twentieth Century, *Journal of Climate*, 34, 5795–5811,](#)
1340 <https://doi.org/10.1175/JCLI-D-20-0498.1>, 2021.

1341 [Fogt, R. L. and Marshall, G. J.: The Southern Annular Mode: Variability, trends, and climate](#)
1342 [impacts across the Southern Hemisphere, *WIREs Climate Change*, 11,](#)
1343 <https://doi.org/10.1002/wcc.652>, 2020.

1344 [Fogt, R. L., Goergens, C. A., Jones, M. E., Witte, G. A., Lee, M. Y., and Jones, J. M.: Antarctic](#)
1345 [station-based seasonal pressure reconstructions since 1905: 1. Reconstruction evaluation:](#)
1346 [Antarctic Pressure Evaluation, *Journal of Geophysical Research: Atmospheres*, 121, 2814–2835,](#)
1347 <https://doi.org/10.1002/2015JD024564>, 2016a.

1348 [Fogt, R. L., Jones, J. M., Goergens, C. A., Jones, M. E., Witte, G. A., and Lee, M. Y.: Antarctic](#)
1349 [station-based seasonal pressure reconstructions since 1905: 2. Variability and trends during the](#)
1350 [twentieth century., *Journal of Geophysical Research: Atmospheres*, 121, 2836–2856,](#)
1351 <https://doi.org/10.1002/2015JD024565>, 2016b.

1352 [Fogt, R. L., Goergens, C. A., Jones, J. M., Schneider, D. P., Nicolas, J. P., Bromwich, D. H., and](#)
1353 [Dusselier, H. E.: A twentieth century perspective on summer Antarctic pressure change and](#)
1354 [variability and contributions from tropical SSTs and ozone depletion, *Geophysical Research*](#)
1355 [Letters](#), 44, 9918–9927, <https://doi.org/10.1002/2017GL075079>, 2017.

1356 [Fogt, R. L., Clark, L. N., and Nicolas, J. P.: A New Monthly Pressure Dataset Poleward of 60°S](#)
1357 [since 1957, *Journal of Climate*, 31, 3865–3874, <https://doi.org/10.1175/JCLI-D-17-0879.1>, 2018.](#)

1358 [Fogt, R. L., Schneider, D. P., Goergens, C. A., Jones, J. M., Clark, L. N., and Garberoglio, M. J.:](#)
1359 [Seasonal Antarctic pressure variability during the twentieth century from spatially complete](#)
1360 [reconstructions and CAM5 simulations, *Climate Dynamics*, \[https://doi.org/10.1007/s00382-\]\(https://doi.org/10.1007/s00382-019-04674-8\)](#)
1361 [019-04674-8, 2019.](#)

1362 [Fogt, R. L., Belak, C. P., Jones, J. M., Slivinski, L. C., and Compo, G. P.: An Assessment of Early](#)
1363 [20th Century Antarctic Pressure Reconstructions using Historical Observations, *International*](#)
1364 [Journal of Climatology](#), <https://doi.org/10.1002/joc.6718>, 2020.

1365 [Fogt, R. L., Sleinkofer, A. M., Raphael, M. N., and Handcock, M. S.: A regime shift in seasonal](#)
1366 [total Antarctic sea ice extent in the twentieth century, *Nat. Clim. Chang.*, 12, 54–62,](#)
1367 [https://doi.org/10.1038/s41558-021-01254-9, 2022a.](#)

1368 [Fogt, R. L., Dalaiden, Q., and Zarembka, M. S.: Understanding differences in Antarctic sea-ice-](#)
1369 [extent reconstructions in the Ross, Amundsen, and Bellingshausen seas since 1900, *PAGES Mag.*,](#)
1370 [30, 74–75, <https://doi.org/10.22498/pages.30.2.74>, 2022b.](#)

1371 [Fogt, R. L., Raphael, M. N., and Handcock, M. S.: Seasonal Antarctic Sea Ice Extent](#)
1372 [Reconstructions, 1905-2020, Version 1, <https://doi.org/10.7265/55X7-WE68>, 2023.](#)

1373 [Goosse, H., Crespin, E., De Montety, A., Mann, M. E., Renssen, H., and Timmermann, A.:](#)
1374 [Reconstructing surface temperature changes over the past 600 years using climate model](#)
1375 [simulations with data assimilation, *J. Geophys. Res.*, 115, D09108,](#)
1376 [https://doi.org/10.1029/2009JD012737, 2010.](#)

1377 [Goyal, R., Jucker, M., Sen Gupta, A., and England, M. H.: Generation of the Amundsen Sea Low](#)
1378 [by Antarctic Orography, *Geophys Res Lett*, 48, <https://doi.org/10.1029/2020GL091487>, 2021.](#)

1379 [Hakim, G. J., Emile-Geay, J., Steig, E. J., Noone, D., Anderson, D. M., Tardif, R., Steiger, N., and](#)
1380 [Perkins, W. A.: The last millennium climate reanalysis project: Framework and first results, *J.*](#)
1381 [Geophys. Res. Atmos., 121, 6745–6764, <https://doi.org/10.1002/2016JD024751>, 2016.](#)

1382 [Hobbs, W. R., Massom, R., Stammerjohn, S., Reid, P., Williams, G., and Meier, W.: A review of](#)
1383 [recent changes in Southern Ocean sea ice, their drivers and forcings, *Global and Planetary*](#)
1384 [Change, 143, 228–250, <https://doi.org/10.1016/j.gloplacha.2016.06.008>, 2016.](#)

1385 [Holland, P. R.: The seasonality of Antarctic sea ice trends, *Geophys. Res. Lett.*, 41, 4230–4237,](#)
1386 [https://doi.org/10.1002/2014GL060172, 2014.](#)

1387 [Holland, P. R. and Kwok, R.: Wind-driven trends in Antarctic sea-ice drift, *Nature Geoscience*, 5,](#)
1388 [872–875, <https://doi.org/10.1038/ngeo1627>, 2012.](#)

1389 [Holland, P. R., O'Connor, G. K., Bracegirdle, T. J., Dutrieux, P., Naughten, K. A., Steig, E. J.,](#)
1390 [Schneider, D. P., Jenkins, A., and Smith, J. A.: Anthropogenic and internal drivers of wind](#)
1391 [changes over the Amundsen Sea, West Antarctica, during the 20th and 21st centuries, *The*](#)
1392 [Cryosphere, 16, 5085–5105, <https://doi.org/10.5194/tc-16-5085-2022>, 2022.](#)

1393 [Hosking, J. S., Orr, A., Marshall, G. J., Turner, J., and Phillips, T.: The Influence of the Amundsen–](#)
1394 [Bellingshausen Seas Low on the Climate of West Antarctica and Its Representation in Coupled](#)
1395 [Climate Model Simulations, *Journal of Climate*, 26, 6633–6648, \[12-00813.1, 2013.\]\(https://doi.org/10.1175/JCLI-D-
1396 <a href=\)](#)

1397 [Jones, J. M., Gille, S. T., Goosse, H., Abram, N. J., Canziani, P. O., Charman, D. J., Clem, K. R.,](#)
1398 [Crosta, X., de Lavergne, C., Eisenman, I., England, M. H., Fogt, R. L., Frankcombe, L. M.,](#)
1399 [Marshall, G. J., Masson-Delmotte, V., Morrison, A. K., Orsi, A. J., Raphael, M. N., Renwick, J. A.,](#)
1400 [Schneider, D. P., Simpkins, G. R., Steig, E. J., Stenni, B., Swingedouw, D., and Vance, T. R.:](#)
1401 [Assessing recent trends in high-latitude Southern Hemisphere surface climate, *Nature Climate*](#)
1402 [Change, 6, 917–926, <https://doi.org/10.1038/nclimate3103>, 2016.](#)

1403 [Lachlan-Cope, T. and Connolley, W.: Teleconnections between the tropical Pacific and the](#)
1404 [Amundsen-Bellinghausens Sea: Role of the El Niño/Southern Oscillation, *Journal of Geophysical*](#)
1405 [Research: Atmospheres, 111, <https://doi.org/10.1029/2005JD006386>, 2006.](#)

1406 [Li, X., Cai, W., Meehl, G. A., Chen, D., Yuan, X., Raphael, M., Holland, D. M., Ding, Q., Fogt, R. L.,](#)
1407 [Markle, B. R., Wang, G., Bromwich, D. H., Turner, J., Xie, S.-P., Steig, E. J., Gille, S. T., Xiao, C.,](#)
1408 [Wu, B., Lazzara, M. A., Chen, X., Stammerjohn, S., Holland, P. R., Holland, M. M., Cheng, X.,](#)
1409 [Price, S. F., Wang, Z., Bitz, C. M., Shi, J., Gerber, E. P., Liang, X., Goosse, H., Yoo, C., Ding, M.,](#)
1410 [Geng, L., Xin, M., Li, C., Dou, T., Liu, C., Sun, W., Wang, X., and Song, C.: Tropical teleconnection](#)
1411 [impacts on Antarctic climate changes, *Nat Rev Earth Environ*, \[021-00204-5, 2021.\]\(https://doi.org/10.1038/s43017-
1412 <a href=\)](#)

1413 [Lorrey, A. M., Pearce, P. R., Allan, R., Wilkinson, C., Woolley, J.-M., Judd, E., Mackay, S., Rawhat,](#)
1414 [S., Slivinski, L., Wilkinson, S., Hawkins, E., Quesnel, P., and Compo, G. P.: Meteorological data](#)
1415 [rescue: Citizen science lessons learned from Southern Weather Discovery, *Patterns*, 3, 100495,](#)
1416 [https://doi.org/10.1016/j.patter.2022.100495, 2022.](#)

1417 [Meier, W., Fetterer, F., Windnagel, A., and Stewart, S.: NOAA/NSIDC Climate Data Record of](#)
1418 [Passive Microwave Sea Ice Concentration, Version 4, <https://doi.org/10.7265/EFMZ-2T65>,](#)
1419 [2021.](#)

1420 [Murphy, E. J., Clarke, A., Symon, C., and Priddle, J.: Temporal variation in Antarctic sea-ice:](#)
1421 [analysis of a long term fast-ice record from the South Orkney Islands, *Deep Sea Research Part I:*](#)
1422 [Oceanographic Research Papers, 42, 1045–1062, \[D, 1995.\]\(https://doi.org/10.1016/0967-0637\(95\)00057-
1423 <a href=\)](#)

1424 [Murphy, E. J., Clarke, A., Abram, N. J., and Turner, J.: Variability of sea-ice in the northern W](#)
1425 [eddell Sea during the 20th century, *J. Geophys. Res. Oceans*, 119, 4549–4572,](#)
1426 <https://doi.org/10.1002/2013JC009511>, 2014.

1427 [O’Connor, G. K., Steig, E. J., and Hakim, G. J.: Strengthening Southern Hemisphere Westerlies](#)
1428 [and Amundsen Sea Low Deepening Over the 20th Century Revealed by Proxy-Data Assimilation,](#)

1429 [Geophysical Research Letters](#), 48, <https://doi.org/10.1029/2021GL095999>, 2021.

1430 [O’Connor, G. K., Holland, P. R., Steig, E. J., Dutrieux, P., and Hakim, G. J.: Characteristics and](#)
1431 [rarity of the strong 1940s westerly wind event over the Amundsen Sea, West Antarctica, *The*](#)
1432 [Cryosphere](#), 17, 4399–4420, <https://doi.org/10.5194/tc-17-4399-2023>, 2023.

1433 [PAGES2k Consortium, Emile-Geay, J., McKay, N. P., Kaufman, D. S., Von Gunten, L., Wang, J.,](#)
1434 [Anchukaitis, K. J., Abram, N. J., Addison, J. A., Curran, M. A. J., Evans, M. N., Henley, B. J., Hao,](#)
1435 [Z., Martrat, B., McGregor, H. V., Neukom, R., Pederson, G. T., Stenni, B., Thirumalai, K., Werner,](#)
1436 [J. P., Xu, C., Divine, D. V., Dixon, B. C., Gergis, J., Mundo, I. A., Nakatsuka, T., Phipps, S. J.,](#)
1437 [Routson, C. C., Steig, E. J., Tierney, J. E., Tyler, J. J., Allen, K. J., Bertler, N. A. N., Björklund, J.,](#)
1438 [Chase, B. M., Chen, M.-T., Cook, E., De Jong, R., DeLong, K. L., Dixon, D. A., Ekaykin, A. A., Ersek,](#)
1439 [V., Filipsson, H. L., Francus, P., Freund, M. B., Frezzotti, M., Gaire, N. P., Gajewski, K., Ge, Q.,](#)
1440 [Goosse, H., Gornostaeva, A., Grosjean, M., Horiuchi, K., Hormes, A., Husum, K., Isaksson, E.,](#)
1441 [Kandasamy, S., Kawamura, K., Kilbourne, K. H., Koç, N., Leduc, G., Linderholm, H. W., Lorrey, A.](#)
1442 [M., Mikhalenko, V., Mortyn, P. G., Motoyama, H., Moy, A. D., Mulvaney, R., Munz, P. M., Nash,](#)
1443 [D. J., Oerter, H., Opel, T., Orsi, A. J., Ovchinnikov, D. V., Porter, T. J., Roop, H. A., Saenger, C.,](#)
1444 [Sano, M., Sauchyn, D., Saunders, K. M., Seidenkrantz, M.-S., Severi, M., Shao, X., Sicre, M.-A.,](#)
1445 [Sigl, M., Sinclair, K., St. George, S., St. Jacques, J.-M., Thamban, M., Kuwar Thapa, U., Thomas, E.](#)
1446 [R., Turney, C., Uemura, R., Viau, A. E., Vladimirova, D. O., Wahl, E. R., White, J. W. C., Yu, Z., and](#)
1447 [Zinke, J.: A global multiproxy database for temperature reconstructions of the Common Era, *Sci*](#)
1448 [Data](#), 4, 170088, <https://doi.org/10.1038/sdata.2017.88>, 2017.

1449 [Parkinson, C. L.: A 40-y record reveals gradual Antarctic sea ice increases followed by decreases](#)
1450 [at rates far exceeding the rates seen in the Arctic, *Proc Natl Acad Sci USA*, 116, 14414–14423,](#)
1451 <https://doi.org/10.1073/pnas.1906556116>, 2019.

1452 [Polvani, L. M., Waugh, D. W., Correa, G. J. P., and Son, S.-W.: Stratospheric Ozone Depletion:](#)
1453 [The Main Driver of Twentieth-Century Atmospheric Circulation Changes in the Southern](#)
1454 [Hemisphere, *Journal of Climate*, 24, 795–812, <https://doi.org/10.1175/2010JCLI3772.1>, 2011.](#)

1455 [Raphael, M. N. and Hobbs, W.: The influence of the large-scale atmospheric circulation on](#)
1456 [Antarctic sea ice during ice advance and retreat seasons, *Geophys. Res. Lett.*, 41, 5037–5045,](#)
1457 <https://doi.org/10.1002/2014GL060365>, 2014.

1458 [Raphael, M. N., Marshall, G. J., Turner, J., Fogt, R. L., Schneider, D., Dixon, D. A., Hosking, J. S.,](#)
1459 [Jones, J. M., and Hobbs, W. R.: The Amundsen Sea Low: Variability, Change, and Impact on](#)
1460 [Antarctic Climate, *Bulletin of the American Meteorological Society*, 97, 111–121,](#)
1461 <https://doi.org/10.1175/BAMS-D-14-00018.1>, 2016.

1462 [Rignot, E., Jacobs, S., Mouginot, J., and Scheuchl, B.: Ice-Shelf Melting Around Antarctica,](#)
1463 [Science, 341, 266–270, https://doi.org/10.1126/science.1235798, 2013.](#)

1464 [Rignot, E., Mouginot, J., Scheuchl, B., van den Broeke, M., van Wessem, M. J., and Morlighem,](#)
1465 [M.: Four decades of Antarctic Ice Sheet mass balance from 1979–2017, Proceedings of the](#)
1466 [National Academy of Sciences, 116, 1095–1103, https://doi.org/10.1073/pnas.1812883116,](#)
1467 [2019.](#)

1468 [Schneider, D. P. and Deser, C.: Tropically driven and externally forced patterns of Antarctic sea](#)
1469 [ice change: reconciling observed and modeled trends, Clim Dyn, 50, 4599–4618,](#)
1470 [https://doi.org/10.1007/s00382-017-3893-5](#), 2018.

1471 [Schneider, D. P. and Fogt, R. L.: Artifacts in Century-Length Atmospheric and Coupled](#)
1472 [Reanalyses Over Antarctica Due to Historical Data Availability, Geophysical Research Letters, 45,](#)
1473 [964–973, https://doi.org/10.1002/2017GL076226, 2018.](#)

1474 [Servettaz, A. P. M., Agosta, C., Kittel, C., and Orsi, A. J.: Control of the temperature signal in](#)
1475 [Antarctic proxies by snowfall dynamics, Ice sheets/Atmospheric Interactions,](#)
1476 [https://doi.org/10.5194/egusphere-2023-1903](#), 2023.

1477 [Slivinski, L. C., Compo, G. P., Whitaker, J. S., Sardeshmukh, P. D., Giese, B. S., McColl, C., Allan,](#)
1478 [R., Yin, X., Vose, R., Titchner, H., Kennedy, J., Spencer, L. J., Ashcroft, L., Brönnimann, S., Brunet,](#)
1479 [M., Camuffo, D., Cornes, R., Cram, T. A., Crouthamel, R., Domínguez-Castro, F., Freeman, J. E.,](#)
1480 [Gergis, J., Hawkins, E., Jones, P. D., Jourdain, S., Kaplan, A., Kubota, H., Le Blancq, F., Lee, T.,](#)
1481 [Lorrey, A., Luterbacher, J., Maugeri, M., Mock, C. J., Moore, G. W. K., Przybylak, R., Pudmenzky,](#)
1482 [C., Reason, C., Slonosky, V. C., Smith, C., Tinz, B., Trewin, B., Valente, M. A., Wang, X. L.,](#)
1483 [Wilkinson, C., Wood, K., and Wyszyn'ski, P.: Towards a more reliable historical reanalysis:](#)
1484 [Improvements for version 3 of the Twentieth Century Reanalysis system, Quarterly Journal of](#)
1485 [the Royal Meteorological Society, https://doi.org/10.1002/qj.3598, 2019.](#)

1486 [Smith, B., Fricker, H. A., Gardner, A. S., Medley, B., Nilsson, J., Paolo, F. S., Holschuh, N.,](#)
1487 [Adusumilli, S., Brunt, K., Csatho, B., Harbeck, K., Markus, T., Neumann, T., Siegfried, M. R., and](#)
1488 [Zwally, H. J.: Pervasive ice sheet mass loss reflects competing ocean and atmosphere processes,](#)
1489 [Science, 368, 1239–1242, https://doi.org/10.1126/science.aaz5845, 2020.](#)

1490 [Steig, E. J., Ding, Q., White, J. W. C., Küttel, M., Rupper, S. B., Neumann, T. A., Neff, P. D.,](#)
1491 [Gallant, A. J. E., Mayewski, P. A., Taylor, K. C., Hoffmann, G., Dixon, D. A., Schoenemann, S. W.,](#)
1492 [Markle, B. R., Fudge, T. J., Schneider, D. P., Schauer, A. J., Teel, R. P., Vaughn, B. H., Burgener, L.,](#)
1493 [Williams, J., and Korotkikh, E.: Recent climate and ice-sheet changes in West Antarctica](#)
1494 [compared with the past 2,000 years, Nature Geosci, 6, 372–375,](#)
1495 [https://doi.org/10.1038/ngeo1778](#), 2013.

1496 [Steiger, N. J., Smerdon, J. E., Cook, E. R., and Cook, B. I.: A reconstruction of global hydroclimate](#)
1497 [and dynamical variables over the Common Era, Sci. Data, 5, 180086,](#)
1498 [https://doi.org/10.1038/sdata.2018.86](#), 2018.

1499 [Stenni, B., Curran, M. A. J., Abram, N. J., Orsi, A., Goursaud, S., Masson-Delmotte, V., Neukom,](#)
1500 [R., Goosse, H., Divine, D., van Ommen, T., Steig, E. J., Dixon, D. A., Thomas, E. R., Bertler, N. A.](#)
1501 [N., Isaksson, E., Ekaykin, A., Werner, M., and Frezzotti, M.: Antarctic climate variability on](#)
1502 [regional and continental scales over the last 2000 years, *Climate of the Past*, 13, 1609–1634,](#)
1503 <https://doi.org/10.5194/cp-13-1609-2017>, 2017.

1504 [Sun, S. and Eisenman, I.: Observed Antarctic sea ice expansion reproduced in a climate model](#)
1505 [after correcting biases in sea ice drift velocity, *Nat Commun*, 12, 1060,](#)
1506 <https://doi.org/10.1038/s41467-021-21412-z>, 2021.

1507 [Thomas, E. R. and Abram, N. J.: Ice core reconstruction of sea ice change in the Amundsen-Ross](#)
1508 [Seas since 1702 A.D., *Geophys. Res. Lett.*, 43, 5309–5317,](#)
1509 <https://doi.org/10.1002/2016GL068130>, 2016.

1510 [Thomas, E. R., Van Wessem, J. M., Roberts, J., Isaksson, E., Schlosser, E., Fudge, T. J., Vallelonga,](#)
1511 [P., Medley, B., Lenaerts, J., Bertler, N., Van Den Broeke, M. R., Dixon, D. A., Frezzotti, M., Stenni,](#)
1512 [B., Curran, M., and Ekaykin, A. A.: Regional Antarctic snow accumulation over the past 1000](#)
1513 [years, *Clim. Past*, 13, 1491–1513, https://doi.org/10.5194/cp-13-1491-2017](#), 2017.

1514 [Thomas, E. R., Allen, C. S., Etourneau, J., King, A. C. F., Severi, M., Winton, V. H. L., Mueller, J.,](#)
1515 [Crosta, X., and Peck, V. L.: Antarctic Sea Ice Proxies from Marine and Ice Core Archives Suitable](#)
1516 [for Reconstructing Sea Ice over the Past 2000 Years, *Geosciences*, 9, 506,](#)
1517 <https://doi.org/10.3390/geosciences9120506>, 2019.

1518 [Turner, J., Colwell, S. R., Marshall, G. J., Lachlan-Cope, T. A., Carleton, A. M., Jones, P. D., Lagun,](#)
1519 [V., Reid, P. A., and Iagovkina, S.: The SCAR READER project: Toward a high-quality database of](#)
1520 [mean Antarctic meteorological observations, *J. Clim.*, 17, 2890–2898,](#)
1521 [https://doi.org/10.1175/1520-0442\(2004\)017<2890:TSRPTA>2.0.CO;2](https://doi.org/10.1175/1520-0442(2004)017<2890:TSRPTA>2.0.CO;2), 2004.

1522 [Turner, J., Phillips, T., Marshall, G. J., Hosking, J. S., Pope, J. O., Bracegirdle, T. J., and Deb, P.:](#)
1523 [Unprecedented springtime retreat of Antarctic sea ice in 2016: The 2016 Antarctic Sea Ice](#)
1524 [Retreat, *Geophysical Research Letters*, 44, 6868–6875, https://doi.org/10.1002/2017GL073656,](#)
1525 [2017.](#)

1526 [Turner, J., Phillips, T., Thamban, M., Rahaman, W., Marshall, G. J., Wille, J. D., Favier, V.,](#)
1527 [Winton, V. H. L., Thomas, E., Wang, Z., Broeke, M., Hosking, J. S., and Lachlan-Cope, T.: The](#)
1528 [Dominant Role of Extreme Precipitation Events in Antarctic Snowfall Variability, *Geophys. Res.*](#)
1529 [*Lett.*, 46, 3502–3511, https://doi.org/10.1029/2018GL081517](#), 2019.

1530 [Turner, J., Marshall, G. J., Clem, K., Colwell, S., Phillips, T., and Lu, H.: Antarctic temperature](#)
1531 [variability and change from station data, *Int J Climatol*, 40, 2986–3007,](#)
1532 <https://doi.org/10.1002/joc.6378>, 2020.

1533 [Turner, J., Holmes, C., Caton Harrison, T., Phillips, T., Jena, B., Reeves-Francois, T., Fogt, R.,](#)
1534 [Thomas, E. R., and Bajish, C. C.: Record Low Antarctic Sea Ice Cover in February 2022,](#)
1535 [Geophysical Research Letters, 49, <https://doi.org/10.1029/2022GL098904>, 2022.](#)

1536 [Wang, J., Luo, H., Yang, Q., Liu, J., Yu, L., Shi, Q., and Han, B.: An Unprecedented Record Low](#)
1537 [Antarctic Sea-ice Extent during Austral Summer 2022, Adv. Atmos. Sci., 39, 1591–1597,](#)
1538 [https://doi.org/10.1007/s00376-022-2087-1, 2022.](#)

1539 [Widmann, M., Goosse, H., Van Der Schrier, G., Schnur, R., and Barkmeijer, J.: Using data](#)
1540 [assimilation to study extratropical Northern Hemisphere climate over the last millennium, Clim.](#)
1541 [Past, 6, 627–644, <https://doi.org/10.5194/cp-6-627-2010>, 2010.](#)

1542 [Zazulie, N., Rusticucci, M., and Solomon, S.: Changes in Climate at High Southern Latitudes: A](#)
1543 [Unique Daily Record at Orcadas Spanning 1903–2008, Journal of Climate, 23, 189–196,](#)
1544 [https://doi.org/10.1175/2009JCLI3074.1, 2010.](#)

1545